Supporting information for

Visible-light photocatalytic selective oxidation of C(sp^3)-H bonds by anion-cation dual-metal-site nanoscale localized carbon nitride

Yingying Wang†,[a] Peihe Li†,*[a] Jinghui Wang,[a] Zhifei Liu,[a] Yin Wang,[a] Ye Lu,[a] Ying Liu,[a] Limei Duan,*[a] Wanfei Li,[b] Sarina Sarina,[c] Huaiyong Zhu*[c] and Jinghai Liu*[a]

[a]*Inner Mongolia Key Laboratory of Carbon Nanomaterials, Nano Innovation Institute (NII), College of Chemistry and Chemical Engineering, Inner Mongolia University for Nationalities, Tongliao 028000, China.*

[b]*Research Center for Nanophotonic and Nanoelectronic Materials, School of Materials Science and Engineering, Suzhou University of Science and Technology, Suzhou 215009, China.*

[c]*School of Chemistry, Physics and Mechanical Engineering, Queensland University of Technology, Brisbane, QLD 4001, Australia*

E-mail: phli2018@foxmail.com, duanlmxie@126.com, hy.zhu@qut.edu.au, jhliu2015@imun.edu.cn.

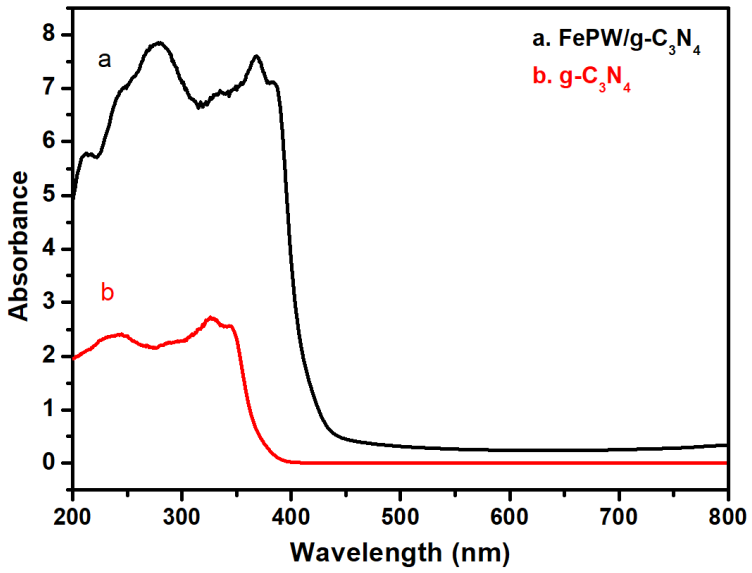

Fig. S1 UV-vis spectra of the (a) g-C_3N_4, and (b) FePW/g-C_3N_4

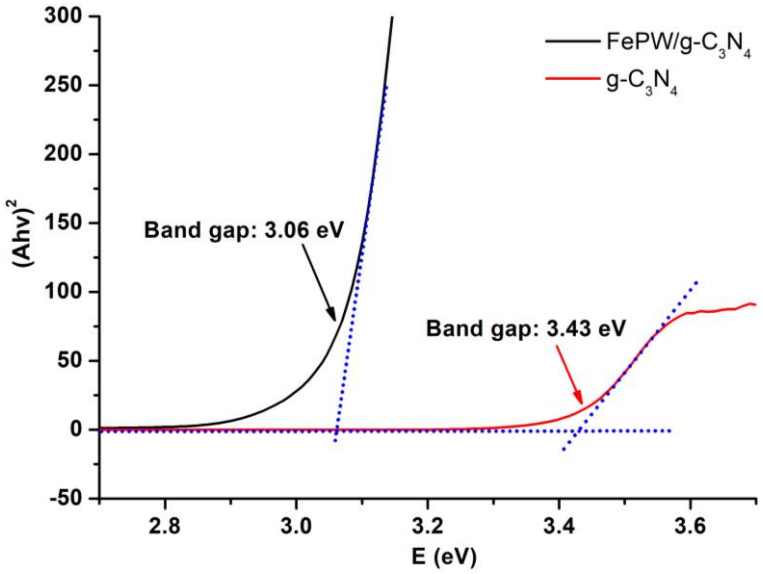

Fig. S2 Band gap of g-C_3N_4 and FePW/g-C_3N_4 obtained from the UV/Vis DR spectrum according to the Kubelka–Munk theory.

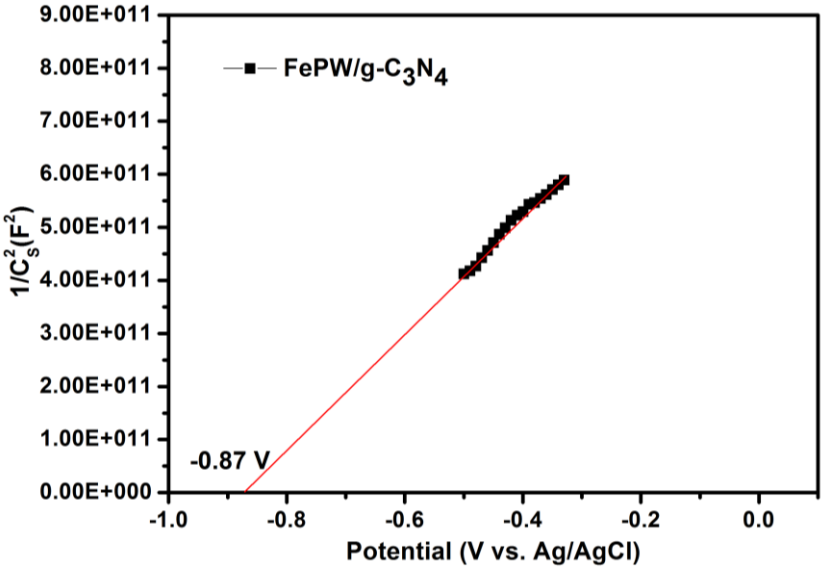

Fig. S3 Mott-Schottky plots.

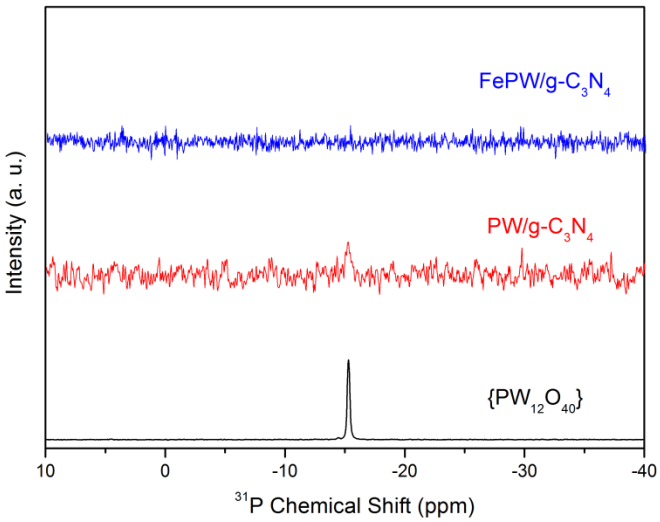

Fig. S4 The ^{31}P NMR of $\{PW_{12}O_{40}\}$, PW/g-C_3N_4 and FePW/g-C_3N_4.

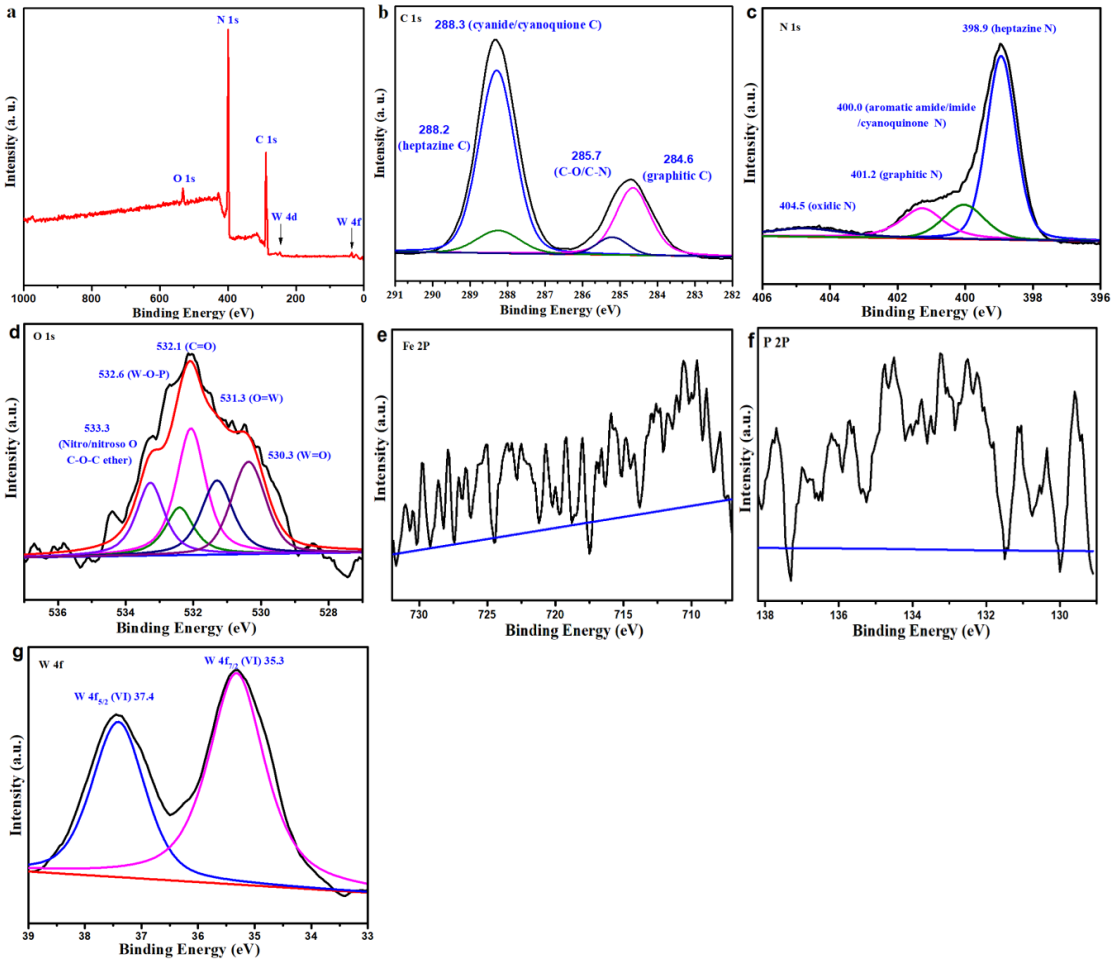

Fig. S5 Surface chemical structures of FePW/g-C_3N_4. (a) XPS survey for FePW/g-C_3N_4. (b) High-resolution C1s spectrum. (c) N1s spectrum. (d) O1s spectrum. (e) Fe2p spectrum. (f) P2p spectrum. (g) High-resolution W4f spectrum.

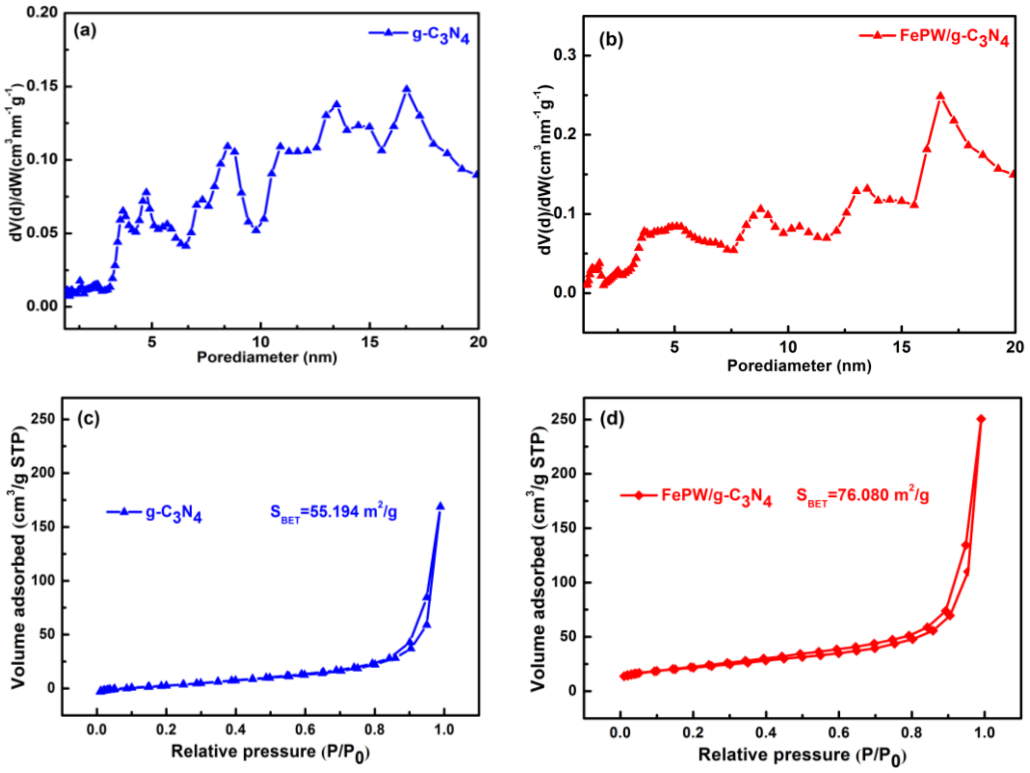

Fig. S6 Specific surface area (SSA) and BJH pore size distributions for g-C_3N_4 and FePW/g-C_3N_4 control. (a) and (b) pore size distribution and pore volume analyzed according to Barret-Joyner-Halenda (BJH) method for g-C_3N_4 and FePW/g-C_3N_4. N_2 adsorption/desorption isotherms: (c) the SSA of g-C_3N_4 is 55.194 m^2/g, and the SSA of FePW/g-C_3N_4 is 76.080 m^2/g.

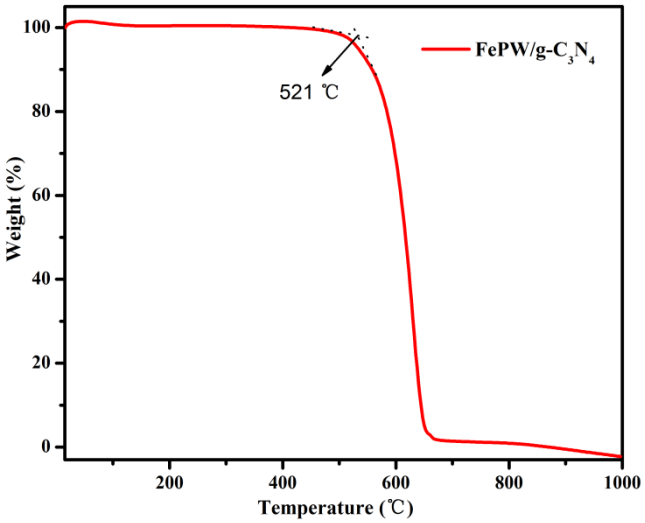

Fig. S7 TGA curve of FePW/g-C_3N_4 obtained under nitrogen atmosphere at a heating rate of 10 °C/min. The FePW/g-C_3N_4 exhibited excellent thermal stability up to 521 ºC and start to loss for the bulk material.

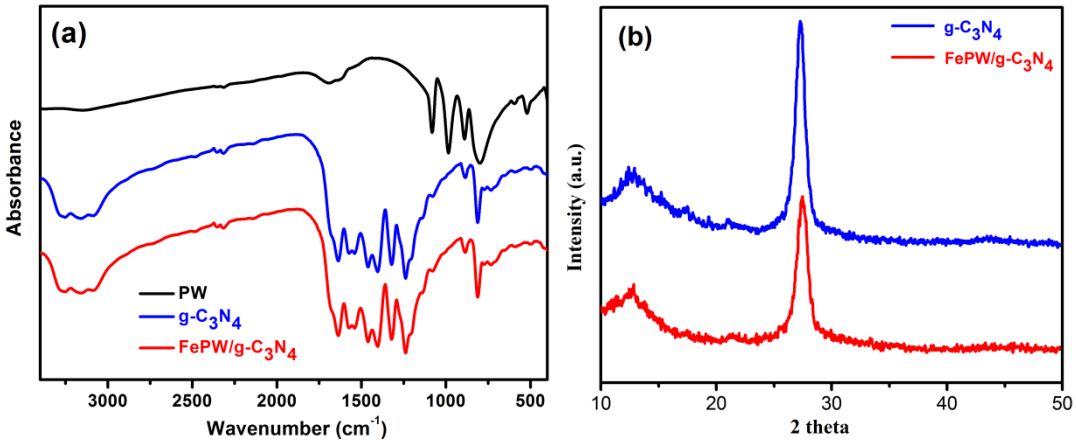

Fig. S8 (a) IR spectra of the $\{PW_{12}O_{40}\}$ = {PW}, g-C_3N_4 and FePW/g-C_3N_4; (b) XRD patterns of the as-synthesized sample: g-C_3N_4 and FePW/g-C_3N_4.

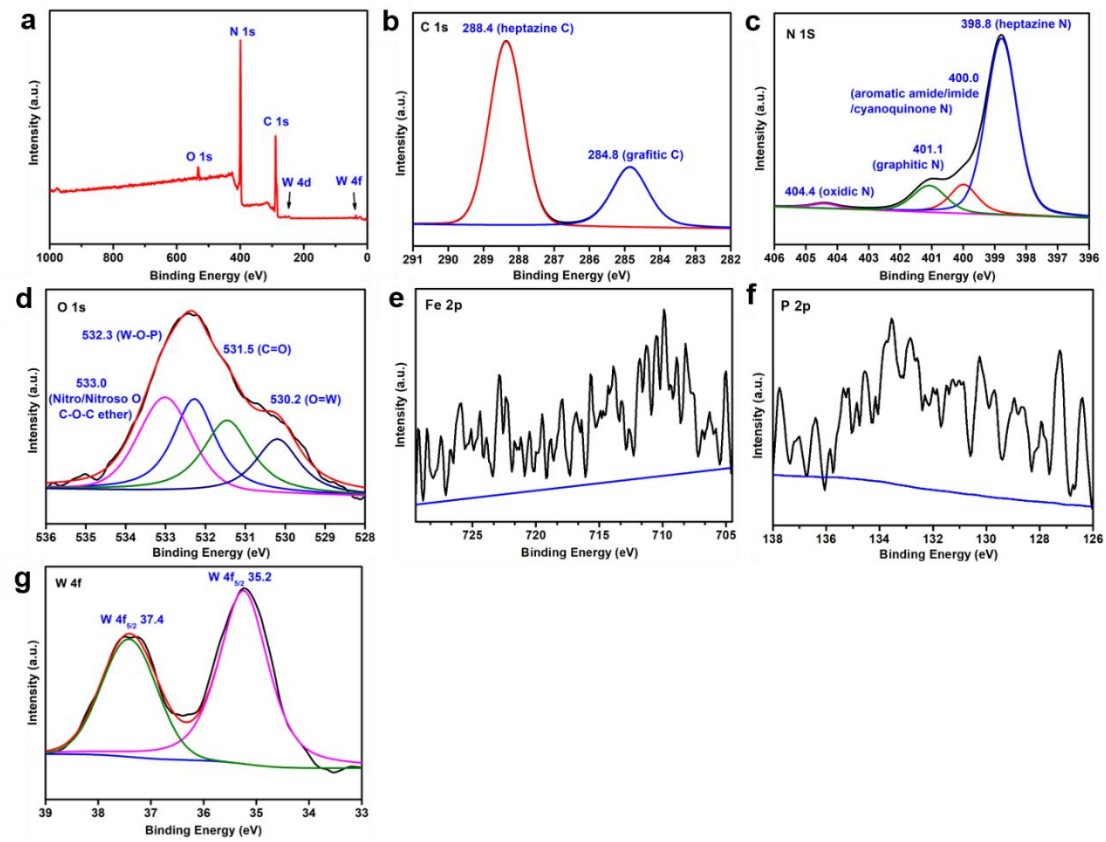

Fig. S9 Surface chemical structures of recovered FePW/g-C_3N_4. (a) XPS survey for FePW/g-C_3N_4. (b) High-resolution C1s spectrum. (c) N1s spectrum. (d) O1s spectrum. (e) Fe2p spectrum. (f) P2p spectrum. (g) High-resolution W4f spectrum.

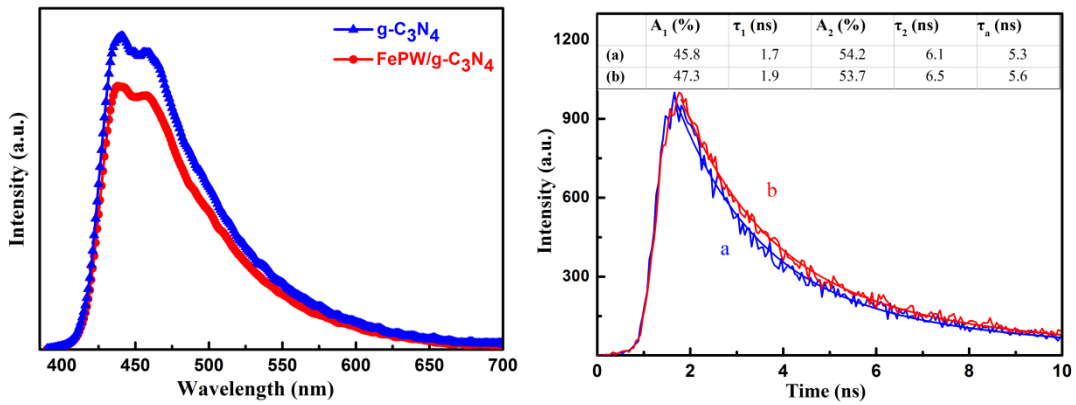

	A_1 (%)	τ_1 (ns)	A_2 (%)	τ_2 (ns)	τ_a (ns)
(a)	45.8	1.7	54.2	6.1	5.3
(b)	47.3	1.9	53.7	6.5	5.6

Fig. S10 Steady-state PL spectra, and time-resolved transient PL decay of (a) g-C_3N_4 and (b) FePW/g-C_3N_4.

Stability of the catalyst (FePW/g-C_3N_4)

After six cycles of the catalyst, we have obtained the catalyst from the simple centrifugation. The catalyst was washed with ethyl acetate, dichloromethane and ethanol, dried in air. The Fourier transform infrared (FT-IR) spectra of (a) "fresh" FePW/g-C_3N_4, and (b) "recovered" FePW/g-C_3N_4 showed that the {g-C_3N_4} was stable in this reaction system by the characteristic peaks appeared at 1636, 1570, 1468, 1402, 1318, 1241, 812 cm^{-1}.

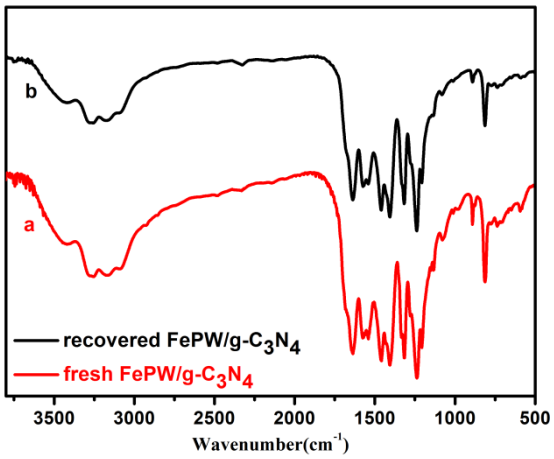

Fig. S11 IR spectra of (a) "fresh" FePW/g-C_3N_4 and (c) "recovered" FePW/g-C_3N_4.

The resources of light

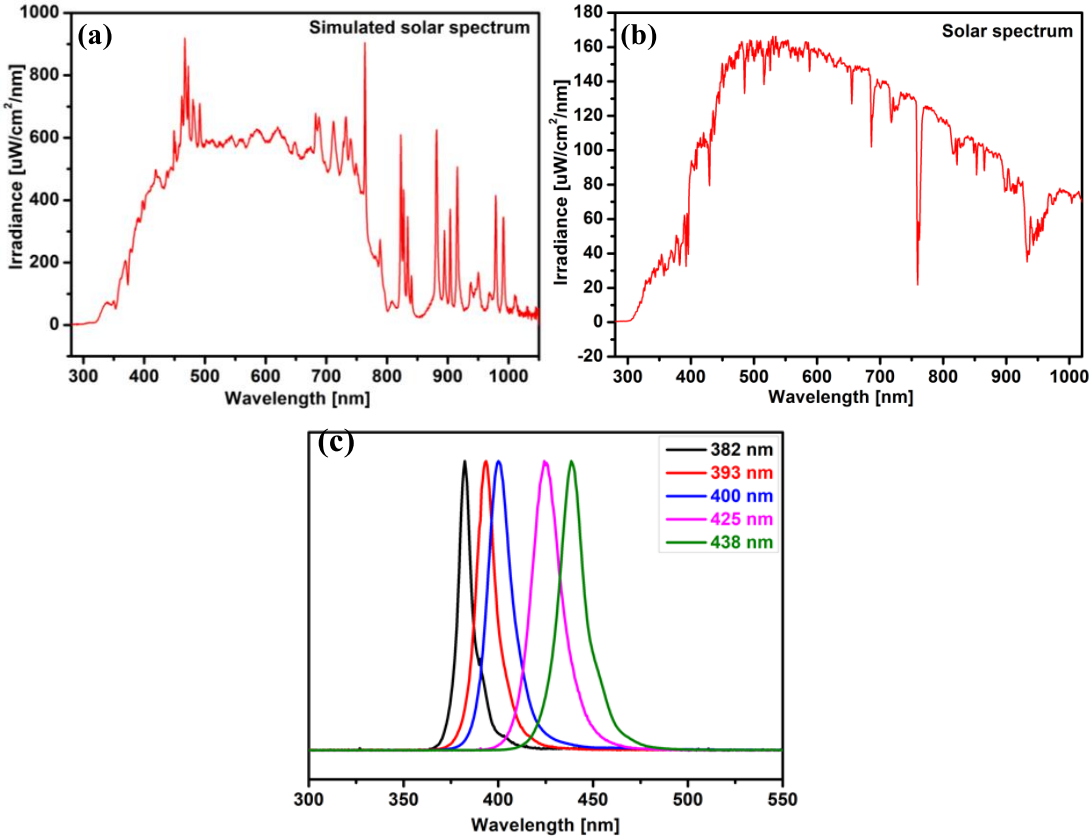

(**d**)

Fig. S12 The spectrum of (a) simulated solar spectrum, (b) solar spectrum, (c) light spectrum; (d) The picture of the reaction under the purple lamp (15 W, 425 nm, 13.4mW/cm^2).

Table S1 ICP-OES/MS for measuring the contents of Fe and P in FePW/g-C_3N_4. **A**: FePW/g-C_3N_4; **B**:PW/g-C_3N_4; **C**:Fe/g-C_3N_4; **D**: recovered FePW/g-C_3N_4.

Entry	Elements	Concentration in solids	Atomic ratio
A	**Fe**	0.68 wt%	
A	**P**	0.0098 wt%	Fe/P/W = 158.7/4.1/1
A	**W**	0.014 wt%	
B	**P**	0.076 wt%	P/W = 1/10.9
B	**W**	4.88 wt%	
C	**Fe**	1.8 wt%	
D	**Fe**	0.65 wt%	
D	**P**	0.0098 wt%	Fe/P/W = 141.6/3.8/1
D	**W**	0.015 wt%	

Optimization of reaction conditions: cyclohexane **1a** as the model substrate for the oxidation reaction. A 10 mL quartz vial was charged with cyclohexane **1a** (0.2 mmol), *tert*-butyl hydroperoxide (2.5 mmol, 2.5 equiv, 65 mg), FePW/g-C_3N_4 (2 mg), and MeCN (2.0 mL). The reaction was monitored by GC analysis using biphenyl as internal standard.

Cyclohexane (1a) standard curve equation:

y = 1.0608x – 0.0231 (R^2 = 0.9983)

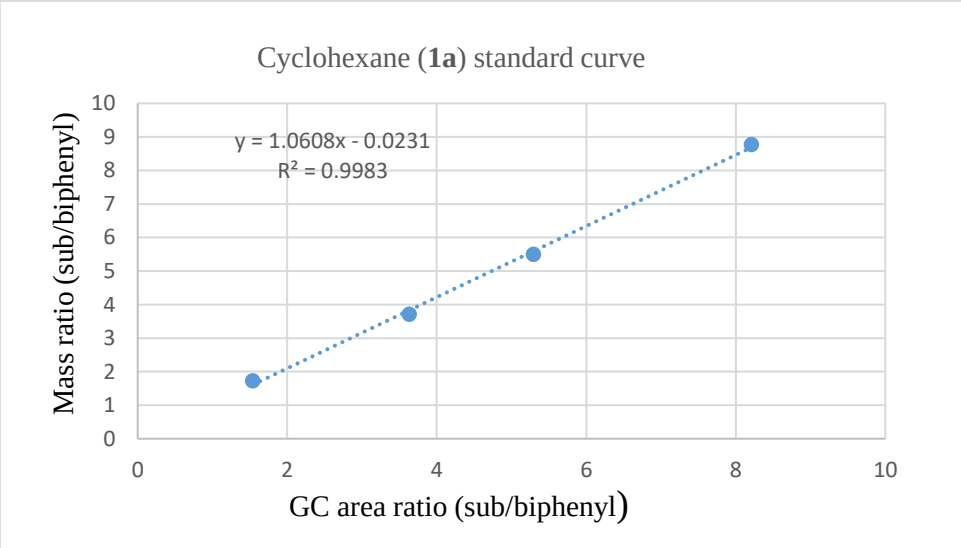

Cyclohexanone (2a) standard curve equation:

y = 1.2232x + 1.3982 (R^2 = 0.998)

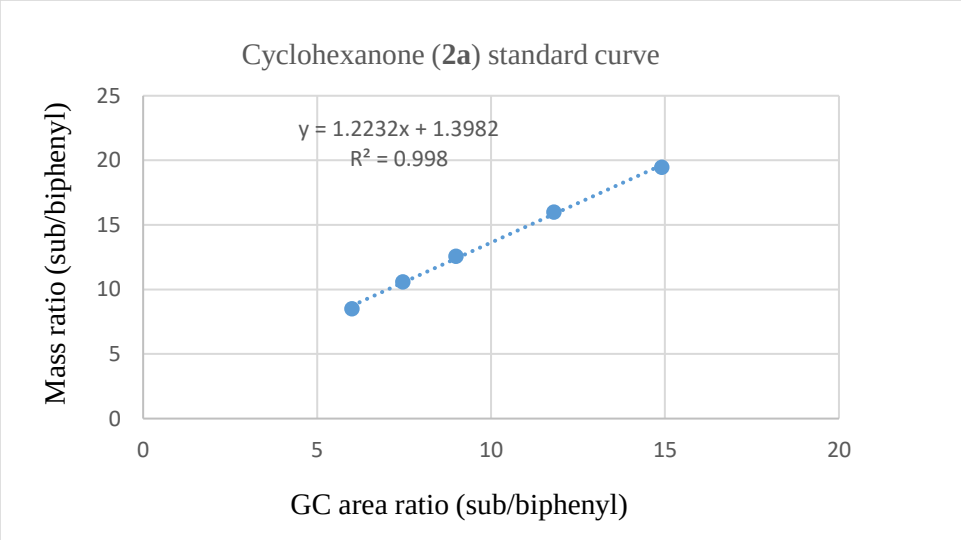

Table S2 Optimization of the reaction conditions.[a]

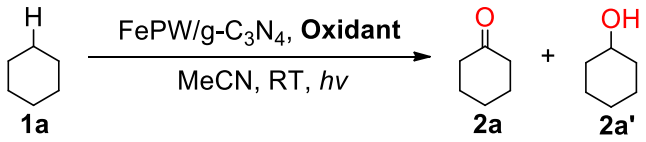

Entry	Oxidant	Con. (%)[b]	Sel. (%)[b]	
			2a	**2a'**
1	O_2 (Air)	0	0	0
2	O_2 (1 atm)	8	56	44
3	H_2O_2 (30%)	36	67	33
4	TBHP (70%)	86	99	1
5[c]	TBHP (70%)	71	99	1
6[d]	TBHP (70%)	87	99	1
7[e]	TBHP (70%)	86	99	1

[a]Reaction conditions: **1a** (0.2 mmol), Catalyst (2 mg), Oxidant (2.5 equiv.), in a solution of MeCN (2.0 mL) under the irradiation of light sunlight at room temperature for 40 h. [b]Corrected gas chromatography yield using biphenyl as an internal standard. [c]TBHP = ^{t}BuOOH (2.0 equiv.). [d]TBHP (3.0 equiv.). [e]TBHP (3.5 equiv.).

Control and trapping experiments

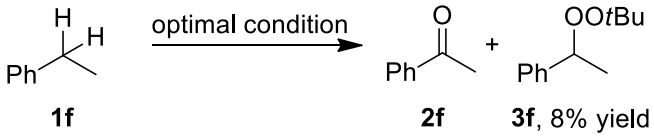

1f **2f** **3f**, 8% yield

(Fig. 1h, (1)) A 20 mL quartz vial was charged with ethylbenzene **1f** (1 mmol), *tert*-butyl hydroperoxide (2.5 mmol, 2.5 equiv, 321 mg), FePW/g-C_3N_4 (10 mg), and MeCN (10.0 mL). The vial was sealed with a polytetrafluoroethylene-lined cap, then the reaction was stirred under light irradiation with a 12-Inch fan at ambient temperature (25-35 ºC). Ater 5 h of the reaction, the reaction was quenched with a saturated NH_4Cl solution. Then the catalyst was filtered and washed with ethyl acetate, and the reaction was diluted with H_2O and ethyl acetate, the organic layer washed with H_2O, brine, dried over $MgSO_4$ and purified by silica gel chromatography using a mixture of hexanes and EtOAc (hexane:EtOAc = 20:1) to provide **2f** (Oil, 62 mg, 52%) and the radical adduct **3f**. (1-(*tert*-butylperoxy)ethyl)benzene **3f**: (Oil, 16 mg, 8% yield), R_f = 0.65 (hexane:EtOAc = 20:1); ^{1}H NMR (500 MHz, $CDCl_3$) δ 7.37–7.25 (m, 5H), 4.99 (q, J = 6.6 Hz, 1H), 1.48 (d, J = 6.6 Hz, 3H), 1.22 (s, 9H); ^{13}C NMR (126 MHz, $CDCl_3$) δ 142.2, 128.2, 127.7, 126.7, 81.6, 80.1, 26.5, 20.4.

^{1}H NMR and ^{13}C NMR Spectrum of **3f**

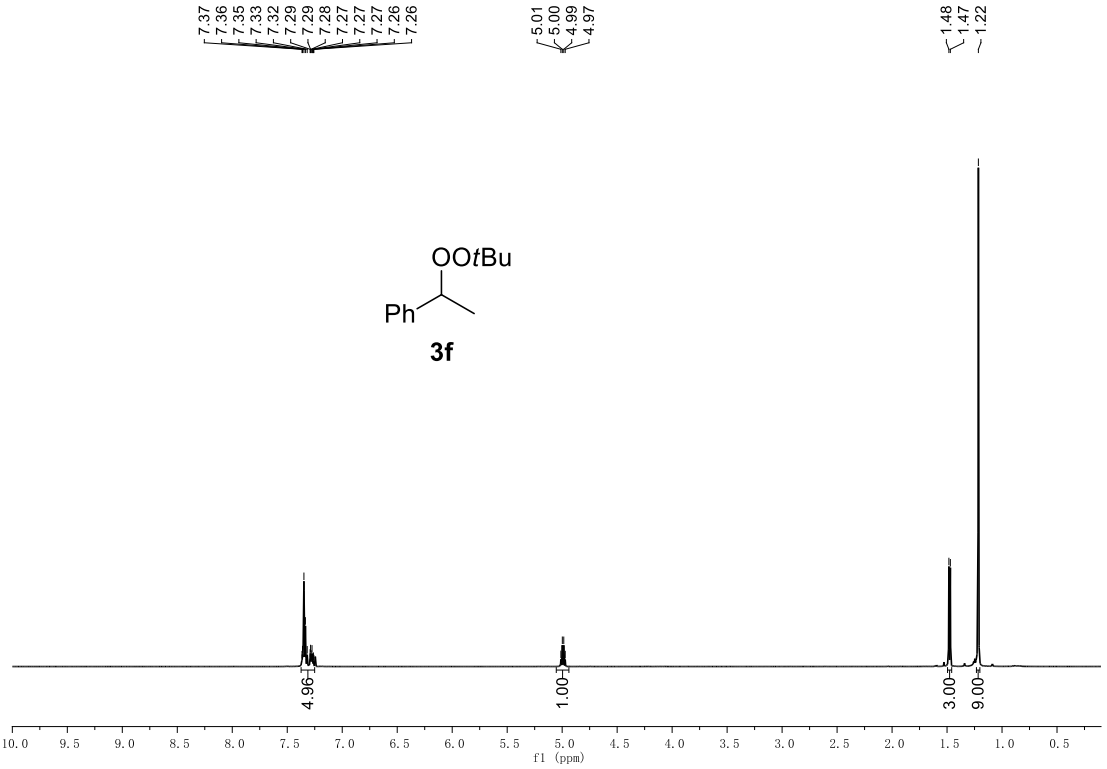

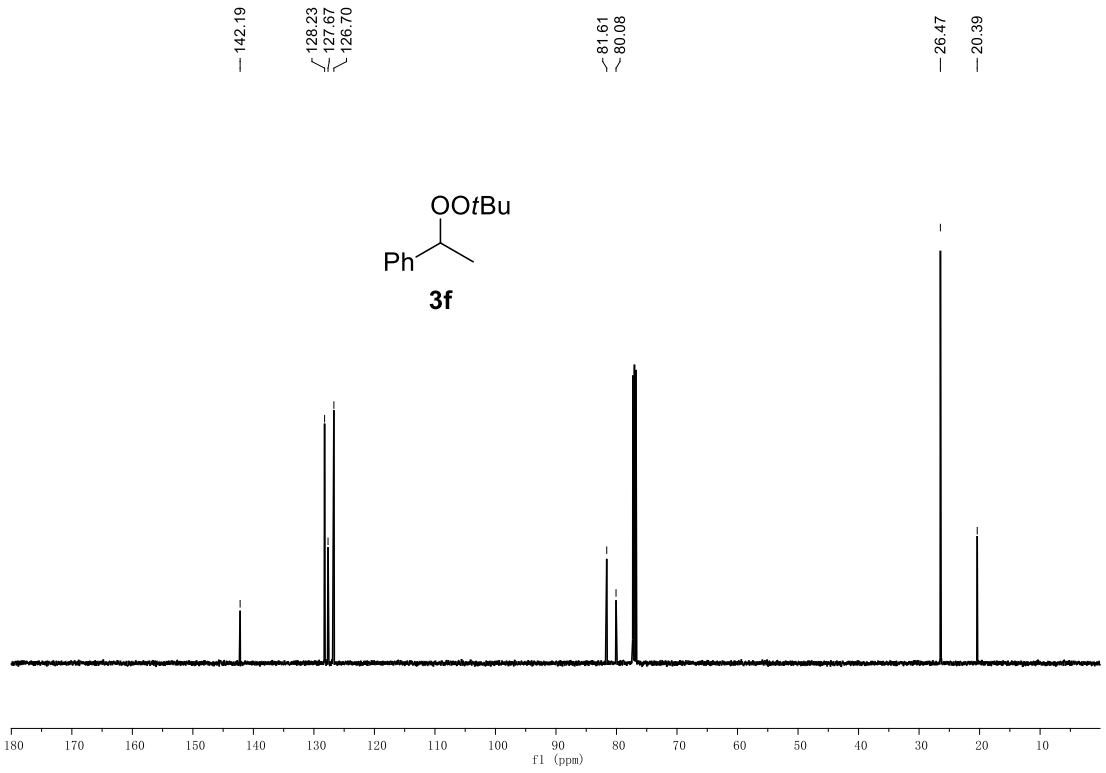

Control and trapping experiments

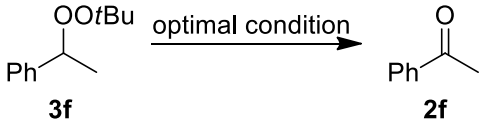

3f **2f**

A 10 mL quartz vial was charged with **3f** (0.2 mmol, 39 mg), *tert*-butyl hydroperoxide (2.5 mmol, 2.5 equiv, 64 mg), FePW/g-C_3N_4 (2 mg), and MeCN (2.0 mL). The vial was sealed with a polytetrafluoroethylene-lined cap, then the reaction was stirred under light irradiation (λ = 425 nm) with a 12-Inch fan at ambient temperature (25-35 ºC). Ater 15 h of the reaction, the reaction was quenched with a saturated NH_4Cl solution. Then the catalyst was filtered and washed with ethyl acetate, and the reaction was diluted with H_2O and ethyl acetate, the organic layer washed with H_2O, brine, dried over $MgSO_4$ and purified by silica gel chromatography using a mixture of hexanes and EtOAc (hexane:EtOAc = 20:1) to provide **2f** (Oil, 22 mg, 92%)

Control and trapping experiments

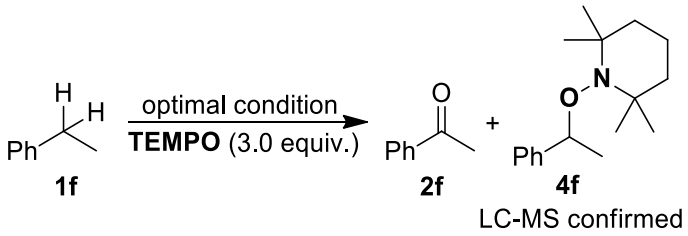

(Fig. 1h, (2)) A 20 mL quartz vial was charged with ethylbenzene **1f** (1 mmol), *tert*-butyl hydroperoxide (2.5 mmol, 2.5 equiv, 321 mg), FePW/g-C_3N_4 (10 mg), 2,2,6,6-tetramethylpiperidine-1-oxyl (TEMPO, 3.0 equiv.) and MeCN (10.0 mL). The vial was sealed with a polytetrafluoroethylene-lined cap, then the reaction was stirred under light irradiation (λ = 425 nm) with a 12-Inch fan at ambient temperature (25-35 ºC). Ater 15 h of the reaction, the reaction was quenched with a saturated NH_4Cl solution. Then the catalyst was filtered and washed with ethyl acetate, and the reaction was diluted with H_2O and ethyl acetate, the organic layer washed with H_2O, brine, dried over $MgSO_4$, **4f** was detected by LC-MS. LC-MS (ESI) *m/z*: Calcd for $C_{17}H_{27}NO$ $[M+H]^+$ 262.2165; found 262.2282.

LC-MS of the reaction **(Fig. 2, (3))**

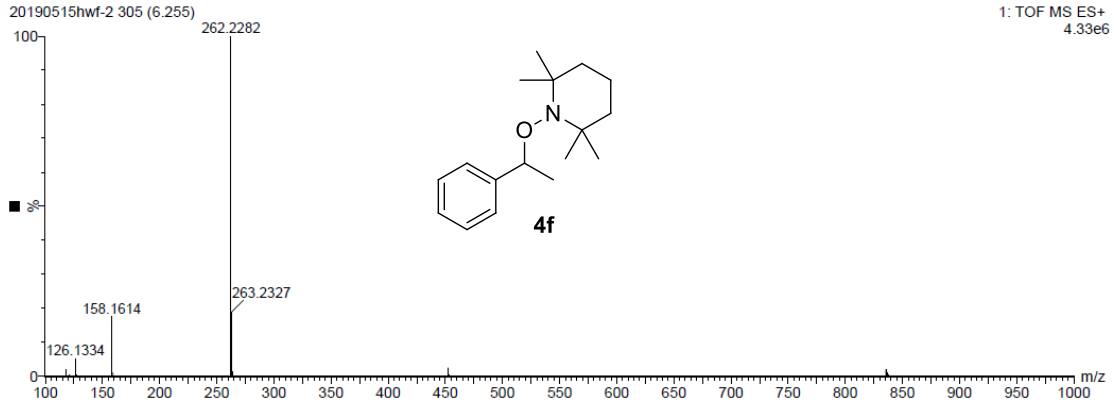

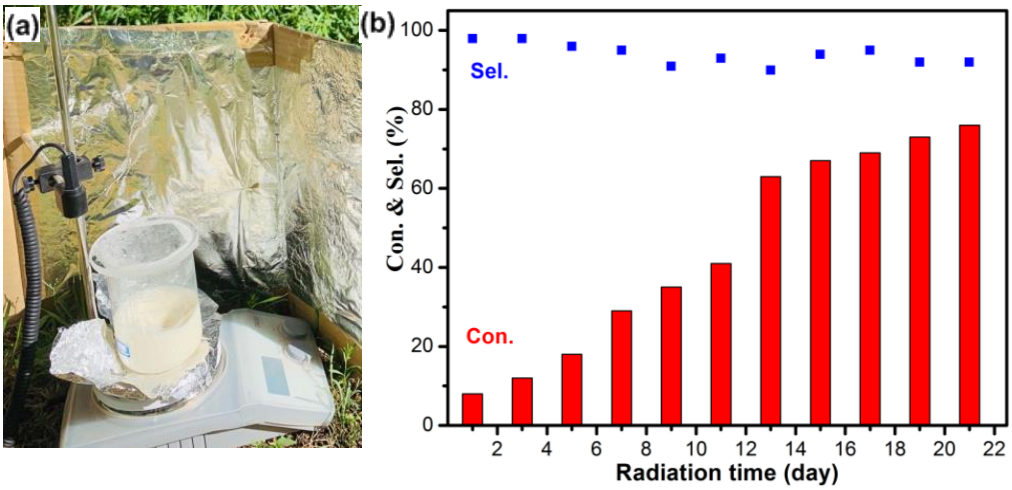

Fig. S13 Estimation of the scale-up effect (300 mL): A 500 mL quartz glass beaker was charged with ethylbenzene **1f** (10 g, 94 mmol), *tert*-butyl hydroperoxide (2.0 equiv, 24 g), FePW/g-C_3N_4 (500 mg), and MeCN (300 mL). The beaker with a quartz lid, then the reaction was stirred under sunlight irradiation. The reaction was performed under natural sunlight in Tongliao (5/6/2019-27/6/2019, 25-35 ºC, only the put the reaction outside on sunny days, otherwise leave it in dark) (9:00 Am-15:00 Pm with 6 hours per day). The averaged solar energy input was ~180 mW as the effective irradiation area was 160 cm^2 and the averaged unit solar power was ~1.125 mW/cm^2.

Table S3 Control and trapping experiments of alcohol oxidation.[a]

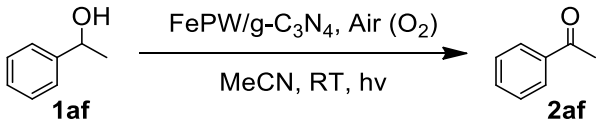

Entry	Variation	Yield (%)
1	In darkness	<5
2	Benzoquinone (1 equiv.)	20
3	$AgNO_3$ (1 equiv.)	16
4	*Tert*-butyl alcohol (1 equiv.)	96
5	Ammonium oxalate (1 equiv.)	68
6	NaN_3 (1 equiv.)	58
7 [b]	Catalase (20 mg)	95

[a]Reaction conditions: FePW/g-C_3N_4 (2 mg), MeCN (2 mL), under the light irradiation (λ = 425 nm). [b]Catalase (3500 units/mg).

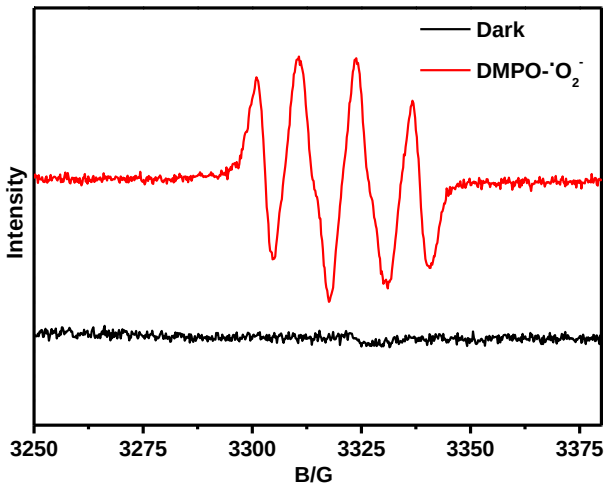

Fig. S14 EPR signals of the reaction solution in the dark (black line) and 425 nm LED light illumination (red line) in the presence of 5,5-dimethyl-1-pyrroline N-oxide (DMPO) as spin-trapping reagents under alcohol oxidation conditions.

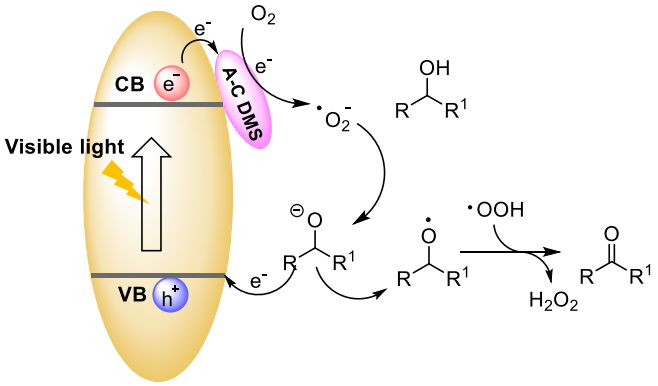

Fig. S15 Proposed mechanism of alcohol photo-oxidation.

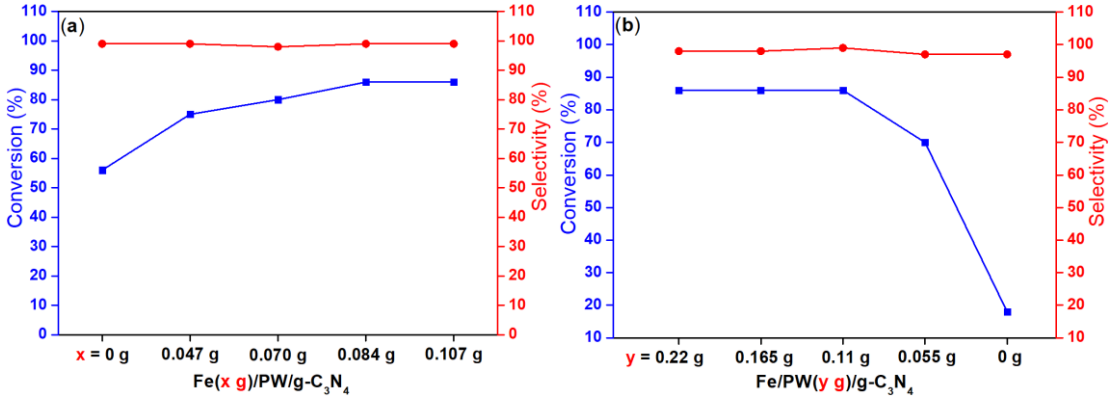

Fig. S16 The photocatalytic activity for conversion and selectivity with increasing amount of Fe^{3+} (a) and decreasing amount of $PW_{12}O_{40}^{3-}$ (b) for FePW/ g-C_3N_4.

Spectroscopic data of products

Table 2, entry 6

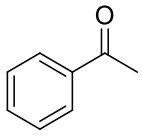

2f

Acetophenone (2f). Oil (119 mg, 99% yield); R_f = 0.48 (hexane:EtOAc = 20:1); ^{1}H NMR (500 MHz, $CDCl_3$) δ 7.97 (d, J = 7.2 Hz, 2H), 7.58 (t, J = 7.4 Hz, 1H), 7.48 (t, J = 7.7 Hz, 2H), 2.62 (s, 3H); ^{13}C NMR (125 MHz, $CDCl_3$) δ 198.3, 137.3, 133.2, 128.7, 128.4, 26.7.

(1) S. Li, B. Zhu, R. Lee, B. Qiao, Visible light-induced selective aerobic oxidative transposition of vinyl halides using a tetrahalogenoferrate(III) complex catalyst, Org. Chem. Front. 5 (2018) 380–385.

Table 2, entry 7

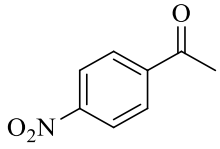

2g

1-(4-nitrophenyl)ethanone (2g). White soild (163 mg, 98% yield); mp: 77-78 °C; R_f = 0.40 (hexane:EtOAc = 15:1); ^{1}H NMR (500 MHz, $CDCl_3$) δ 8.29 (d, J = 8.7 Hz, 2H), 8.11 (d, J = 8.7 Hz, 2H), 2.68 (s, 3H); ^{13}C NMR (125 MHz, $CDCl_3$) δ 196.2, 150.2, 141.2, 129.1, 123.7, 26.8.

(1) J. Zhang, Z. Wang, Y. Wang, C. Wan, X. Zheng, Z. Wang, A metal-free catalytic system for the oxidation of benzylic methylenes and primary amines under solvent-free conditions, Green Chem. 11 (2009) 1973–1978.

Table 2, entry 8

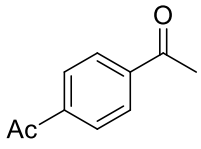

2h

1,1'-(1,4-phenylene)diethanone (2h). White soild (128 mg, 79% yield); mp: 114-115 °C; R_f = 0.30 (hexane:EtOAc = 10:1); ^{1}H NMR (500 MHz, $CDCl_3$) δ 8.0-7.99 (m, 4H), 2.61 (s, 6H); ^{13}C NMR (125 MHz, $CDCl_3$) δ 197.4, 140.1, 128.4, 26.8.

(1) J. Liu, K.-F. Hu, J.-P. Qu, Y.-B. Kang, Organopromoted Selectivity-Switchable Synthesis of Polyketones, Org. Lett., 19 (2017), 5593−5596.

Table 2, entry 9

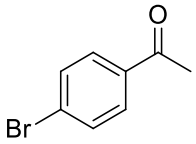

2i

1-(4-bromophenyl)ethanone (2i). White soild (185 mg, 93% yield); mp: 49-50 °C; R_f = 0.4 (hexane:EtOAc = 20:1); ^{1}H NMR (500 MHz, $CDCl_3$) δ 7.80 (d, J = 8.5 Hz, 2H), 7.59 (d, J = 8.5 Hz, 2H), 2.57 (s, 3H); ^{13}C NMR (125 MHz, $CDCl_3$) δ 197.1, 135.9, 131.9, 129.9, 128.4, 26.6.

(1) S. Li, B. Zhu, R. Lee, B. Qiao, Visible light-induced selective aerobic oxidative transposition of vinyl halides using a tetrahalogenoferrate(III) complex catalyst, Org. Chem. Front. 5 (2018) 380–385.

Table 2, entry 10

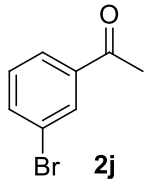

2j

1-(3-bromophenyl)ethanone (2j). Oil (159 mg, 80% yield); R_f = 0.47 (hexane:EtOAc = 20:1); ^{1}H NMR (500 MHz, $CDCl_3$) δ 8.06 (s, 1H), 7.85 (d, *J* = 7.7 Hz, 1H), 7.66 (d, *J* = 7.9 Hz, 1H), 7.33 (t, *J* = 7.8 Hz, 1H), 2.58 (s, 3H); ^{13}C NMR (125 MHz, $CDCl_3$) δ 196.7, 138.8, 136.0, 131.4, 130.3, 126.9, 123.0, 26.7.

(1) S. Li, B. Zhu, R. Lee, B. Qiao, Visible light-induced selective aerobic oxidative transposition of vinyl halides using a tetrahalogenoferrate(III) complex catalyst, Org. Chem. Front. 5 (2018) 380–385.

Table 2, entry 11

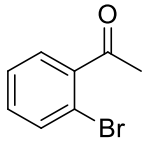

2k

1-(2-bromophenyl)ethanone (2k). Oil (149 mg, 75% yield); R_f = 0.5 (hexane:EtOAc = 20:1); ^{1}H NMR (500 MHz, $CDCl_3$) δ 7.59 (d, *J* = 7.9 Hz, 1H), 7.44 (d, *J* = 9.3 Hz,

1H), 7.35 (t, *J* = 7.5 Hz, 1H), 7.26 (t, *J* = 6.8 Hz, 1H), 2.61 (s, 3H); ^{13}C NMR (125 MHz, $CDCl_3$) δ 201.3, 141.4, 133.8, 131.7, 128.8, 127.4, 118.8, 30.3.

(1) S. Li, B. Zhu, R. Lee, B. Qiao, Visible light-induced selective aerobic oxidative transposition of vinyl halides using a tetrahalogenoferrate(III) complex catalyst, Org. Chem. Front. 5 (2018) 380–385.

Table 2, entry 12

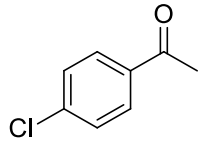

2l

1-(4-chlorophenyl)ethanone (2l). Oil (140 mg, 91% yield); R_f = 0.49 (hexane:EtOAc = 20:1); ^{1}H NMR (500 MHz, $CDCl_3$) δ 7.90 (*d*, *J* = 8.6 Hz, 2H), 7.44 (*d*, *J* = 8.6 Hz, 2H), 2.59 (s, 3H); ^{13}C NMR (125MHz, $CDCl_3$) δ 196.8, 139.5, 135.4, 129.7, 128.9, 26.5.

(1) S. Li, B. Zhu, R. Lee, B. Qiao, Visible light-induced selective aerobic oxidative transposition of vinyl halides using a tetrahalogenoferrate(III) complex catalyst, Org. Chem. Front. 5 (2018) 380–385.

Table 2, entry 13

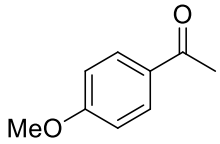

2m

1-(4-methoxyphenyl)ethanone (2m). Oil (126 mg, 85% yield); R_f = 0.30 (hexane:EtOAc = 20:1); ^{1}H NMR (500 MHz, $CDCl_3$) δ 7.96 (d, *J* = 8.7 Hz, 2H), 6.95 (d, *J* = 8.7 Hz, 2H), 3.89 (s, 3H), 2.58 (s, 3H); ^{13}C NMR (125 MHz, $CDCl_3$) δ 196.8, 163.5, 130.6, 130.3, 113.7, 55.5, 26.4.

(1) H. Peng, A. Lin, Y. Zhang, H. Jiang, J. Zhou, Y. Cheng, C. Zhu, H. Hu, Oxidation and amination of benzylic sp^3 C-H bond catalyzed by rhenium(V) complexes, ACS Catal. 2 (2012) 163−167.

Table 2, entry 14

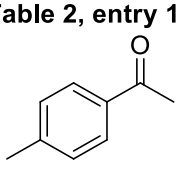

2n

1-(*p*-tolyl)ethanone (2n). Oil (107 mg, 80% yield); R_f = 0.5 (hexane:EtOAc = 20:1); ^{1}H NMR (500 MHz, $CDCl_3$) δ 7.87 (d, J = 8.1 Hz, 2H), 7.25 (d, J = 8.0 Hz, 2H), 2.59 (s, 3H), 2.42 (s, 3H); ^{13}C NMR (125 MHz, $CDCl_3$) δ 197.9, 143.9, 134.7, 129.3, 128.5, 26.6, 21.7.

(1) H. Peng, A. Lin, Y. Zhang, H. Jiang, J. Zhou, Y. Cheng, C. Zhu, H. Hu, Oxidation and amination of benzylic sp^3 C-H bond catalyzed by rhenium(V) complexes, ACS Catal. 2 (2012) 163−167.

Table 2, entry 15

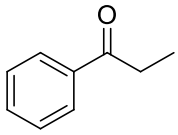

2o

propiophenone (2o). Oil (82 mg, 61% yield); R_f = 0.67 (hexane:EtOAc = 20:1); ^{1}H NMR (500 MHz, $CDCl_3$) δ 7.96 (d, J = 7.2 Hz, 2H), 7.54 (t, J = 7.4 Hz, 1H), 7.45 (t, J = 7.6 Hz, 2H), 3.00 (q, J = 7.2 Hz, 2H), 1.22 (t, J = 7.2 Hz, 3H); ^{13}C NMR (125 MHz, $CDCl_3$) δ 200.8, 136.9, 132.8, 128.5, 127.9, 31.7, 8.2.

(1) H. Peng, A. Lin, Y. Zhang, H. Jiang, J. Zhou, Y. Cheng, C. Zhu, H. Hu, Oxidation and amination of benzylic sp^3 C-H bond catalyzed by rhenium(V) complexes, ACS Catal. 2 (2012) 163−167.

Table 2, entry 16

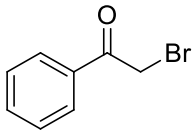

2p

2-bromo-1-phenylethanone (2p). White soild (99 mg, 50% yield); mp: 42-43 °C; R_f = 0.43 (hexane:EtOAc = 20:1); ^{1}H NMR (500 MHz, $CDCl_3$) δ 8.01 (d, J = 8.4 Hz, 2H), 7.64 (t, J = 7.4 Hz, 1H), 7.52 (t, J = 7.8 Hz, 2H), 4.49 (s, 2H); ^{13}C NMR (125 MHz, $CDCl_3$) δ 191.3, 134.0, 129.0, 128.9, 30.9.

(1) S. Li, B. Zhu, R. Lee, B. Qiao, Visible light-induced selective aerobic oxidative transposition of vinyl halides using a tetrahalogenoferrate(III) complex catalyst, Org. Chem. Front. 5 (2018) 380–385.

Table 2, entry 17

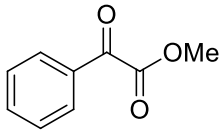

2q

methyl 2-oxo-2-phenylacetate (2q). Oil (157 mg, 96% yield); R_f = 0.45 (hexane:EtOAc = 20:1); ^{1}H NMR (500 MHz, $CDCl_3$) δ 8.03 (d, J = 7.2 Hz, 2H), 7.68 (t, J = 7.4 Hz, 1H), 7.53 (t, J = 7.9 Hz, 2H), 4.0 (s, 3H); ^{13}C NMR (125 MHz, $CDCl_3$) δ 186.1, 164.0, 135.0, 132.4, 130.1, 128.9, 52.8.

(1) A. Stergiou, A. Bariotaki, D. Kalaitzakis, I. Smonou, Oxone-mediated oxidative cleavage of β-keto esters and 1,3-diketones to α-keto esters and 1,2-diketones in aqueous medium, J. Org. Chem. 78 (2013) 7268–7273.

Table 2, entry 18

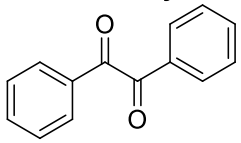

2r

benzil (2r). Oil (178 mg, 85% yield); R_f = 0.45 (hexane:EtOAc = 20:1); ^{1}H NMR (500 MHz, $CDCl_3$) δ 7.98 (d, J = 7.2 Hz, 4H), 7.66 (t, J = 7.4 Hz, 2H), 7.52 (t, J = 7.9 Hz, 4H); ^{13}C NMR (125 MHz, $CDCl_3$) δ 194.6, 134.9, 133.0, 129.9, 129.1.

(1) G. Urgoitia, R. SanMartin, M. T. Herrero, E. Domínguez, Palladium NCN and CNC pincer complexes as exceptionally active catalysts for aerobic oxidation in sustainable media, Green Chem. 13 (2011) 2161–2166.

Table 2, entry 19

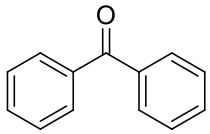

2s

benzophenone (2s). Oil (160 mg, 88% yield); R_f = 0.46 (hexane:EtOAc = 15:1); ^{1}H NMR (500 MHz, $CDCl_3$) δ 7.81 (d, J = 7.1 Hz, 4H), 7.60 (t, J = 7.4 Hz, 2H), 7.49 (t, J = 7.7 Hz, 4H); ^{13}C NMR (125 MHz, $CDCl_3$) δ 196.8, 137.7, 132.5, 130.1, 128.4.

(1) S. Li, B. Zhu, R. Lee, B. Qiao, Visible light-induced selective aerobic oxidative transposition of vinyl halides using a tetrahalogenoferrate(III) complex catalyst, Org. Chem. Front. 5 (2018) 380–385.

Table 2, entry 20

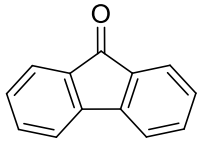

2t

9*H*-fluoren-9-one (2t). Yellow soild (165 mg, 92% yield); mp: 81-82 °C; R_f = 0.56 (hexane:EtOAc = 20:1); ^{1}H NMR (500 MHz, $CDCl_3$) δ 7.63 (d, J = 8.0 Hz, 2H), 7.48-7.44 (m, 4H), 7.28-7.25 (m, 2H); ^{13}C NMR (125 MHz, $CDCl_3$) δ 193.9, 144.4, 134.7, 129.1, 124.3, 120.3.

(1) H. Peng, A. Lin, Y. Zhang, H. Jiang, J. Zhou, Y. Cheng, C. Zhu, H. Hu, Oxidation and amination of benzylic sp^3 C-H bond catalyzed by rhenium(V) complexes, ACS Catal. 2 (2012) 163−167.

Table 2, entry 21

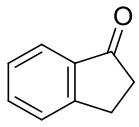

2u

2,3-dihydro-1H-inden-1-one (2u). Oil (112 mg, 85% yield); R_f = 0.47 (hexane:EtOAc = 20:1); ^{1}H NMR (500 MHz, $CDCl_3$) δ 7.75 (d, J = 7.5 Hz, 1H), 7.58 (t, J = 7.4 Hz, 1H), 7.47 (d, J = 7.2 Hz, 1H), 7.35 (t, J = 7.3 Hz, 1H), 3.15-3.13 (m, 2H), 2.69-2.67 (m, 2H); ^{13}C NMR (125 MHz, $CDCl_3$) δ 207.0, 155.1, 137.0, 134.5, 127.2, 126.6, 123.6, 36.1, 25.7.

(1) H. Peng, A. Lin, Y. Zhang, H. Jiang, J. Zhou, Y. Cheng, C. Zhu, H. Hu, Oxidation and amination of benzylic sp^3 C-H bond catalyzed by rhenium(V) complexes, ACS Catal. 2 (2012) 163−167.

Table 2, entry 22

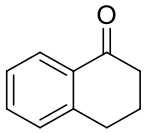

2v

3,4-dihydronaphthalen-1(2*H*)-one (2v). Yellow Oil (112 mg, 77% yield); R_f = 0.45 (hexane:EtOAc = 20:1); ^{1}H NMR (500 MHz, $CDCl_3$) δ 8.03 (d, J = 7.9 Hz, 1H), 7.57 (t, J = 7.5 Hz, 1H), 7.36 (t, J = 7.5 Hz, 1H), 7.35 (d, J = 7.9 Hz, 1H), 2.99 (t, J = 6.0 Hz, 2H), 2.70-2.62 (m, 2H), 2.17-2.10 (m, 2H); ^{13}C NMR (125 MHz, $CDCl_3$) δ 198.4,

144.5, 133.4, 132.6, 128.8, 127.2, 126.6, 39.1, 29.7, 23.3.

(1) G. Urgoitia, R. SanMartin, M. T. Herrero, E. Domínguez, Palladium NCN and CNC pincer complexes as exceptionally active catalysts for aerobic oxidation in sustainable media, Green Chem. 13 (2011) 2161–2166.

Table 2, entry 23

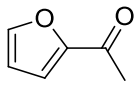

2w

1-(furan-2-yl)ethanone (2w). Oil (71 mg, 65% yield); R_f = 0.35 (hexane:EtOAc = 20:1); ^{1}H NMR (500 MHz, $CDCl_3$) δ 7.56 (s, 1H), 7.16 (d, J = 3.5 Hz, 1H), 6.51 (d, J = 3.2 Hz, 1H), 2.45 (s, 3H); ^{13}C NMR (125 MHz, $CDCl_3$) δ 186.8, 152.8, 146.4, 117.3, 112.2, 26.0.

(1) Y. Liu, A. Xie, J. Li, X. Xu, W. Dong, B. Wang, Heterocycle-substituted tetrazole ligands for copper-catalysed aerobic oxidation of alcohols, Tetrahedron, 70 (2014) 9791−9796.

Table 2, entry 24

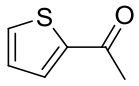

2x

1-(thiophen-2-yl)ethanone (2x). Oil (79 mg, 63% yield); R_f = 0.5 (hexane:EtOAc = 15:1); ^{1}H NMR (500 MHz, $CDCl_3$) δ 7.69 (s, 1H), 7.63-7.62 (m, 1H), 7.13-7.12 (m, 1H), 2.54 (s, 3H); ^{13}C NMR (125 MHz, $CDCl_3$) δ 190.8, 144.6, 133.8, 132.5, 128.2, 26.9.

(1) Y. Liu, A. Xie, J. Li, X. Xu, W. Dong, B. Wang, Heterocycle-substituted tetrazole ligands for copper-catalysed aerobic oxidation of alcohols, Tetrahedron, 70 (2014) 9791−9796.

Table 2, entry 25

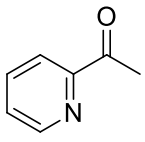

2y

1-(pyridin-2-yl)ethanone (2y). Oil (72 mg, 60% yield); R_f = 0.35 (hexane:EtOAc = 10:1); ^{1}H NMR (500 MHz, $CDCl_3$) δ 8.66 (d, J = 4.7 Hz, 1H), 8.01 (d, J = 7.9 Hz, 1H),

7.81 (t, J = 7.7 Hz, 1H), 7.46-4.43 (m, 1H), 2.70 (s, 3H); ^{13}C NMR (125 MHz, $CDCl_3$) δ 200.1, 153.5, 148.9, 136.8, 127.1, 121.6, 25.8.

(1) G. Urgoitia, R. SanMartin, M. T. Herrero, E. Domínguez, Palladium NCN and CNC pincer complexes as exceptionally active catalysts for aerobic oxidation in sustainable media, Green Chem. 13 (2011) 2161–2166.

Table 2, entry 33

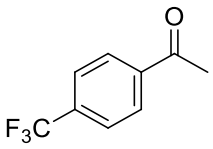

2ag

4-(Trifluoromethyl) acetophenone (2ag). Oil (178 mg, 95% yield); R_f = 0.5 (hexane: EtOAc = 10:1); ^{1}H NMR (500 MHz, $CDCl_3$) δ 8.08 (d, J = 8.1 Hz, 2H), 7.75 (d, J = 8.2 Hz, 2H), 2.67 (s, 3H); ^{13}C NMR (125 MHz, $CDCl_3$) δ 197.0, 139.7, 134.5 (q, $^2J_{FC}$ = 32.5 Hz), 128.6, 125.7 (q, $^3J_{FC}$ = 3.75 Hz), 124.0 (q, $^1J_{FC}$ = 235 Hz), 26.8.

(1) F. Li, N. Wang, L. Lu, G. Zhu, Regioselective hydration of terminal alkynes catalyzed by a neutral gold(I) complex [(IPr)AuCl] and one-pot synthesis of optically active secondary alcohols from terminal alkynes by the combination of [(IPr)AuCl] and Cp*RhCl[(R,R)-TsDPEN], J. Org. Chem. 80 (2015) 3538−3546.

Table 2, entry 34

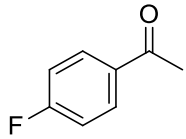

2ah

1-(4-Fluoropheny)ethanone (2ah). Oil (122 mg, 89% yield); R_f = 0.5 (hexane: EtOAc = 10:1); ^{1}H NMR (500 MHz, $CDCl_3$) δ 8.01 (dd, J = 7.4, 5.4 Hz, 2H), 7.16 (t, J = 8.0 Hz, 2H), 2.61 (s, 3H); ^{13}C NMR (125 MHz, $CDCl_3$) δ 196.4, 165.7 (d, J_{C-F} = 254.6 Hz), 133.5 (d, J_{C-F} = 2.9 Hz), 130.9 (d, J_{C-F} = 9.3 Hz), 115.6 (d, J_{C-F} = 21.9 Hz), 26.5.

(1) F. Li, N. Wang, L. Lu, G. Zhu, Regioselective hydration of terminal alkynes catalyzed by a neutral gold(I) complex [(IPr)AuCl] and one-pot synthesis of optically active secondary alcohols from terminal alkynes by the combination of [(IPr)AuCl] and Cp*RhCl[(R,R)-TsDPEN], J. Org. Chem. 80 (2015) 3538−3546.

Table 2, entry 37

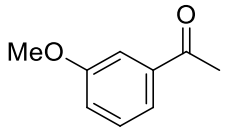

2ak

1,1'-(1,3-phenylene)diethanone (2ak). Oil (132 mg, 88% yield); R_f = 0.33 (hexane: EtOAc = 20:1); ^{1}H NMR (500 MHz, $CDCl_3$) δ 7.57–7.55 (m, 1H), 7.51 (dd, J = 2.5, 1.6 Hz, 1H), 7.39 (t, J = 7.9 Hz, 1H), 7.14 (ddd, J = 8.2, 2.7, 0.8 Hz, 1H), 3.88 (s, 3H), 2.62 (s, 3H); ^{13}C NMR (125 MHz, $CDCl_3$) δ 197.7, 159.5, 138.2, 129.3, 120.9, 119.4, 112.1, 55.2, 26.4.

(1) G. Zhang, S. K. Hanson, Cobalt-catalyzed acceptorless alcohol dehydrogenation: synthesis of imines from alcohols and amines, Org. Lett. 15 (2013) 650−653.

Table 2, entry 38

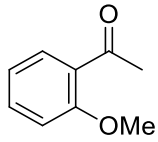

2al

1,1'-(1,2-phenylene)diethanone (2al). Oil (127 mg, 85% yield); R_f = 0.33 (hexane: EtOAc = 20:1); ^{1}H NMR (500 MHz, $CDCl_3$) δ 7.76 (dd, J = 7.7, 1.8 Hz, 1H), 7.49 (ddd, J = 8.5, 7.4, 1.8 Hz, 1H), 7.02 (t, J = 7.6 Hz, 1H), 6.99 (d, J = 8.4 Hz, 1H), 3.94 (s, 3H), 2.64 (s, 3H); ^{13}C NMR (125 MHz, $CDCl_3$) δ 199.6, 158.6, 133.4, 130.1, 120.3, 111.3, 55.2, 31.5.

(1) G. Urgoitia, R. SanMartin, M. T. Herrero, E. Domínguez, Palladium NCN and CNC pincer complexes as exceptionally active catalysts for aerobic oxidation in sustainable media, Green Chem. 13 (2011) 2161–2166.

Table 2, entry 45

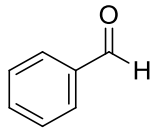

2as

Benzaldehyde (2as). Oil (101 mg, 96% yield); R_f = 0.35 (hexane: EtOAc = 20:1); ^{1}H NMR (500 MHz, $CDCl_3$) δ 10.05 (s, 1H), 7.91 (d, J = 7.0 Hz, 2H), 7.66 (t, J = 7.4 Hz, 1H), 7.56 (t, J = 7.6 Hz, 2H); ^{13}C NMR (125 MHz, $CDCl_3$) δ 192.5, 136.4, 134.5, 130.2, 129.8, 129.0, 128.5.

(1) S. Verma, R. B. N. Baig, M. N. Nadagouda, R. S. Varma, Photocatalytic C-H activation of hydrocarbons over VO@g-C_3N_4, ACS Sustainable Chem. Eng. 4

(2016) 2333−2336.

Table 2, entry 46

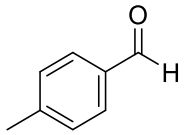

2at

4-methylbenzaldehyde (2at). Oil (109 mg, 91%); R_f = 0.55 (hexane:EtOAc = 10:1); ^{1}H NMR (500 MHz, $CDCl_3$) δ 9.94 (s, 1H), 7.75 (d, J = 8.1 Hz, 2H), 7.30 (d, J = 8.1 Hz, 2H), 2.41 (s, 3H); ^{13}C NMR (126 MHz, $CDCl_3$) δ 191.9, 145.5, 134.1, 129.8, 129.7, 21.8.

(1) X.-J. Yang, Y.-W. Zheng, L.-Q. Zheng, L.-Z. Wu, C.-H. Tung, B. Chen, Visible light-catalytic dehydrogenation of benzylic alcohols to carbonyl compounds by using an eosin Y and nickel-thiolate complex dual catalyst system, Green Chem. 21 (2019) 1401–1405.

Table 2, entry 47

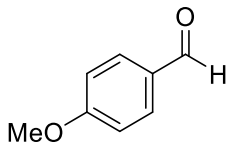

2au

4-methoxybenzaldehyde (2au). Oil (133 mg, 98%); R_f = 0.55 (hexane:EtOAc = 10:1); ^{1}H NMR (500 MHz, $CDCl_3$) δ 9.88 (s, 1H), 7.84 (d, J = 8.6 Hz, 2H), 7.00 (d, J = 8.7 Hz, 2H), 3.89 (s, 3H); ^{13}C NMR (126 MHz, $CDCl_3$) δ 190.8, 164.6, 131.9, 129.9, 114.3, 55.5.

(1) X.-J. Yang, Y.-W. Zheng, L.-Q. Zheng, L.-Z. Wu, C.-H. Tung, B. Chen, Visible light-catalytic dehydrogenation of benzylic alcohols to carbonyl compounds by using an eosin Y and nickel-thiolate complex dual catalyst system, Green Chem. 21 (2019) 1401–1405.

Table 2, entry 48

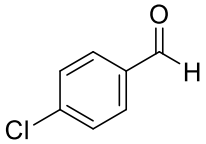

2av

4-chlorobenzaldehyde (2av). Oil (126 mg, 90%); R_f = 0.56 (hexane:EtOAc = 10:1); ^{1}H NMR (500 MHz, $CDCl_3$) δ 9.98 (s, 1H), 7.82 (d, J = 7.6 Hz, 2H), 7.51 (d, J = 7.9 Hz, 2H); ^{13}C NMR (126 MHz, $CDCl_3$) δ 190.8, 140.9, 134.7, 130.9, 129.4.

(1) X.-J. Yang, Y.-W. Zheng, L.-Q. Zheng, L.-Z. Wu, C.-H. Tung, B. Chen, Visible light-catalytic dehydrogenation of benzylic alcohols to carbonyl compounds by using an eosin Y and nickel-thiolate complex dual catalyst system, Green Chem. 21 (2019) 1401–1405.

Table 2, entry 49

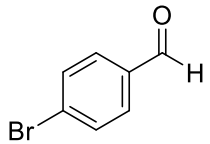

2aw

4-bromobenzaldehyde (2aw). White solid (164 mg, 89%); mp: 58-59 ℃; R_f = 0.55 (hexane:EtOAc = 10:1); ^{1}H NMR (500 MHz, $CDCl_3$) δ 9.99 (s, 1H), 7.76 (d, J = 8.3 Hz, 2H), 7.69 (d, J = 8.4 Hz, 2H); ^{13}C NMR (126 MHz, $CDCl_3$) δ 191.1, 135.0, 132.4, 130.9, 129.8.

(1) Z. Wei, S. Ru, Q. Zhao, H. Yu, G. Zhang, Y. Wei, Highly efficient and practical aerobic oxidation of alcohols by inorganic-ligand supported copper catalysis, Green Chem. 21 (2019) 4069–4075.

Table 2, entry 50

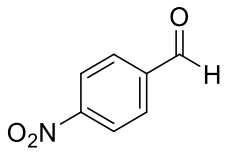

2ax

4-nitrobenzaldehyde (2ax). yellow solid (128 mg, 85%); mp: 105-106 ℃; R_f = 0.43 (hexane:EtOAc = 10:1); ^{1}H NMR (500 MHz, $CDCl_3$) δ 10.17 (s, 1H), 8.40 (dd, J = 8.5, 1.3 Hz, 2H), 8.09 (dd, J = 8.6, 1.5 Hz, 2H); ^{13}C NMR (126 MHz, $CDCl_3$) δ 190.3, 151.1, 140.0, 130.5, 124.3.

(1) Z. Wei, S. Ru, Q. Zhao, H. Yu, G. Zhang, Y. Wei, Highly efficient and practical aerobic oxidation of alcohols by inorganic-ligand supported copper catalysis, Green Chem. 21 (2019) 4069–4075.

Table 2, entry 51

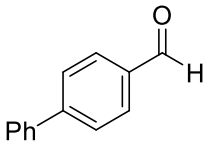

2ay

[1,1'-biphenyl]-4-carbaldehyde (2ay). White solid (138 mg, 76%); mp: 57-59 ℃; R_f = 0.53 (hexane:EtOAc = 10:1); ^{1}H NMR (500 MHz, $CDCl_3$) δ 10.08 (s, 1H), 7.97 (d, J = 8.3 Hz, 2H), 7.77 (d, J = 8.2 Hz, 2H), 7.70–7.64 (m, 2H), 7.51 (dd, J = 10.3, 4.7 Hz,

2H), 7.45 (dd, J = 8.4, 6.3 Hz, 1H). ^{13}C NMR (126 MHz, $CDCl_3$) δ 191.9, 147.2, 139.7, 135.2, 130.3, 129.0, 128.5, 127.7, 127.4.

(1) S. Lan, X. Yang, K. Shi, R. Fan, D. Ma, Pillarquinone-based porous polymer for a highly-efficient heterogeneous organometallic catalysis, ChemCatChem 11 (2019) 2864–2869.

Table 2, entry 52

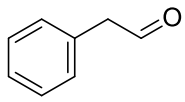

2az

2-phenylacetaldehyde (2aa). Oil (95 mg, 79%); R_f = 0.65 (hexane:EtOAc = 10:1); ^{1}H NMR (500 MHz, $CDCl_3$) δ 9.77 (t, J = 2.4 Hz, 1H), 7.41 (t, J = 7.4 Hz, 2H), 7.35 (t, J = 7.4 Hz, 1H), 7.26 (d, J = 7.2 Hz, 2H), 3.72 (d, J = 2.3 Hz, 2H); ^{13}C NMR (126 MHz, $CDCl_3$) δ 199.5, 131.9, 129.6, 129.0, 127.4, 50.5.

(1) M. Schönberger, D. Trauner, A Photochromic Agonist for μ-Opioid Receptors, Angew. Chem. Int. Ed. 53 (2014) 3264–3267.

Table 2, entry 53

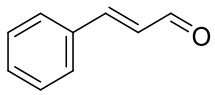

2aaa

Cinnamaldehyde (2aaa). Oil (46 mg, 35%); R_f = 0.60 (hexane:EtOAc = 10:1); ^{1}H NMR (500 MHz, $CDCl_3$) δ 9.71 (d, J = 7.7 Hz, 1H), 7.60–7.54 (m, 2H), 7.52–7.40 (m, 4H), 6.73 (dd, J = 16.0, 7.7 Hz, 1H); ^{13}C NMR (126 MHz, $CDCl_3$) δ 193.7, 152.8, 134.0, 131.3, 129.1, 128.5, 128.5.

(1) W. Huang, B. C. Ma, H. Lu, R. Li, L. Wang, K. Landfester, K. A. I. Zhang, Visible-light-promoted selective oxidation of alcohols using a covalent triazine framework, ACS Catal. 7 (2017) 5438–5442.

^{1}H NMR and ^{13}C NMR Spectrum of **2f**

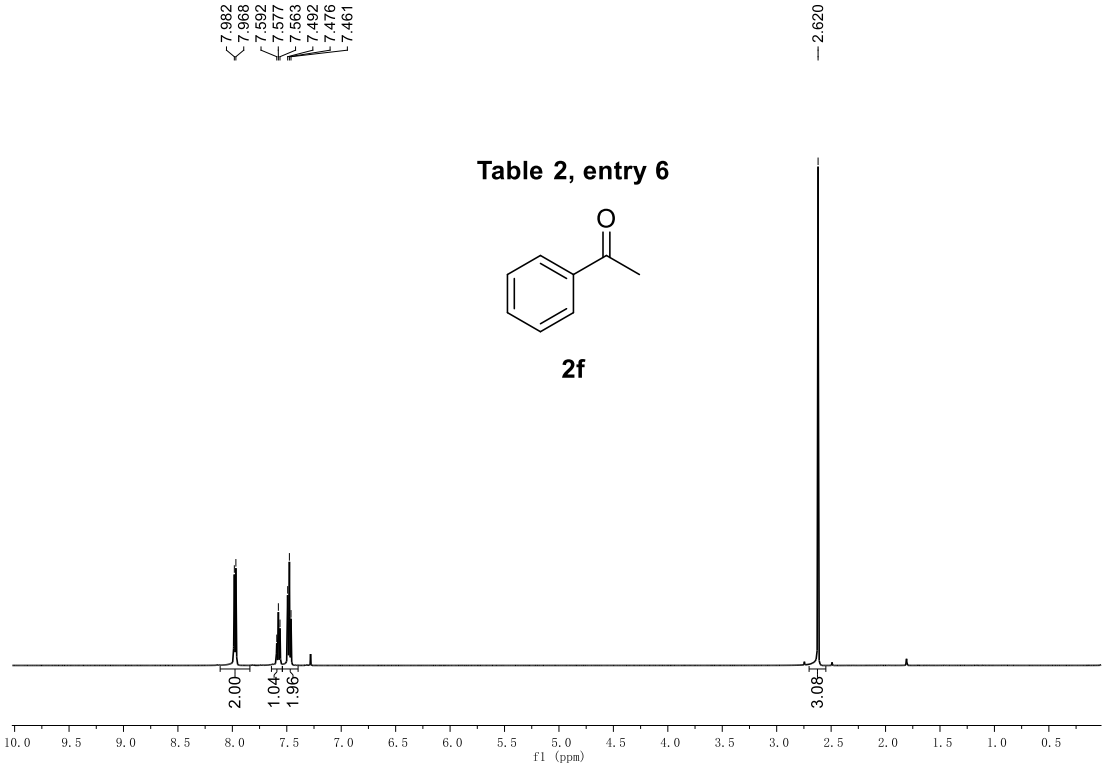

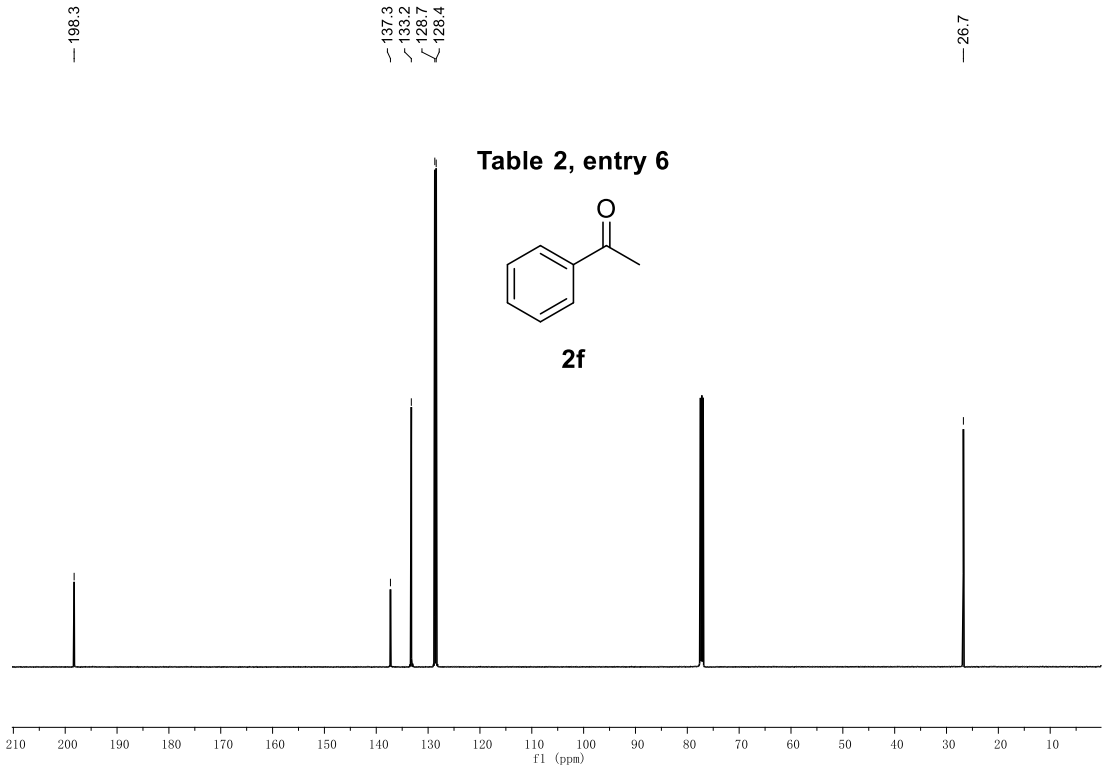

^{1}H NMR and ^{13}C NMR Spectrum of **2g**

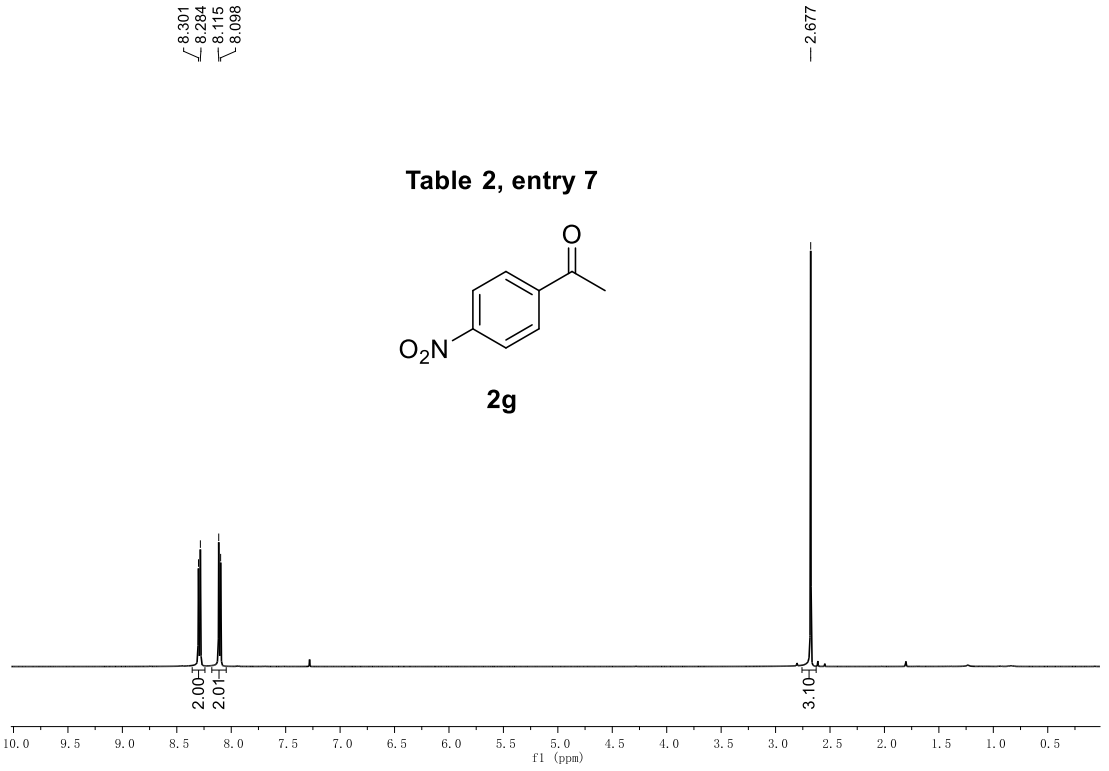

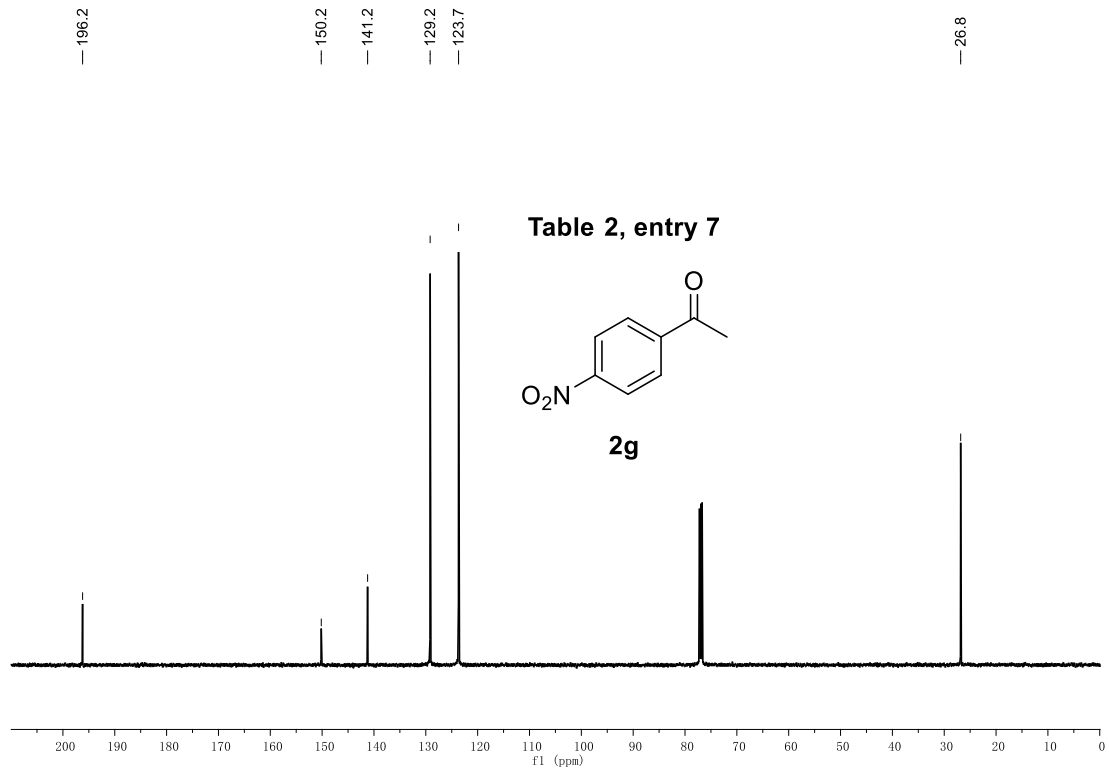

^{1}H NMR and ^{13}C NMR Spectrum of **2h**

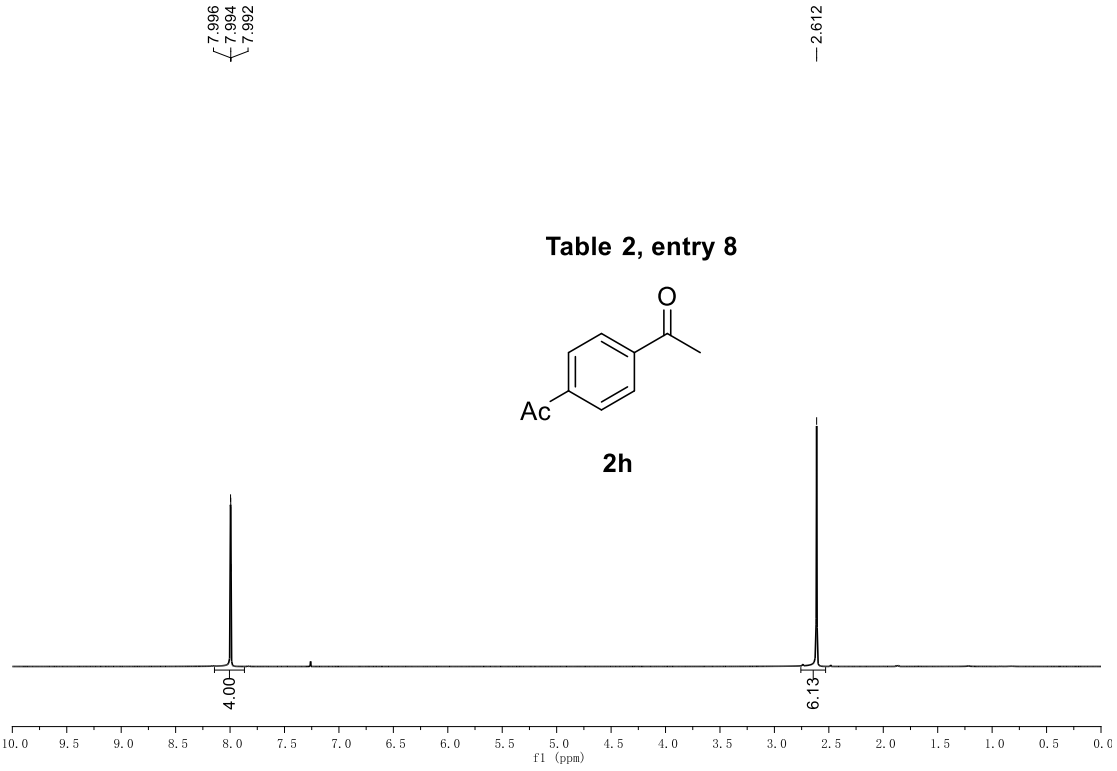

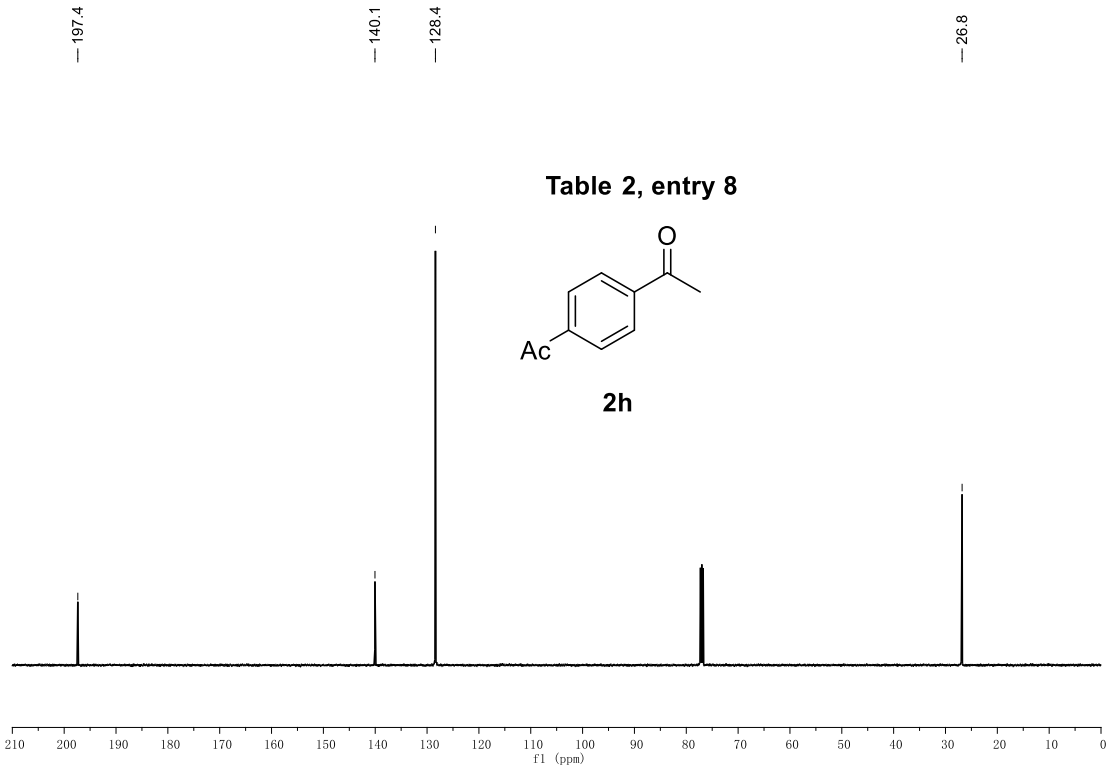

^{1}H NMR and ^{13}C NMR Spectrum of **2i**

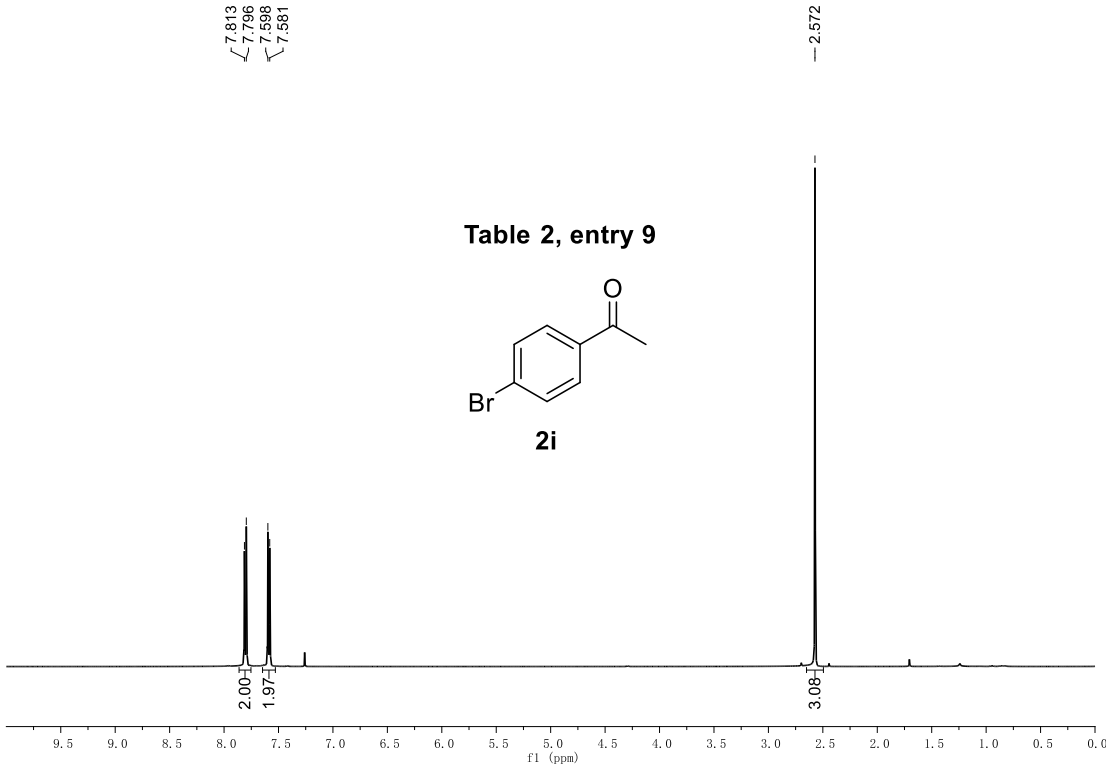

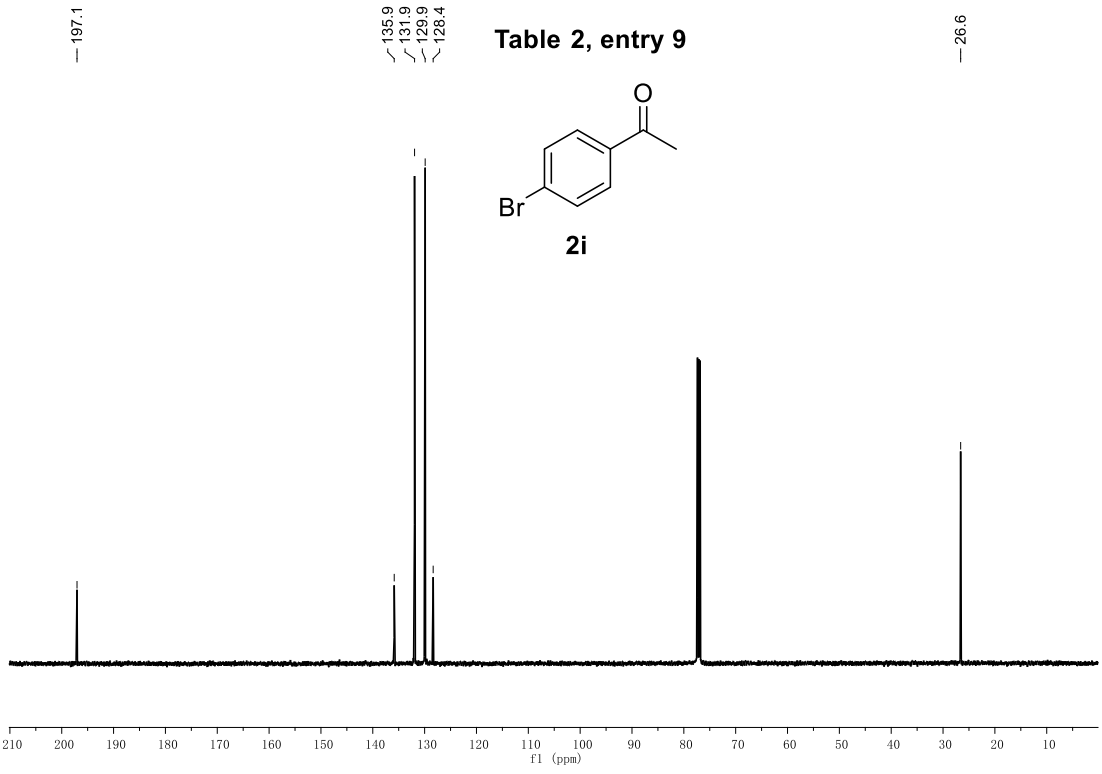

^{1}H NMR and ^{13}C NMR Spectrum of **2j**

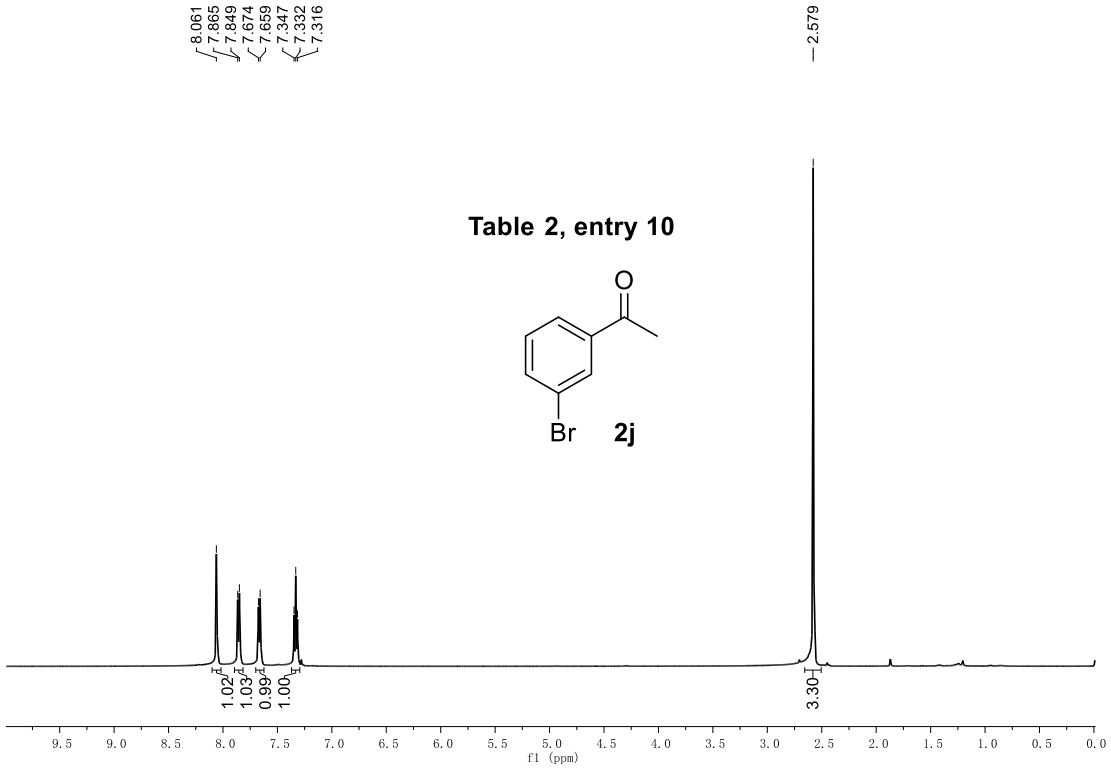

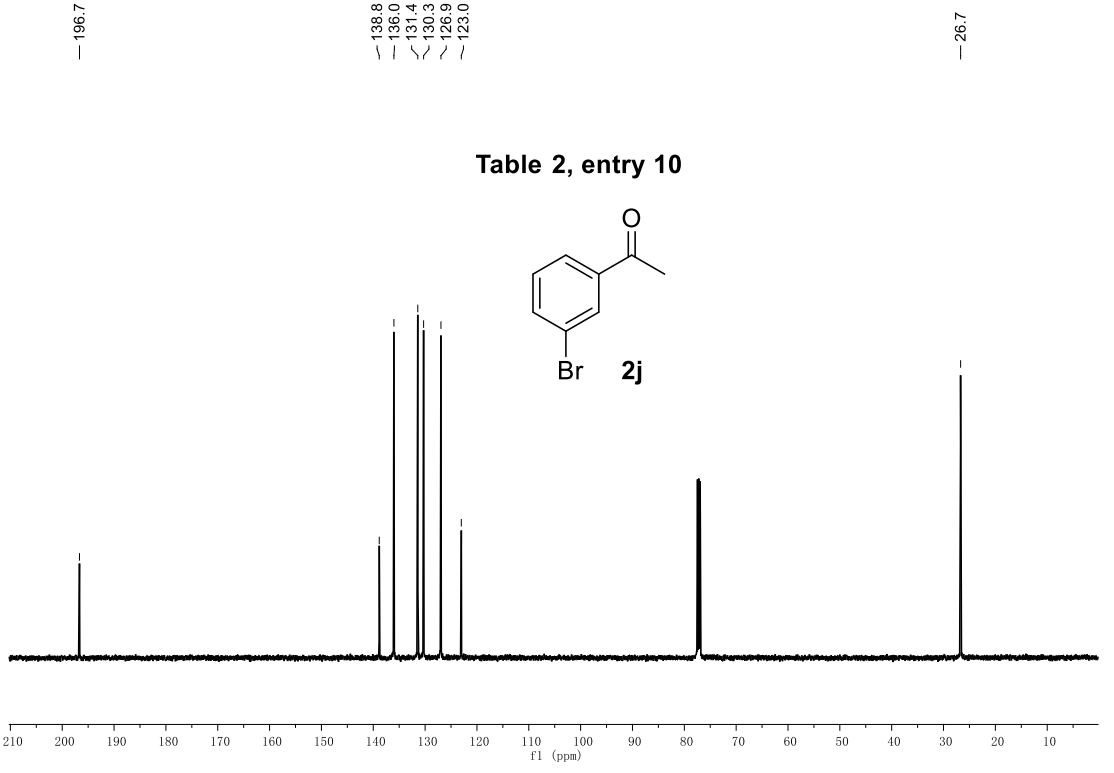

^{1}H NMR and ^{13}C NMR Spectrum of **2k**

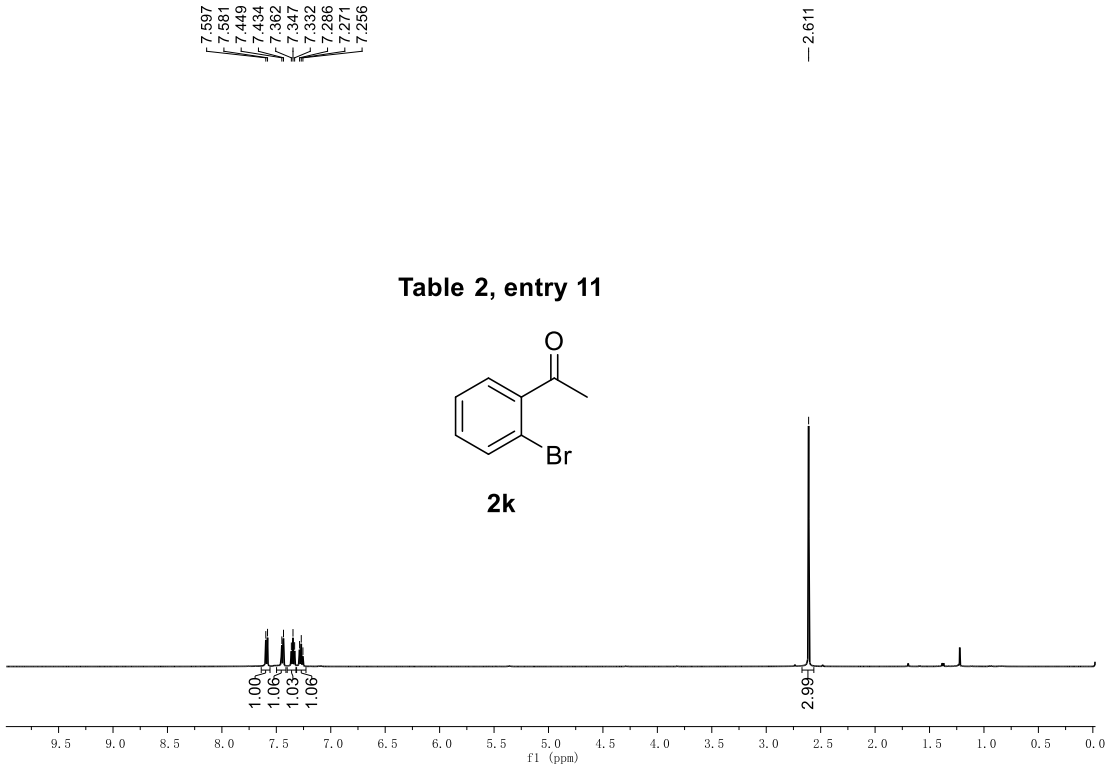

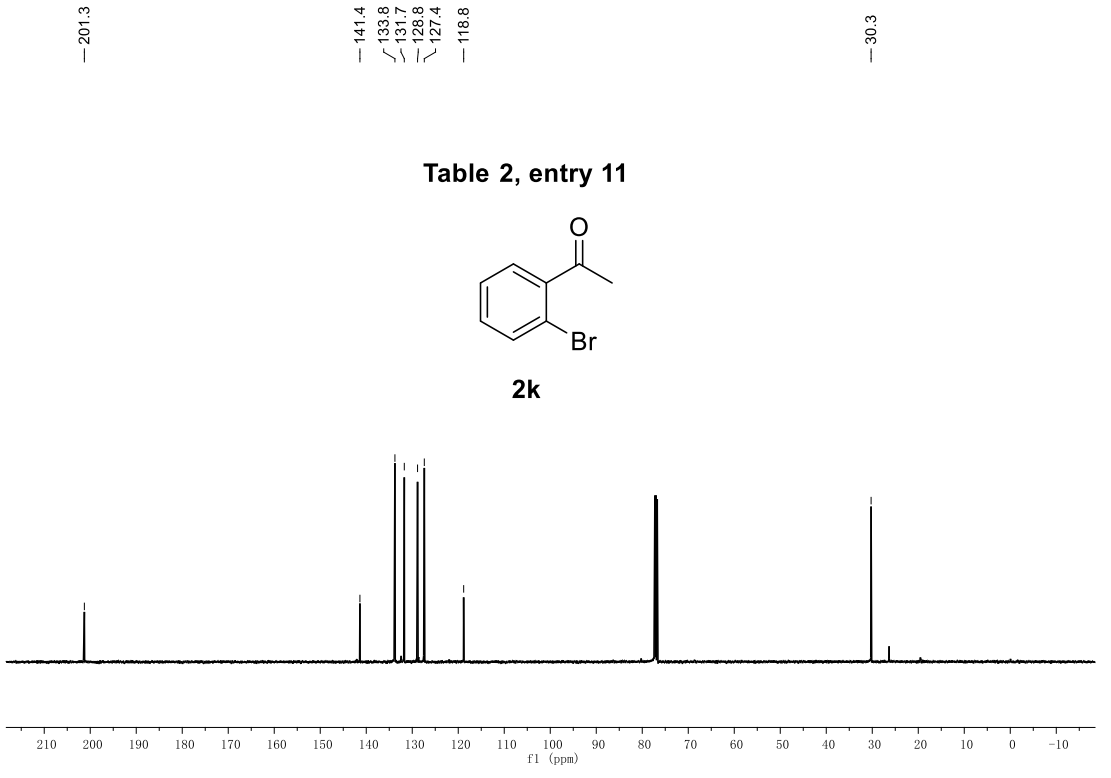

^{1}H NMR and ^{13}C NMR Spectrum of **2l**

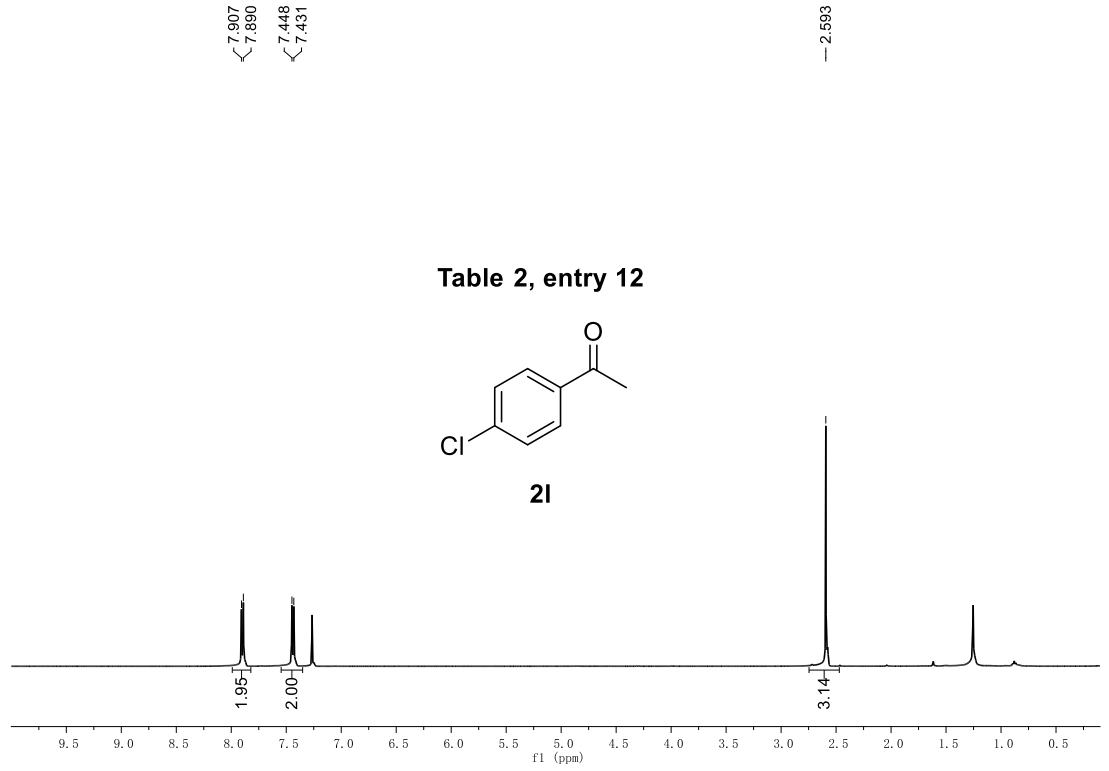

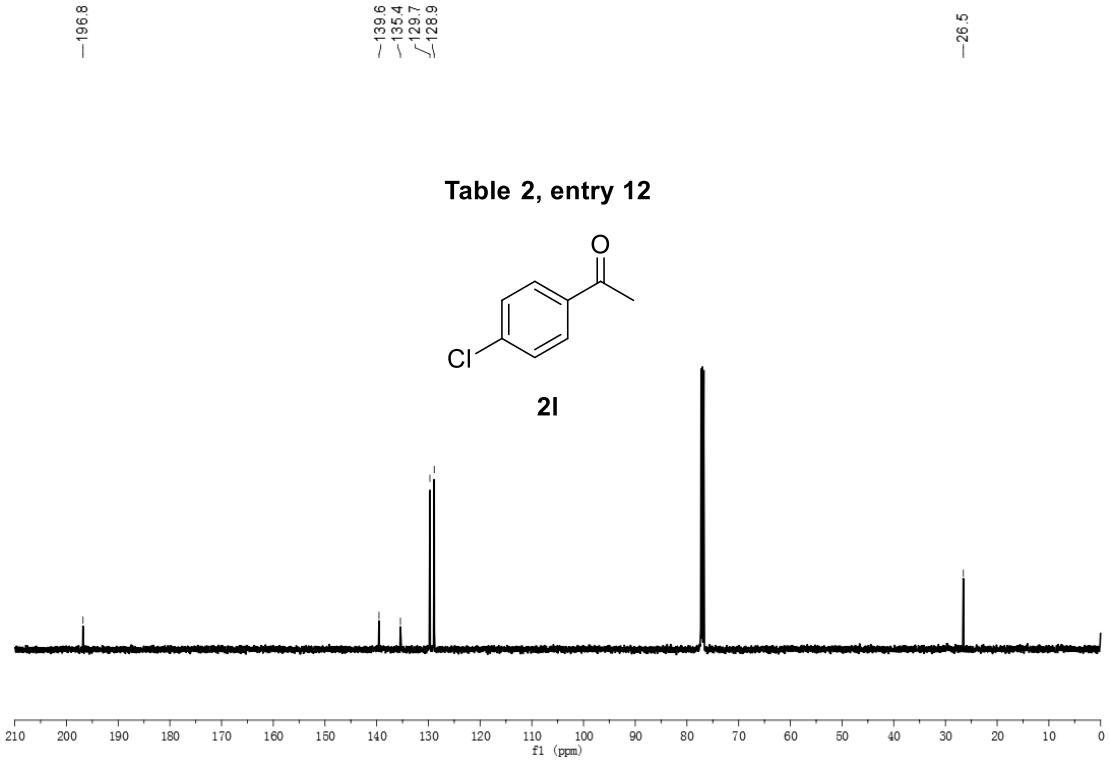

^{1}H NMR and ^{13}C NMR Spectrum of **2m**

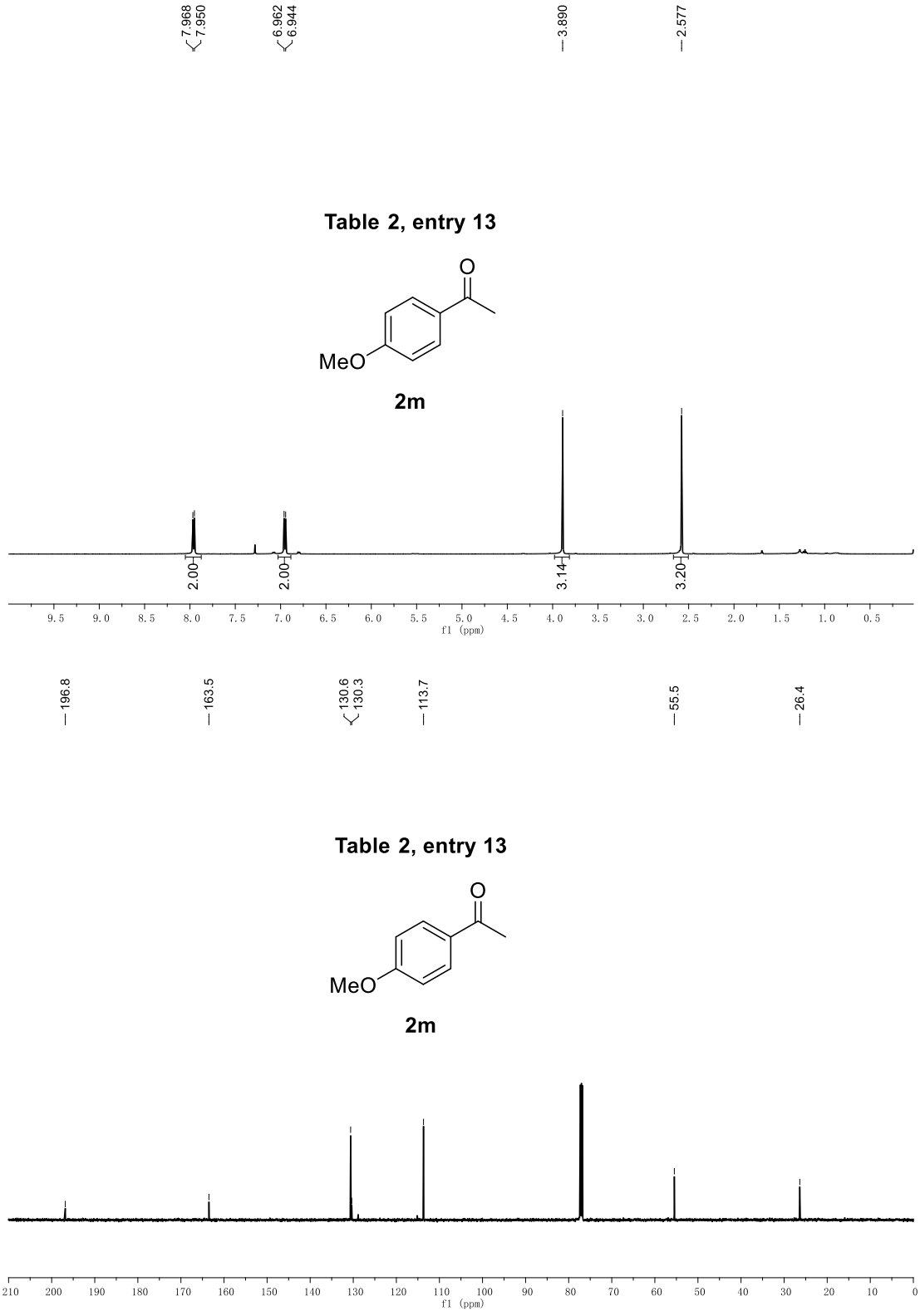

^{1}H NMR and ^{13}C NMR Spectrum of **2n**

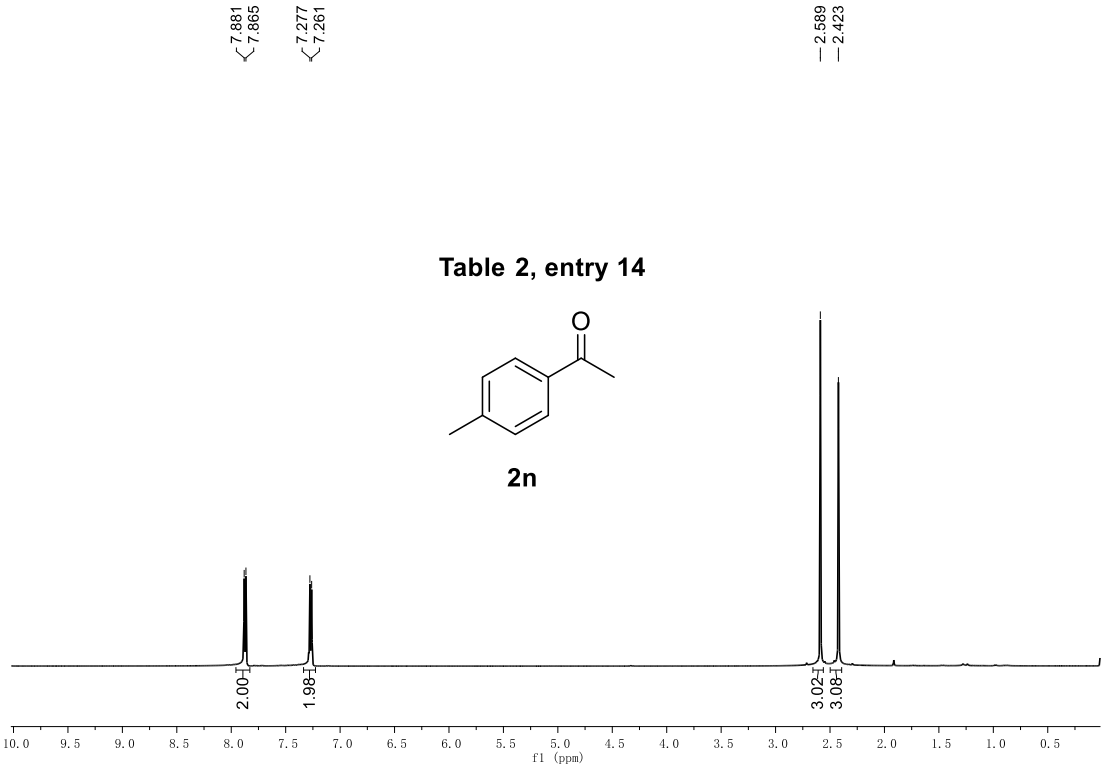

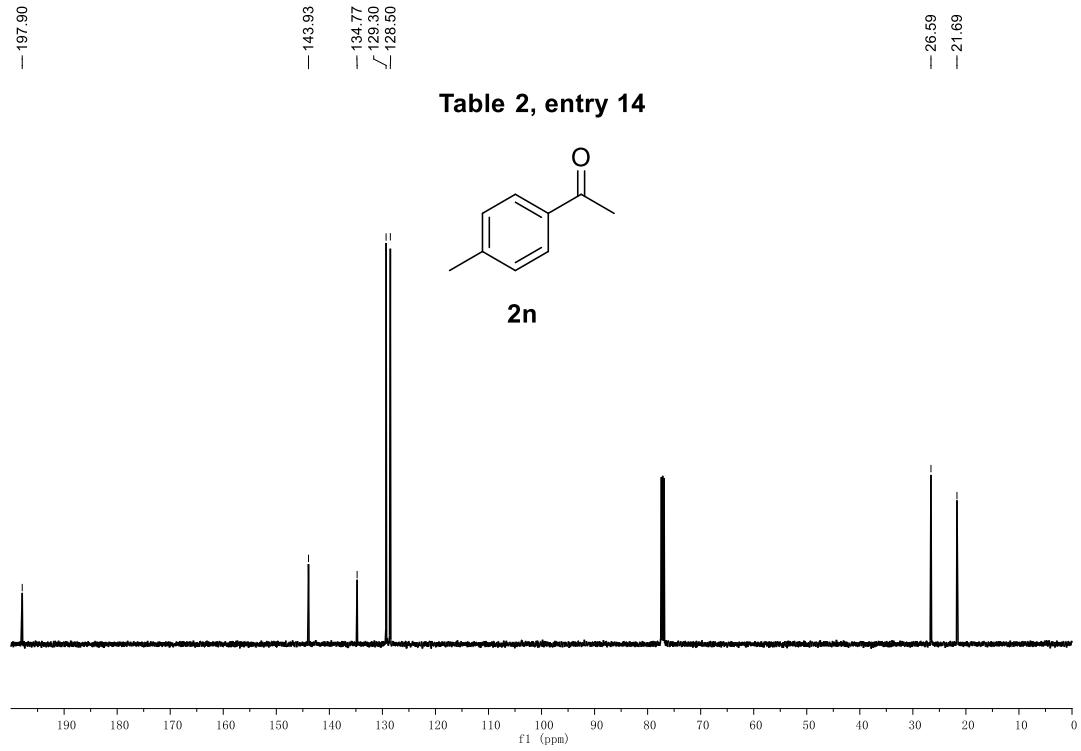

^{1}H NMR and ^{13}C NMR Spectrum of **2o**

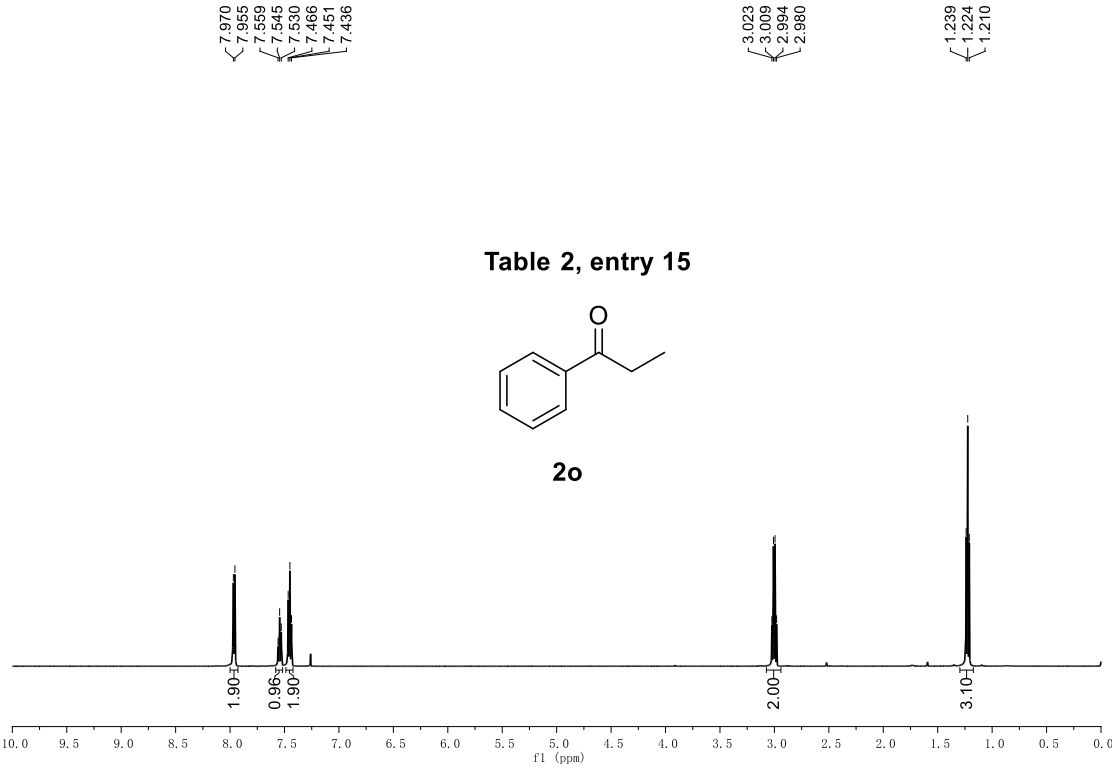

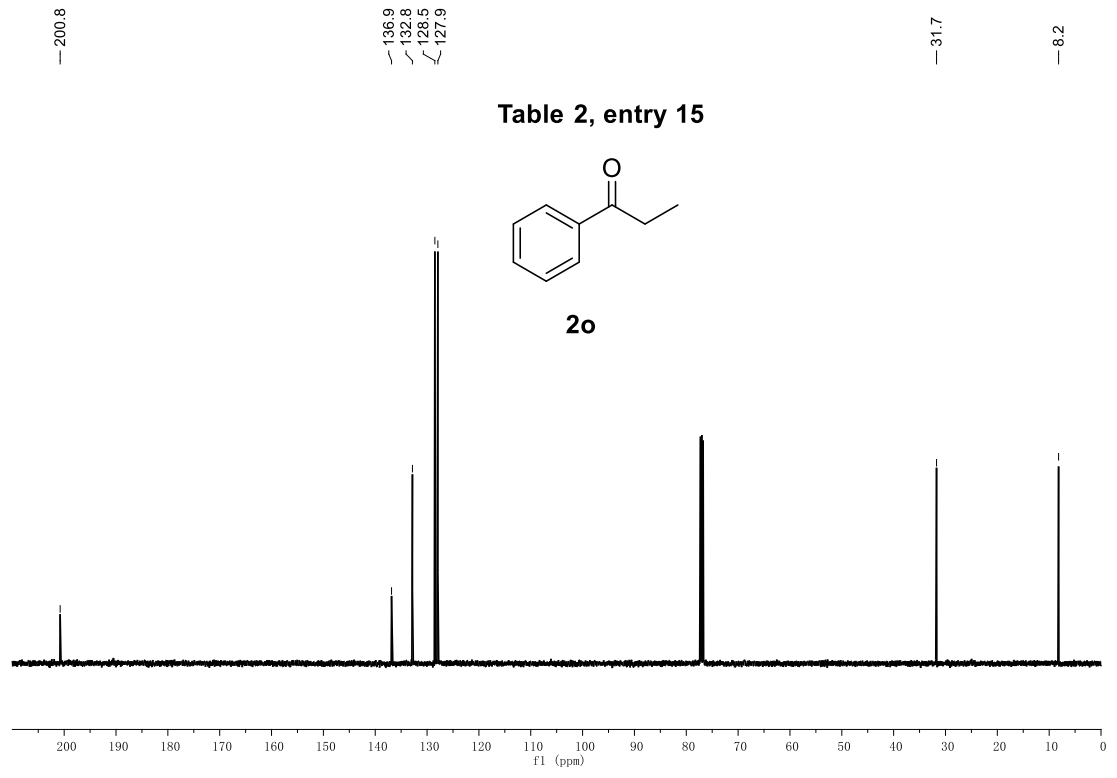

^{1}H NMR and ^{13}C NMR Spectrum of **2p**

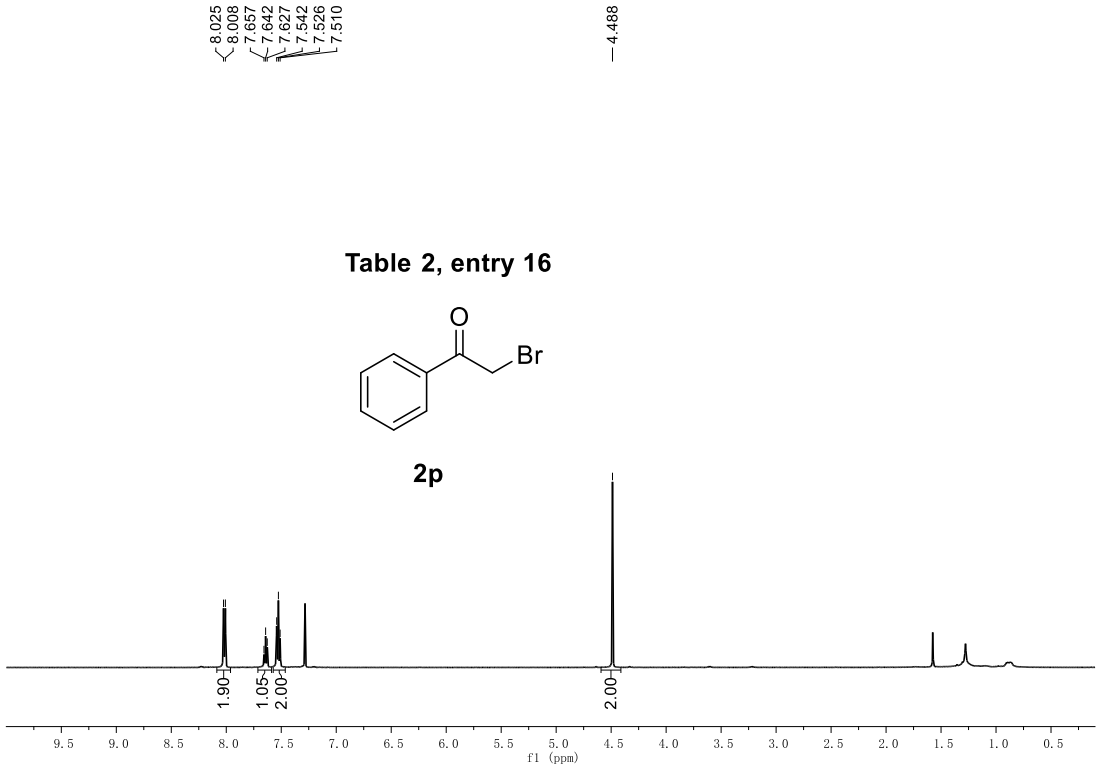

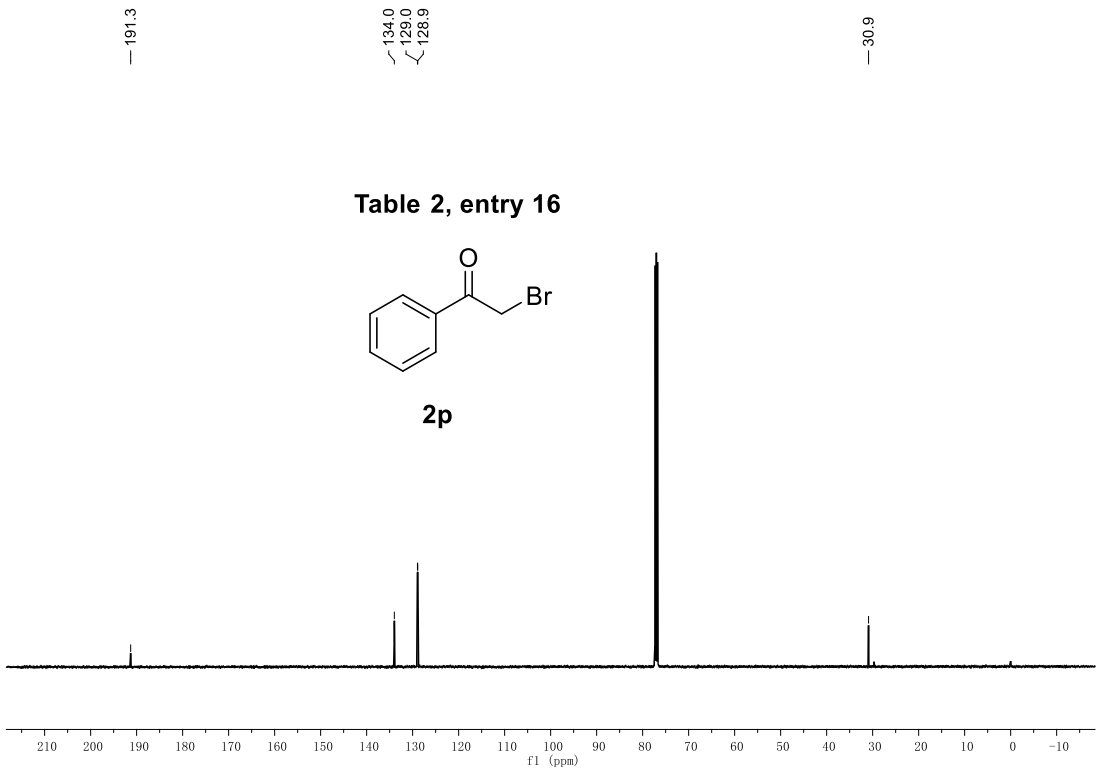

^{1}H NMR and ^{13}C NMR Spectrum of **2q**

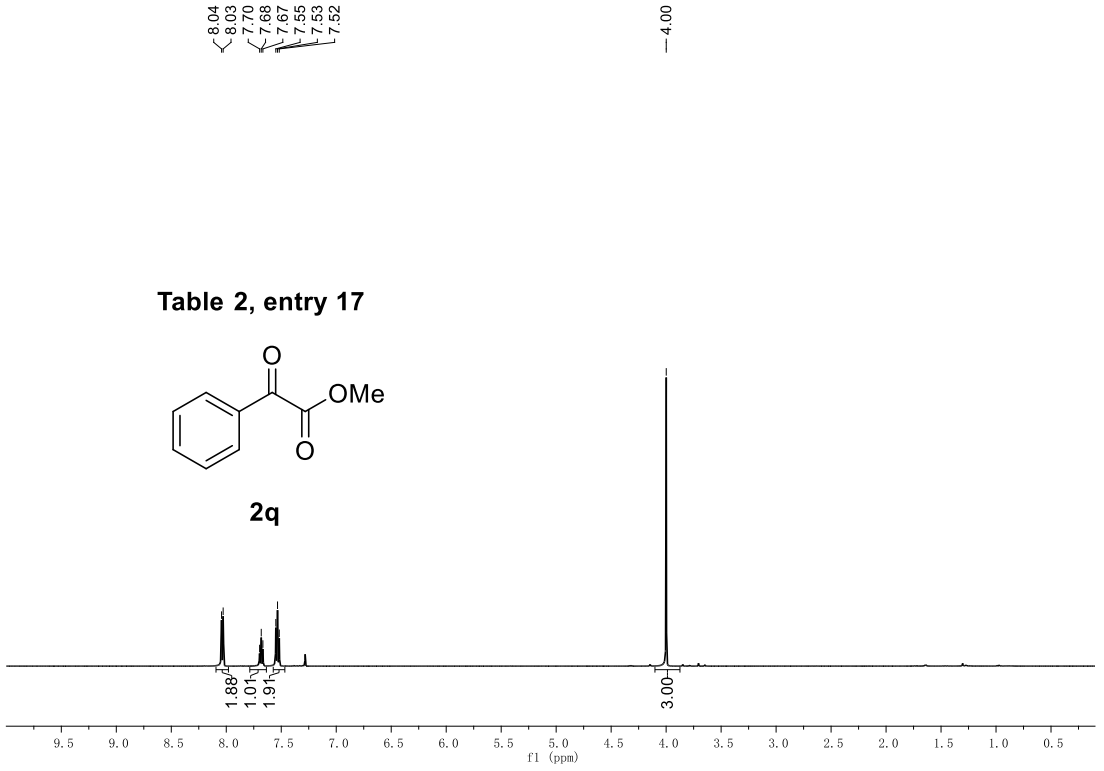

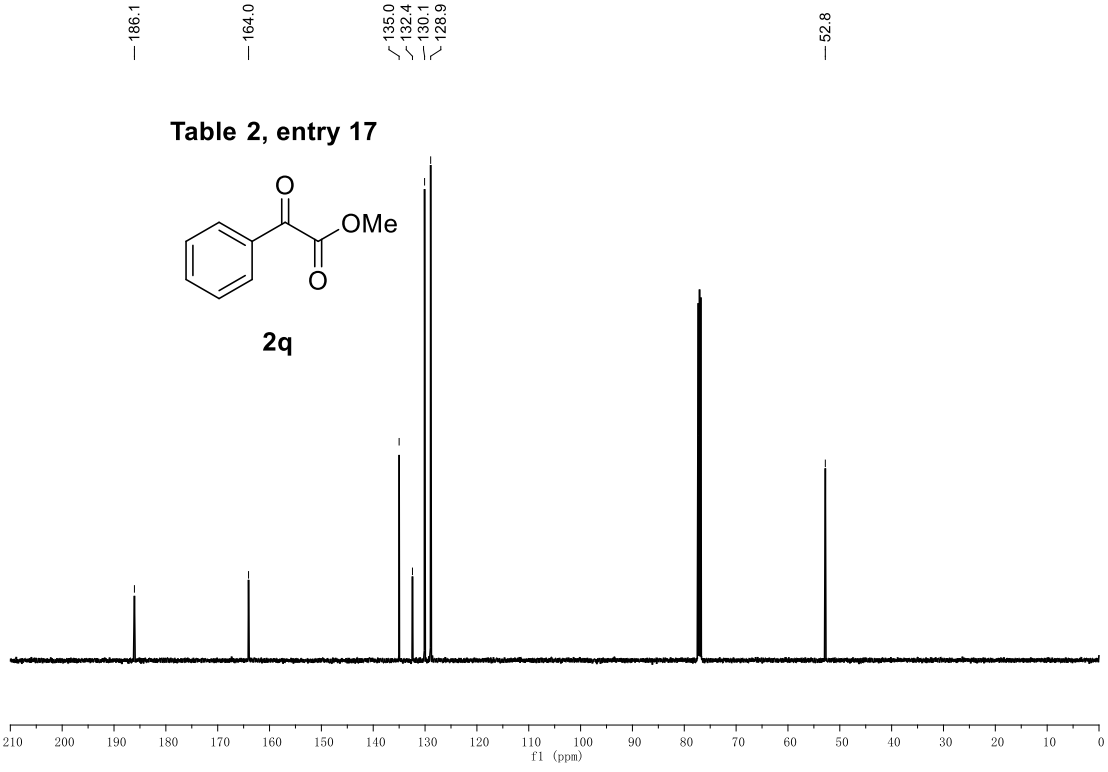

^{1}H NMR and ^{13}C NMR Spectrum of **2r**

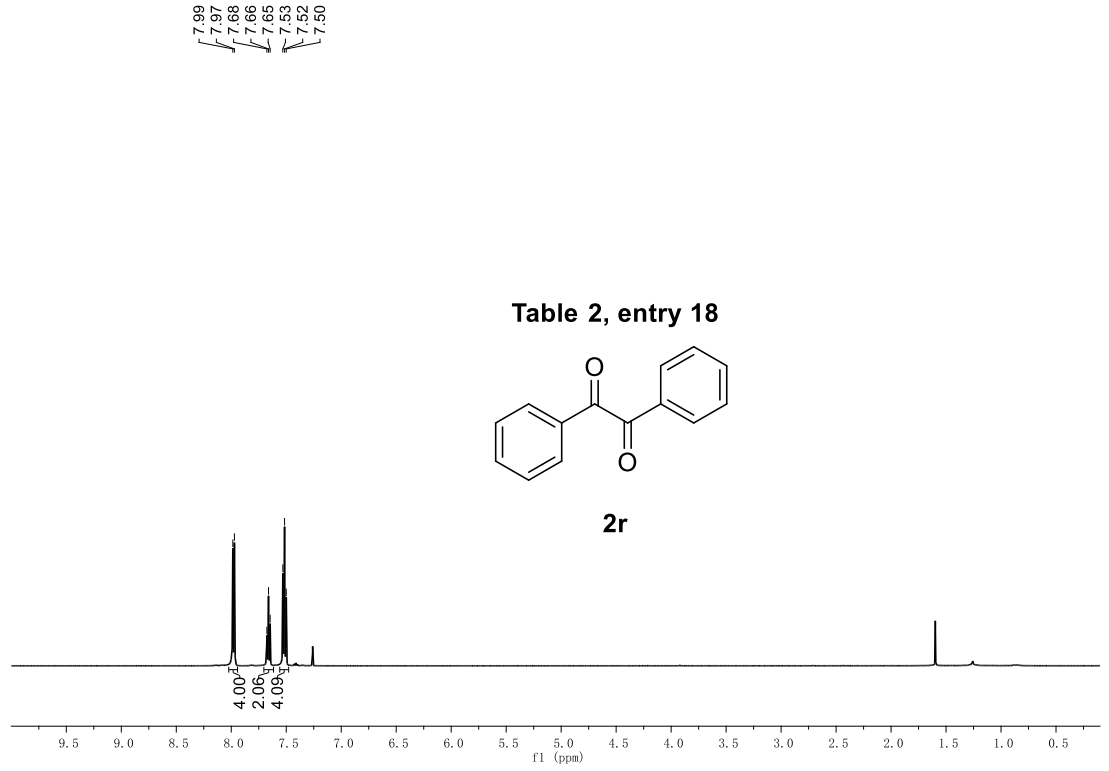

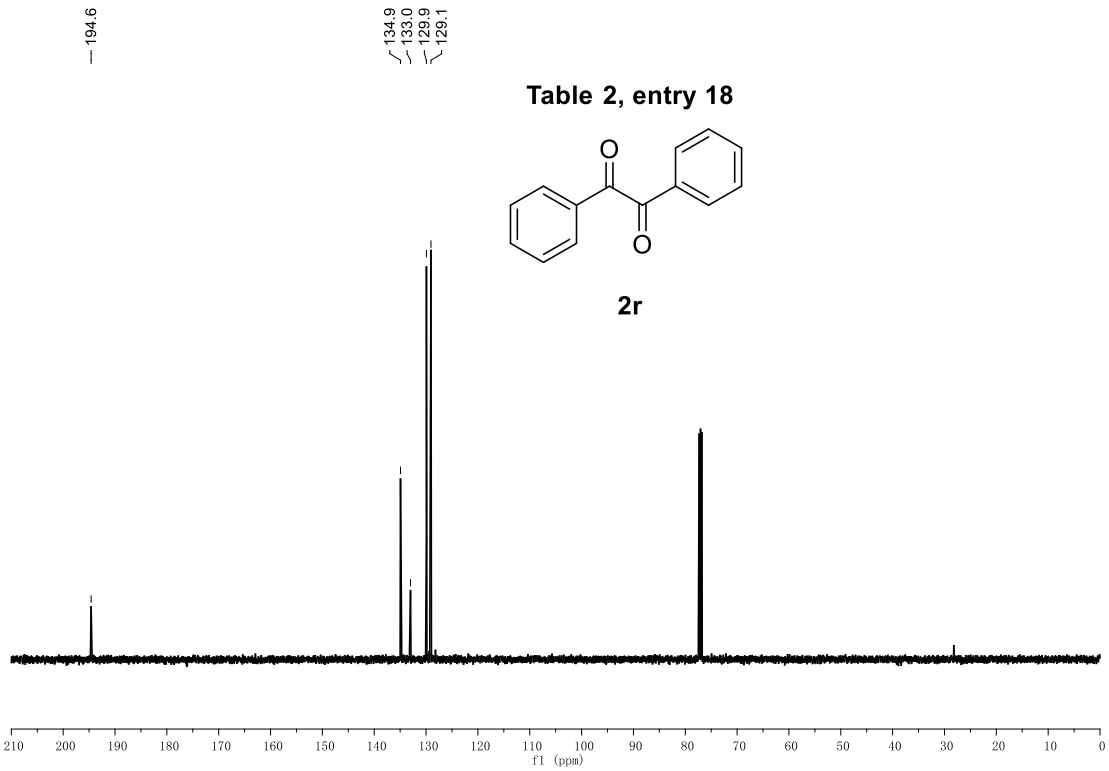

^{1}H NMR and ^{13}C NMR Spectrum of **2s**

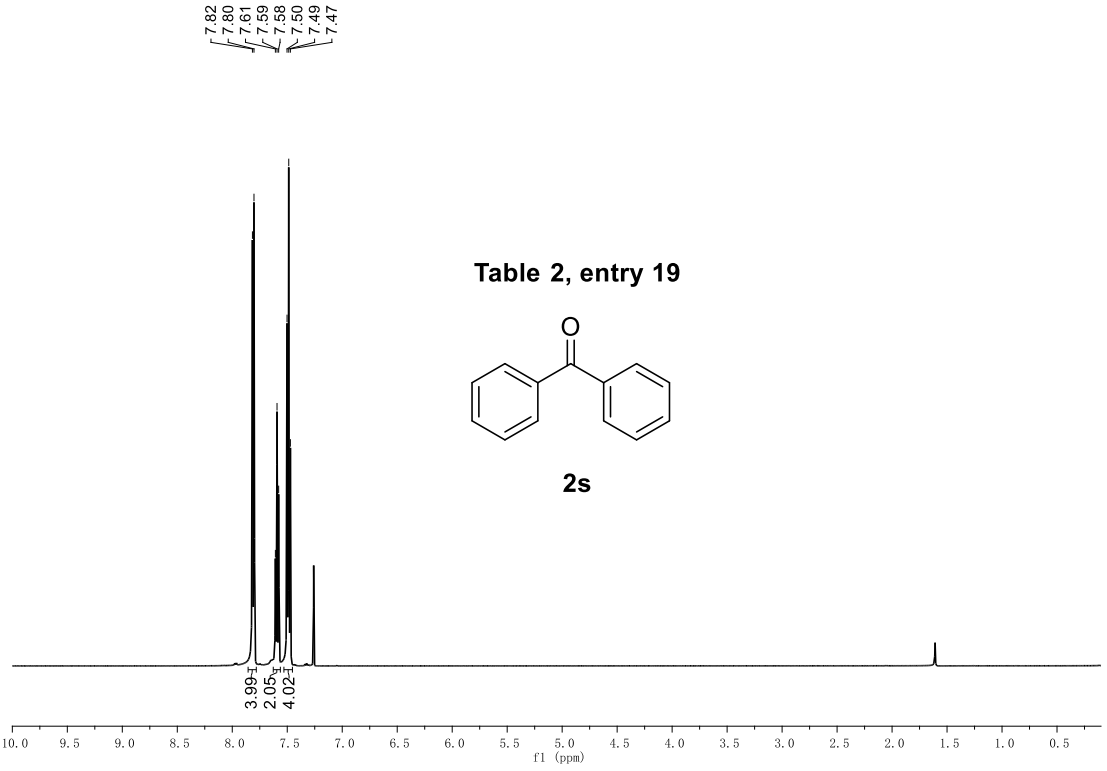

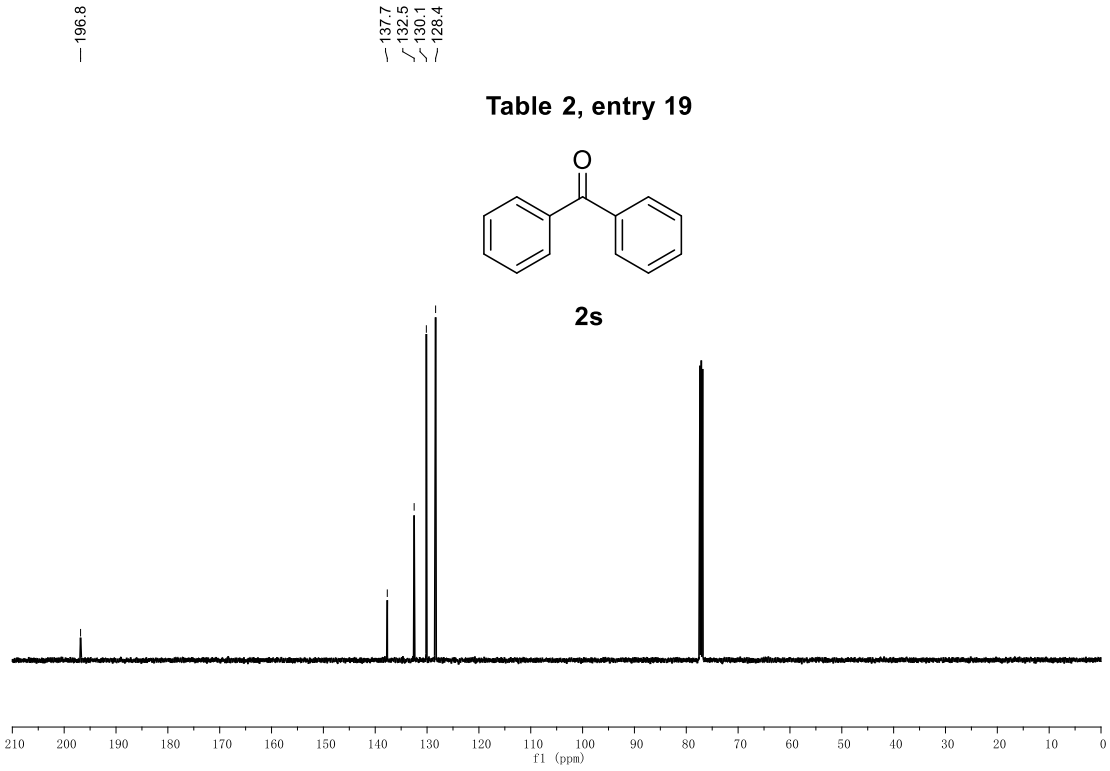

^{1}H NMR and ^{13}C NMR Spectrum of **2t**

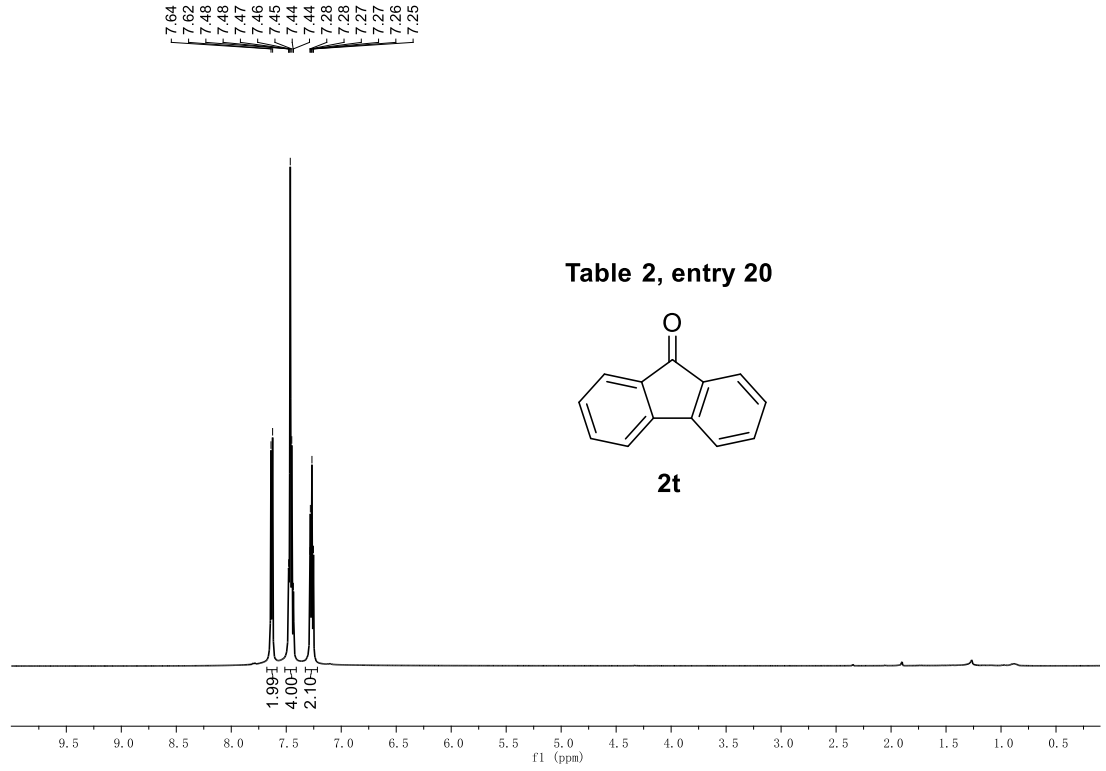

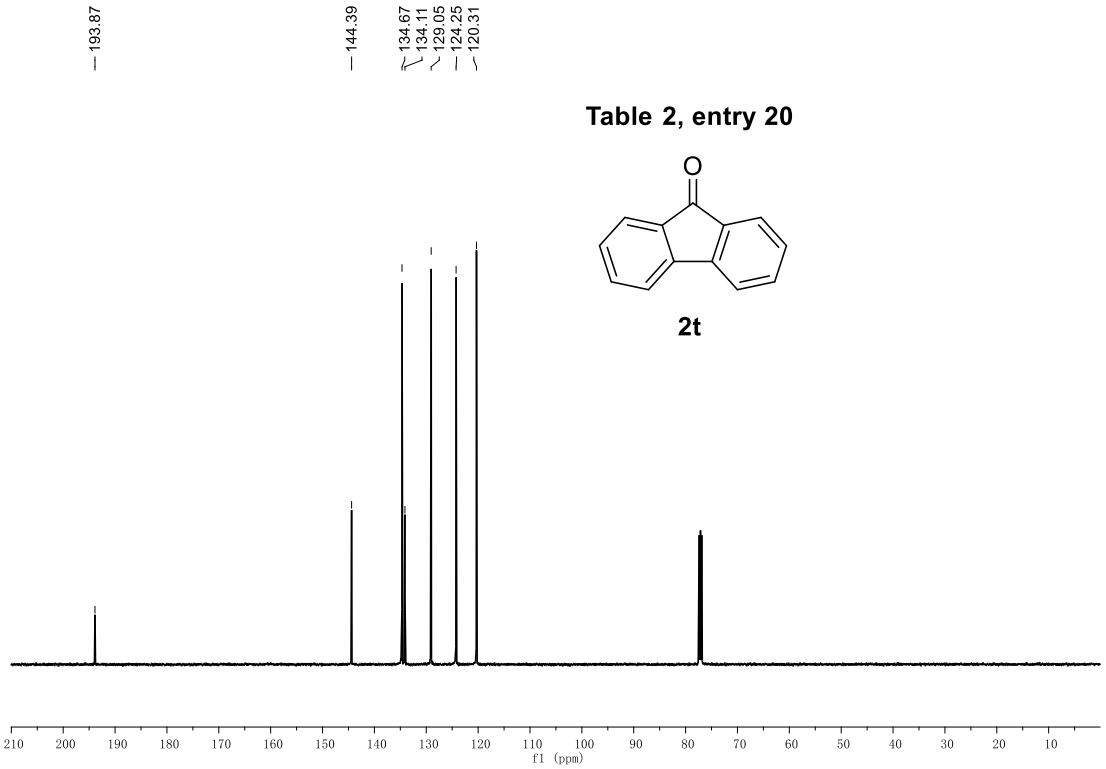

^{1}H NMR and ^{13}C NMR Spectrum of **2u**

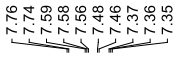

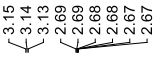

Table 2, entry 21

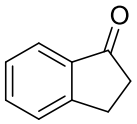

2u

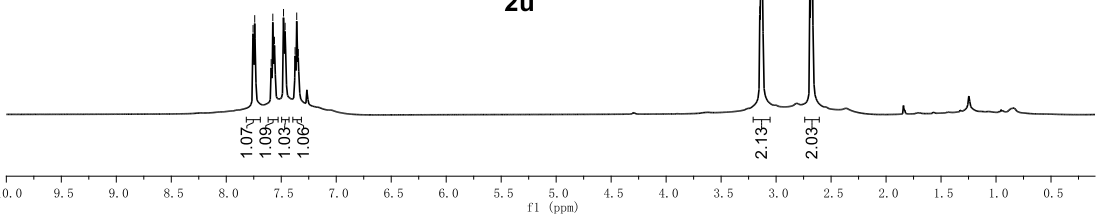

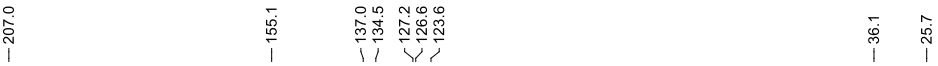

Table 2, entry 21

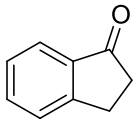

2u

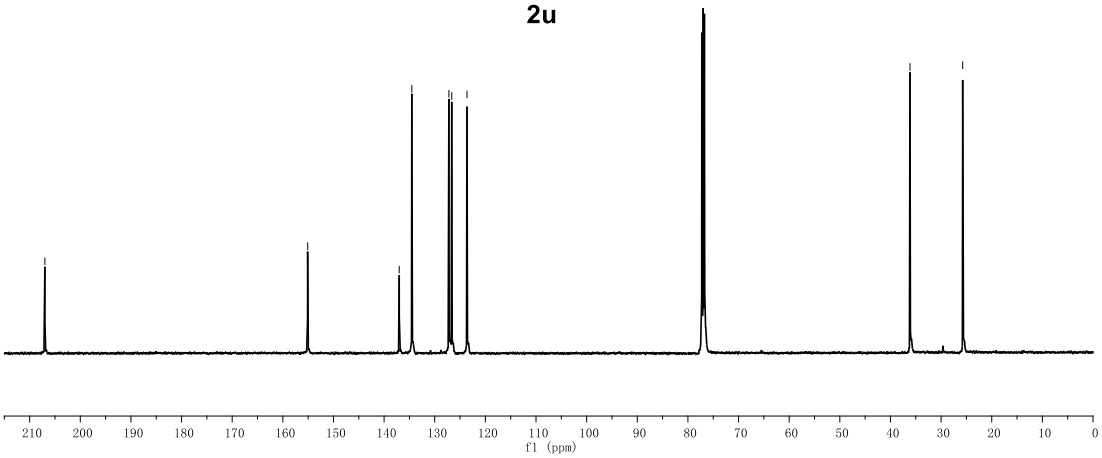

^{1}H NMR and ^{13}C NMR Spectrum of **2v**

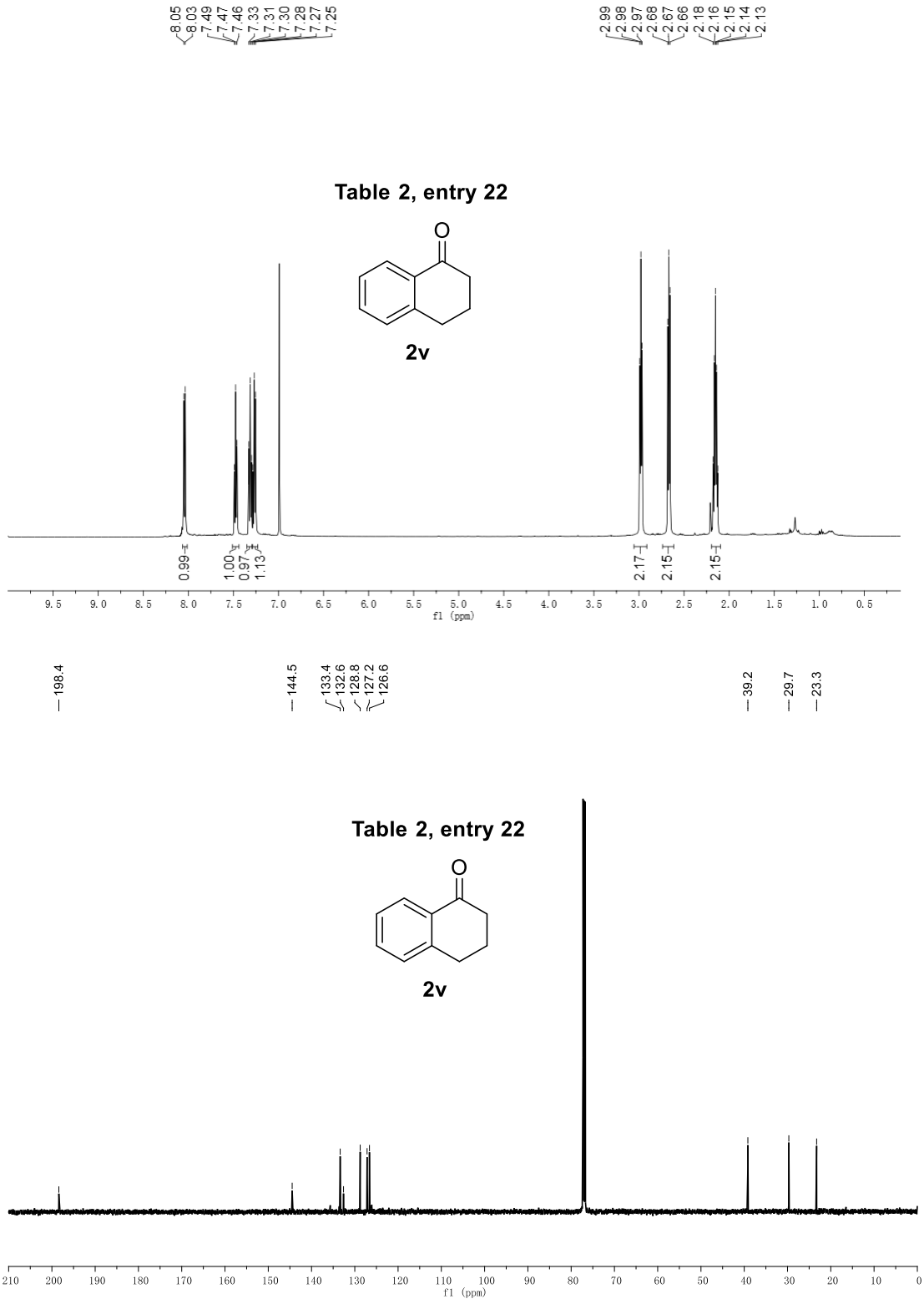

^{1}H NMR and ^{13}C NMR Spectrum of **2w**

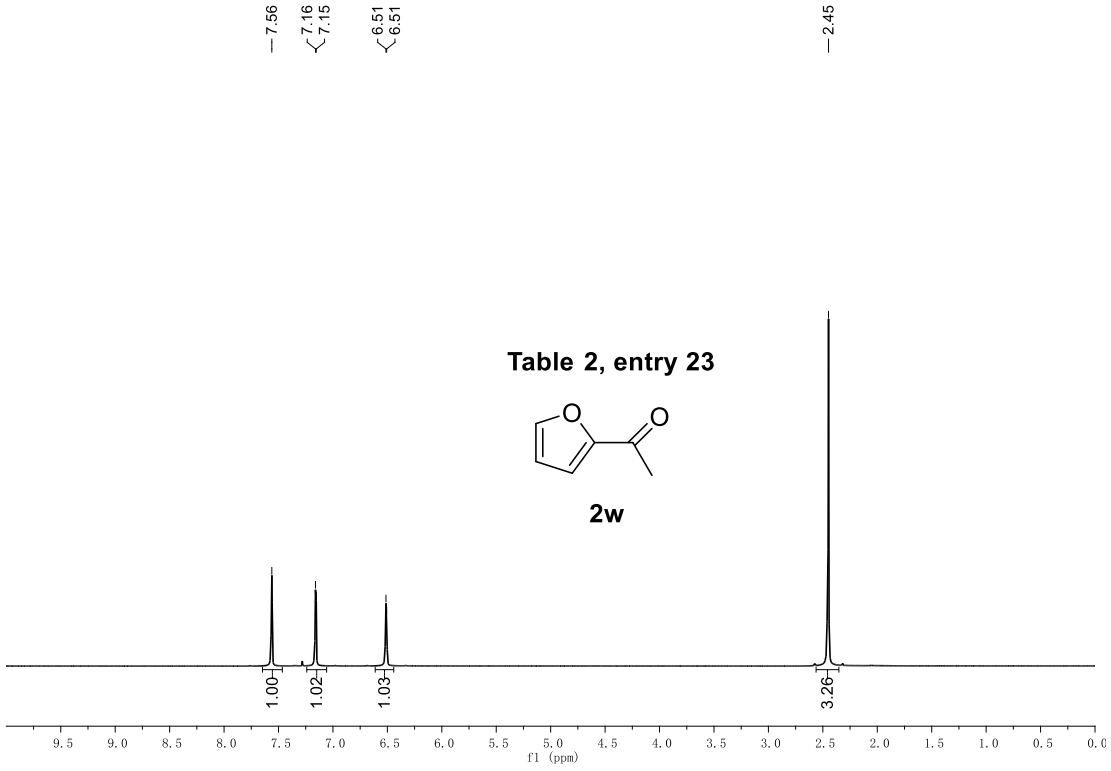

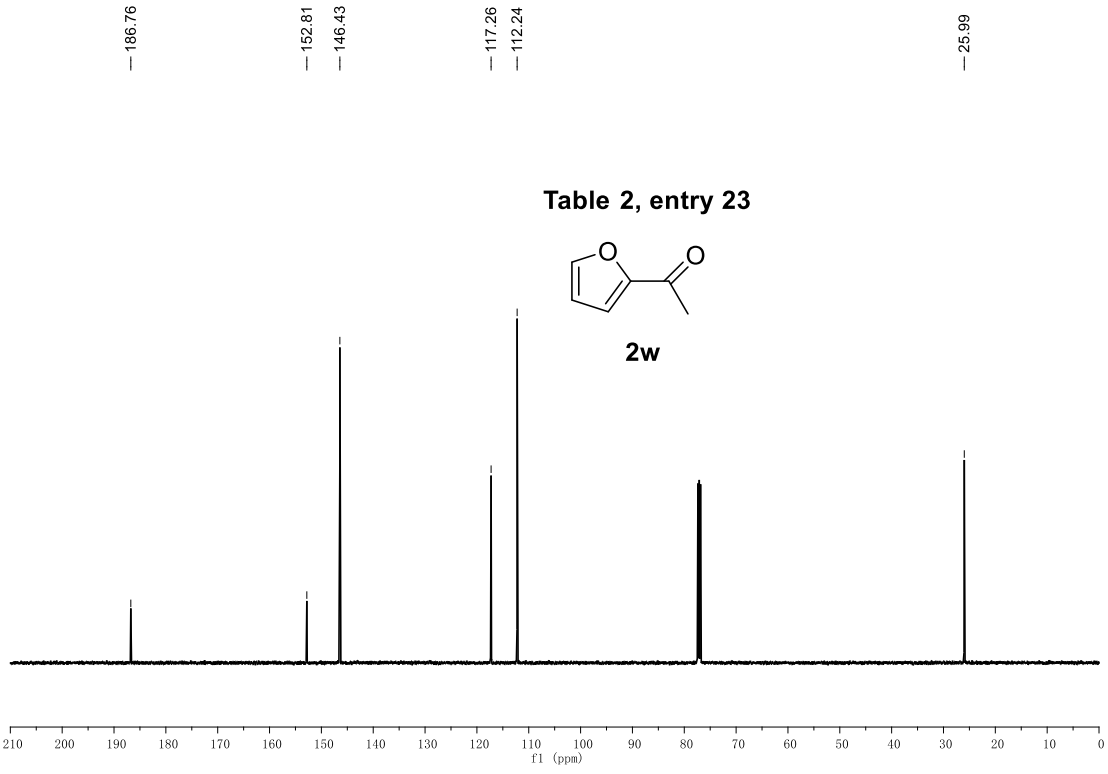

^{1}H NMR and ^{13}C NMR Spectrum of **2x**

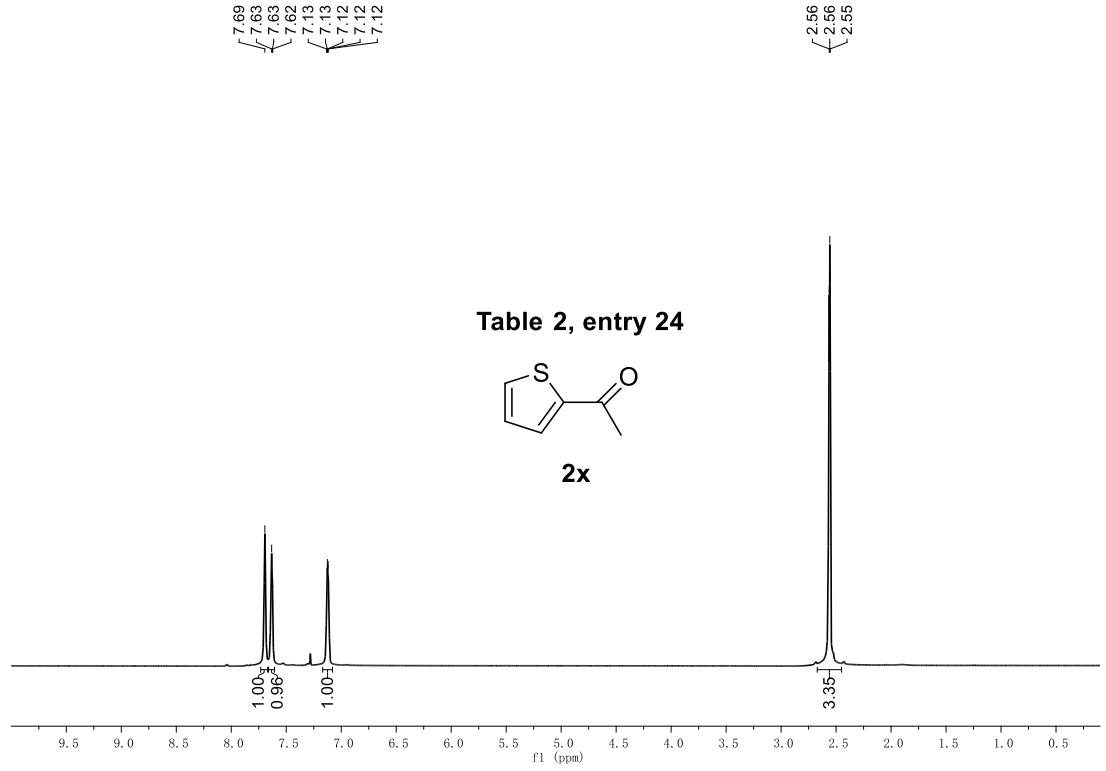

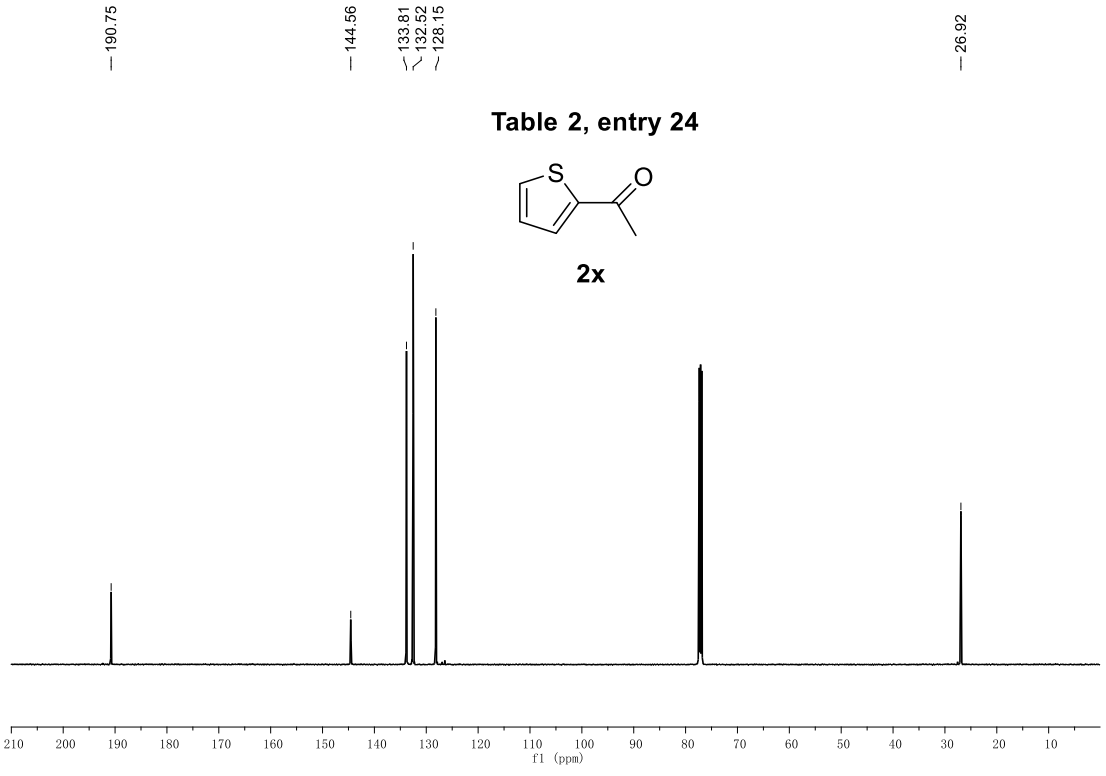

^{1}H NMR and ^{13}C NMR Spectrum of **2y**

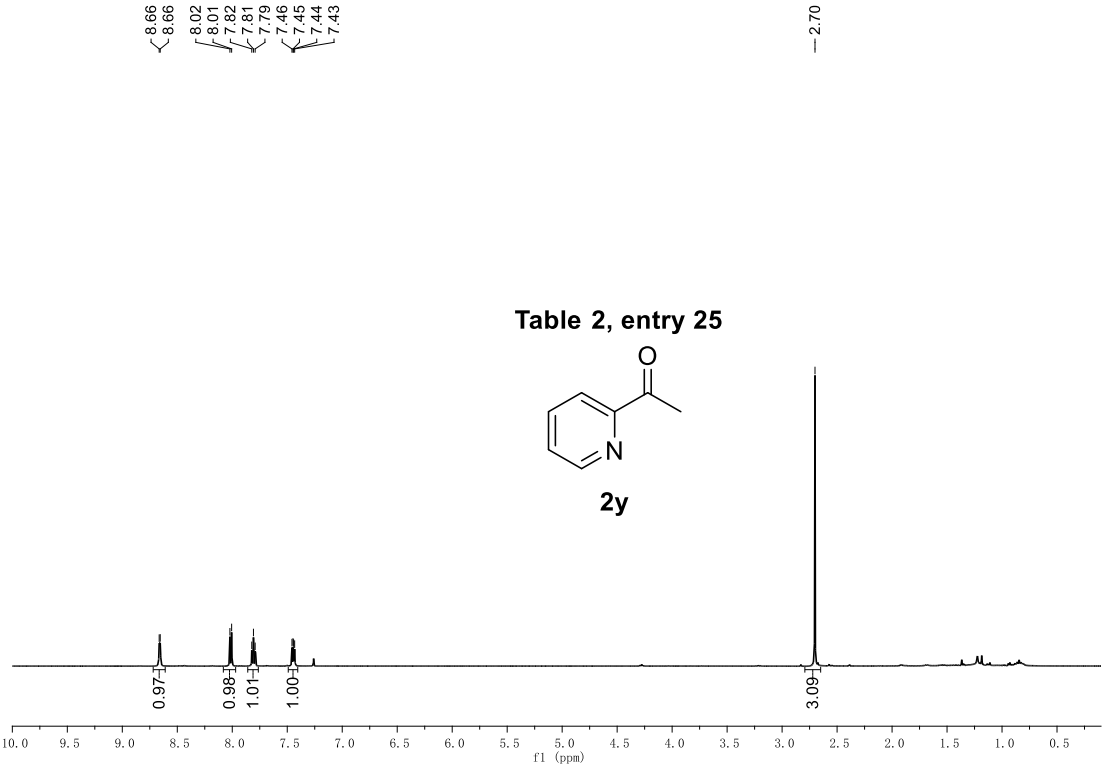

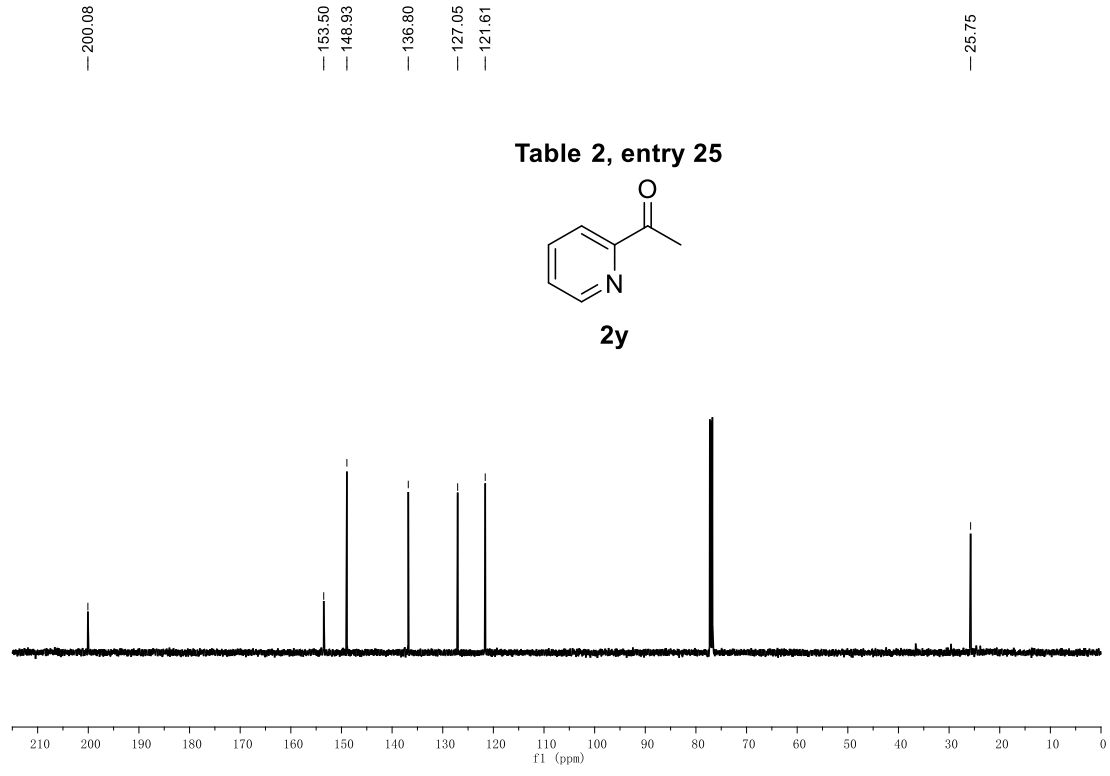

^{1}H NMR and ^{13}C NMR Spectrum of **2ag**

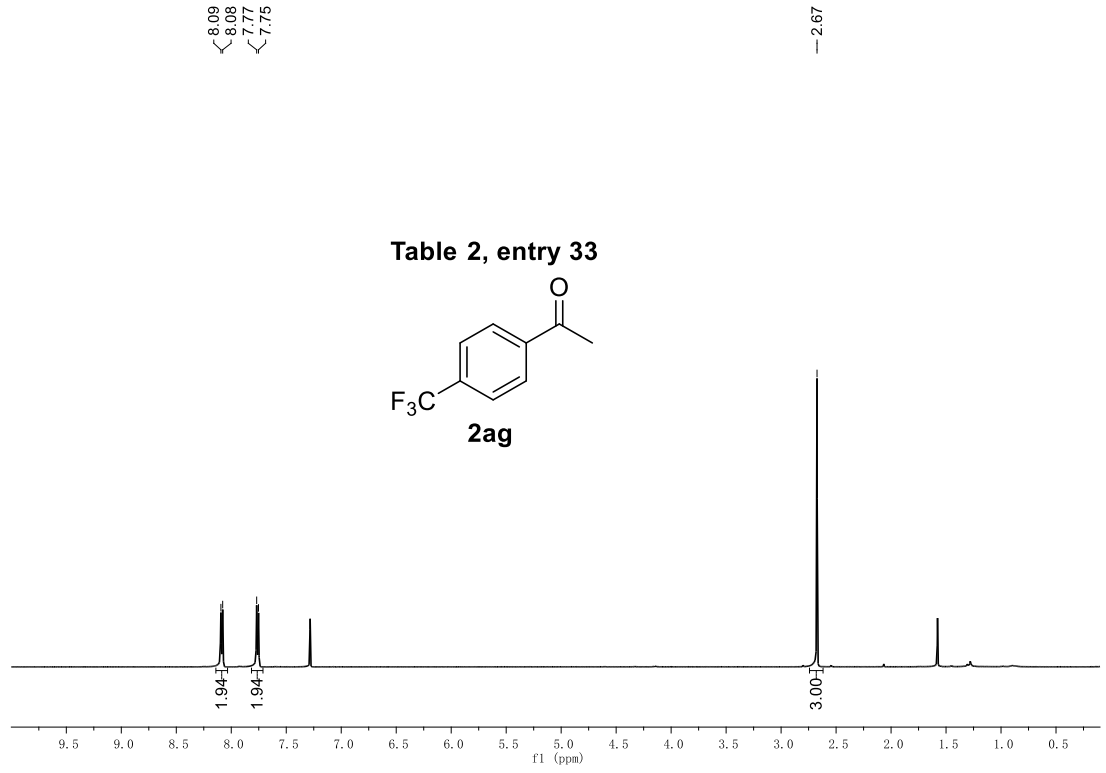

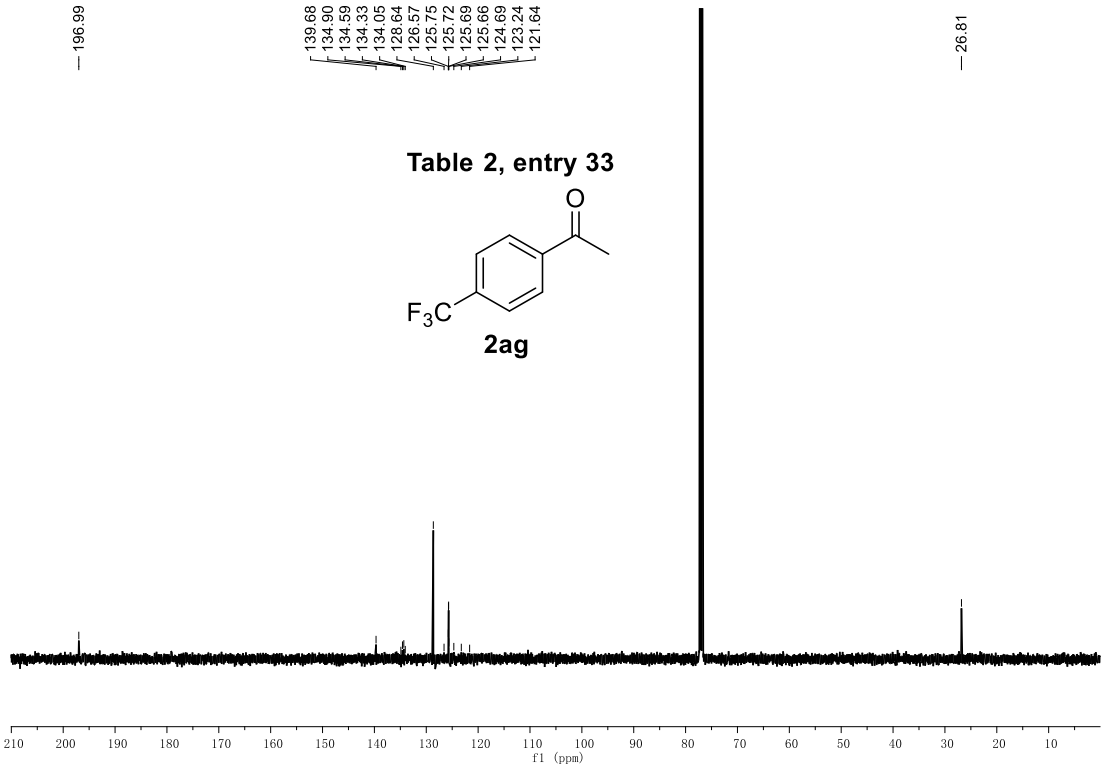

^{1}H NMR and ^{13}C NMR Spectrum of **2ah**

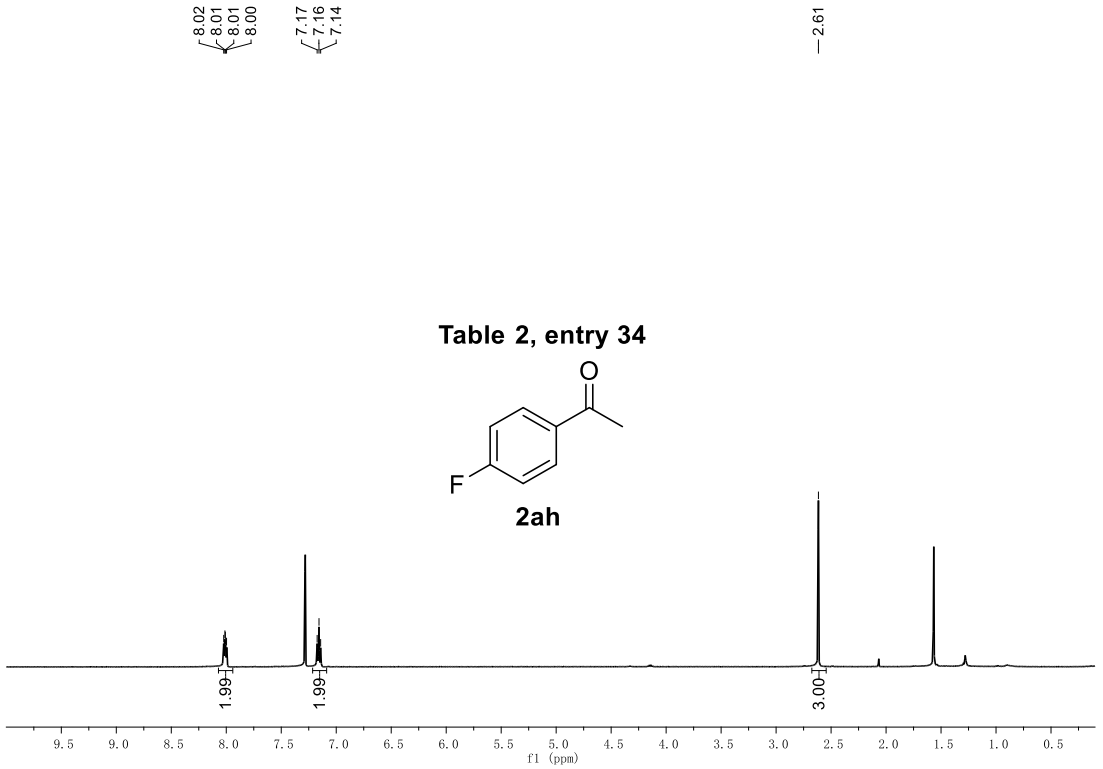

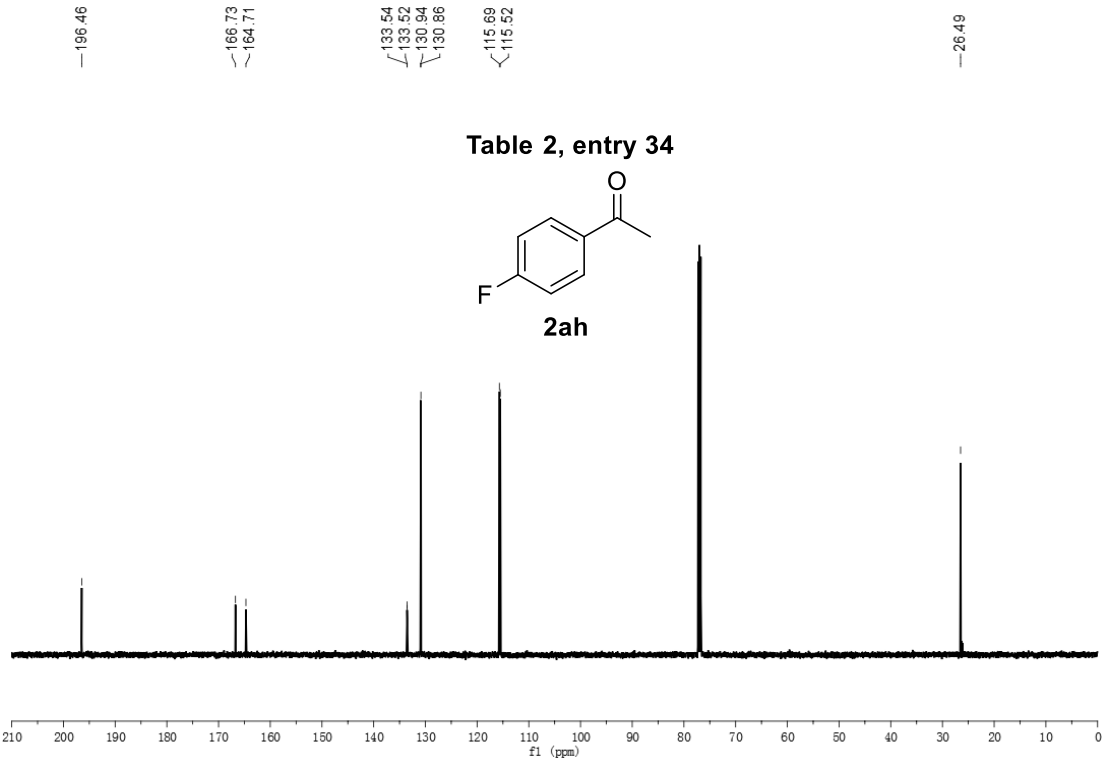

^{1}H NMR and ^{13}C NMR Spectrum of **2ak**

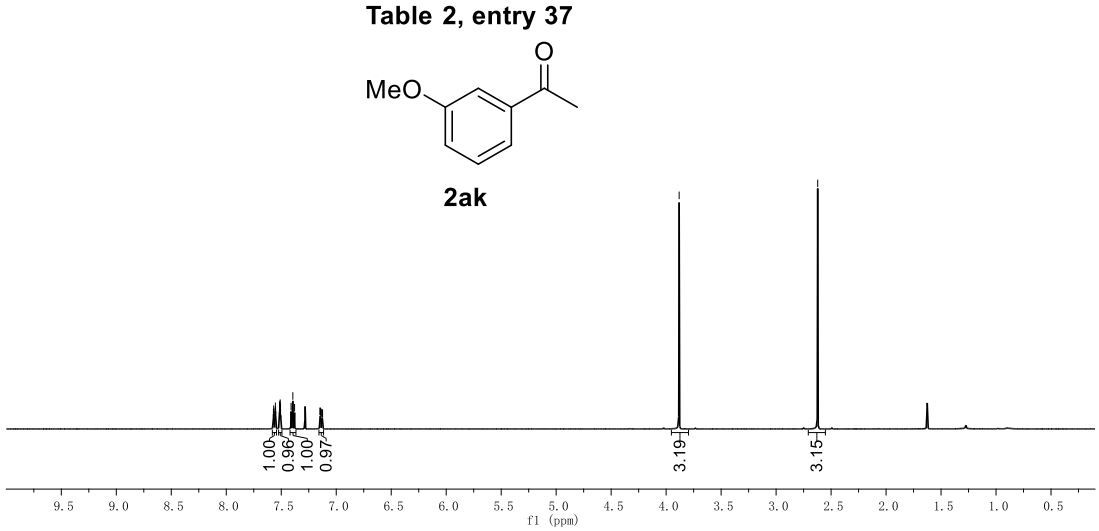

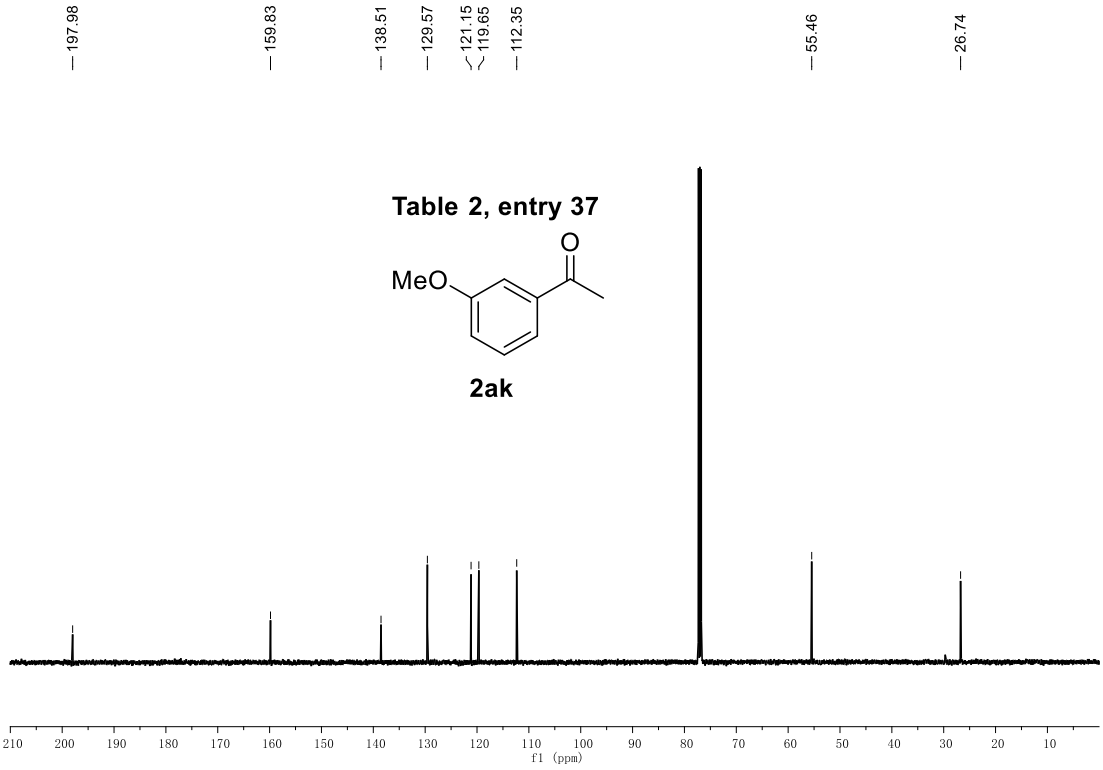

^{1}H NMR and ^{13}C NMR Spectrum of **2al**

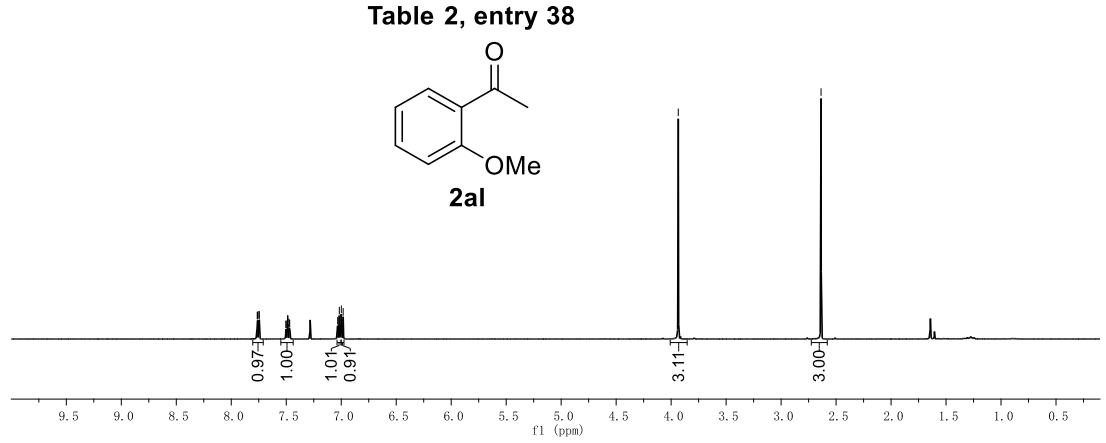

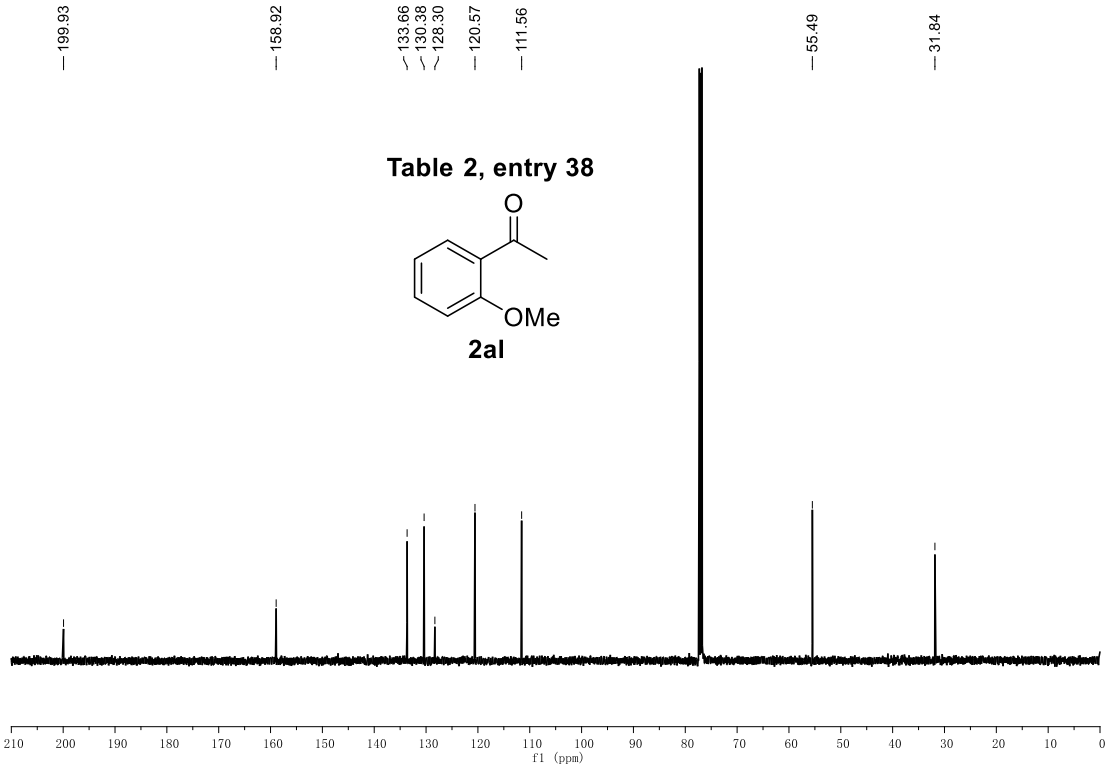

^{1}H NMR and ^{13}C NMR Spectrum of **2as**

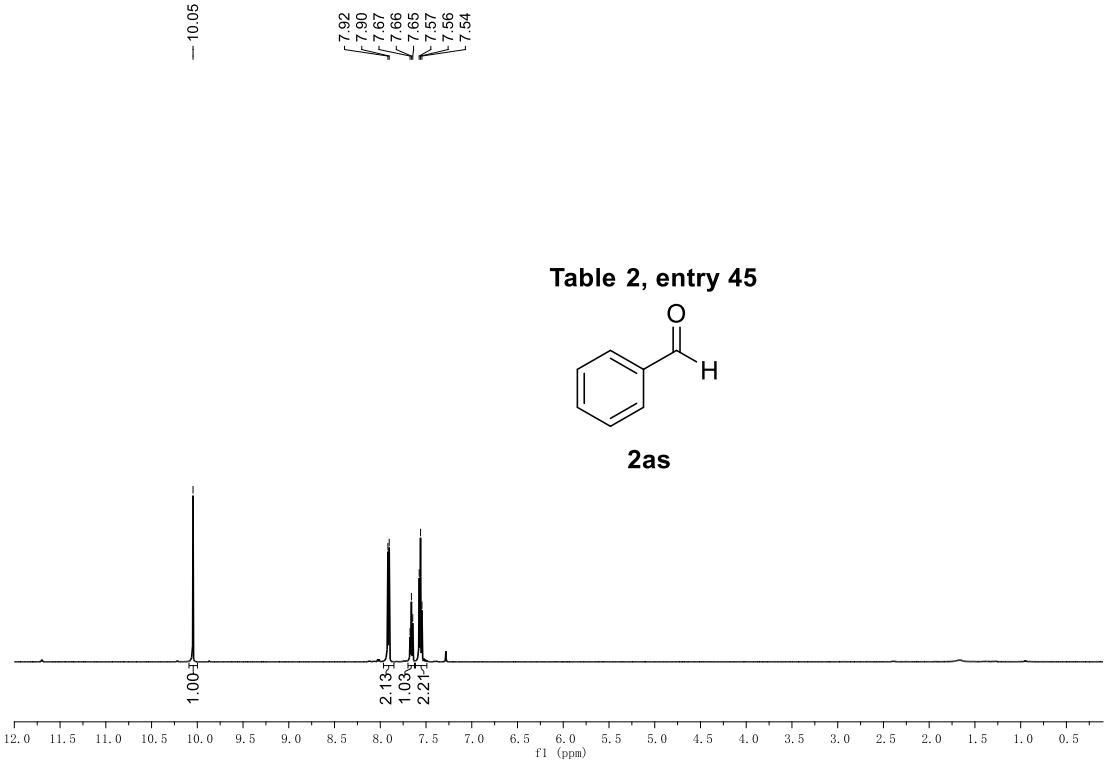

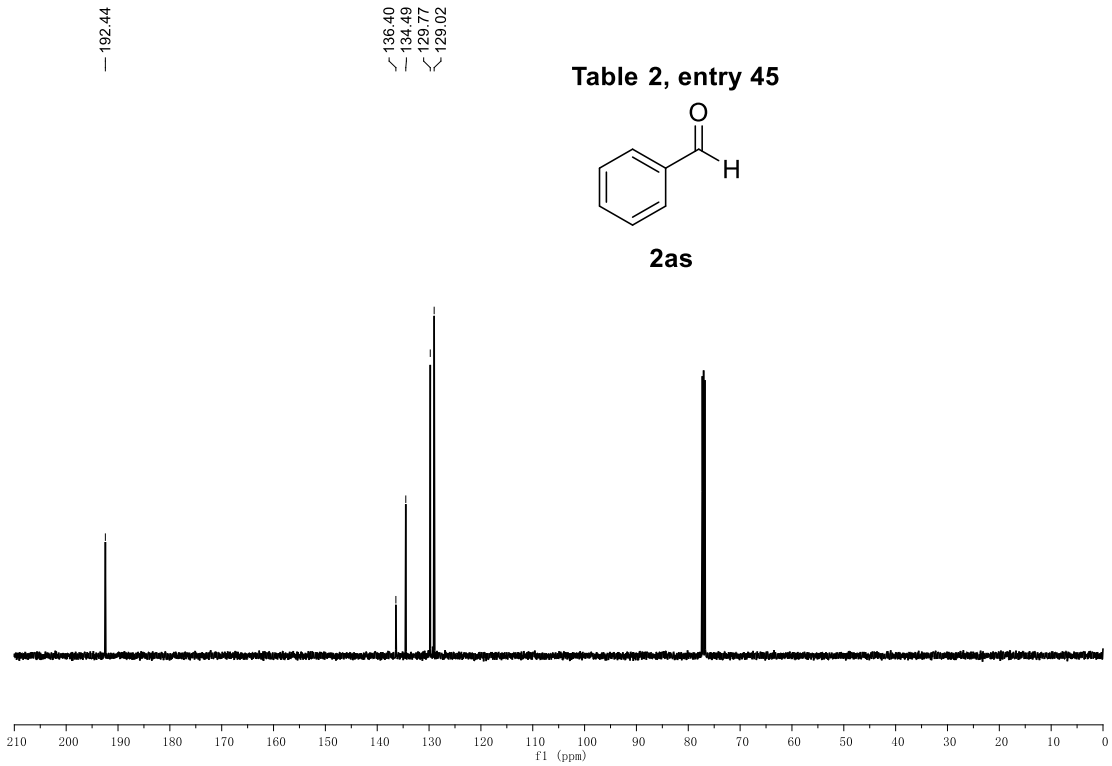

^{1}H NMR and ^{13}C NMR Spectrum of **2at**

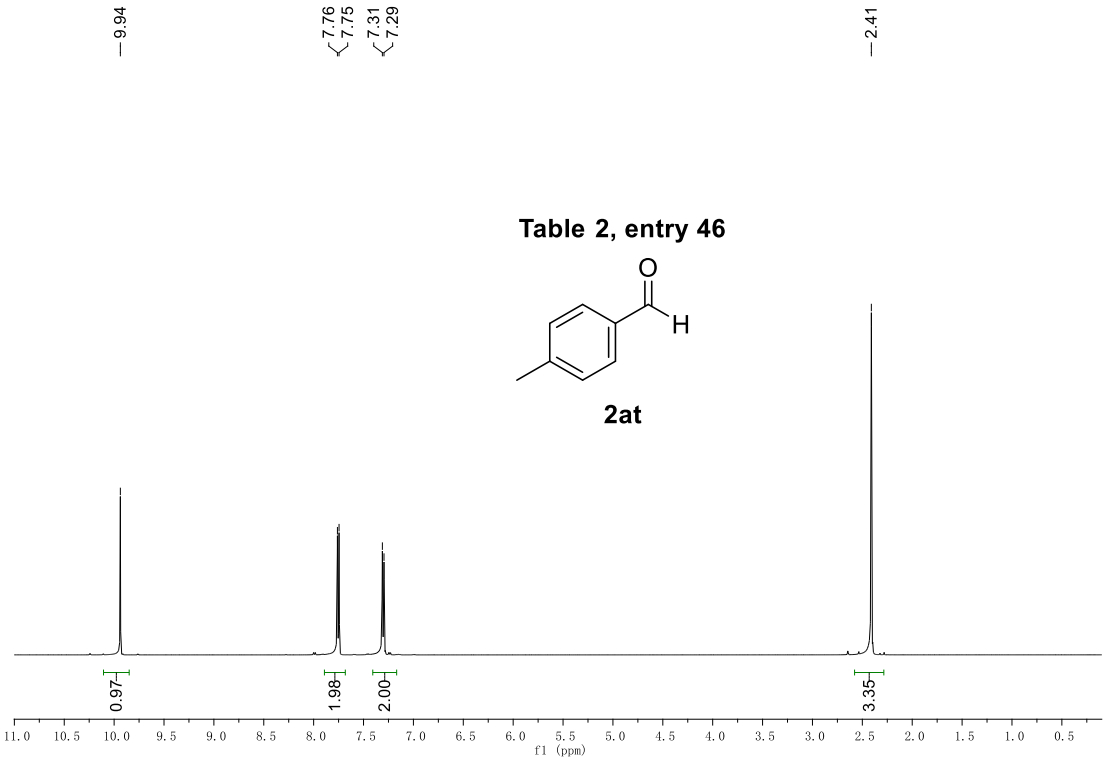

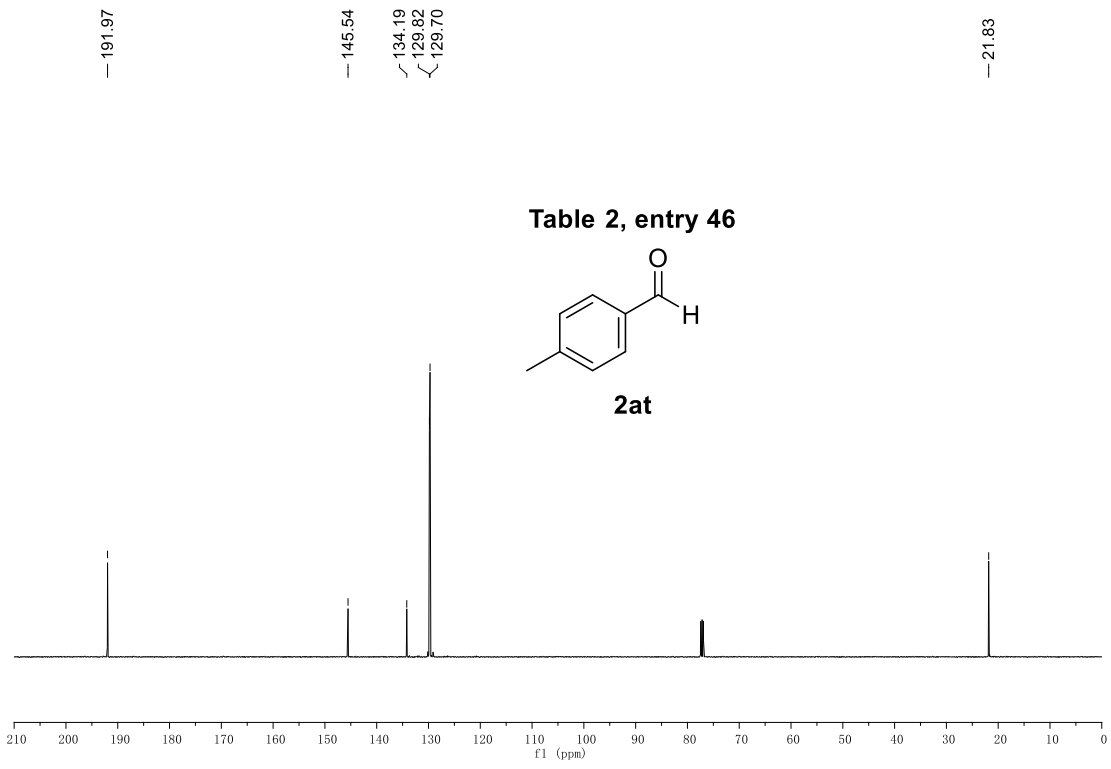

^{1}H NMR and ^{13}C NMR Spectrum of **2au**

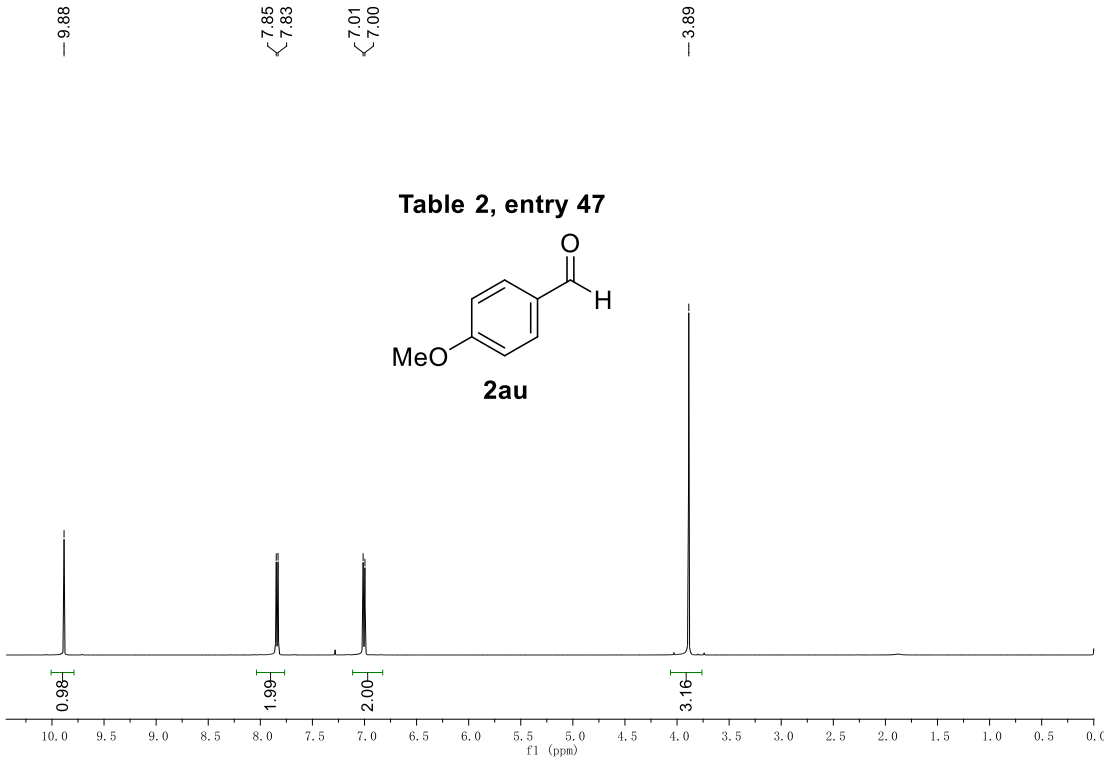

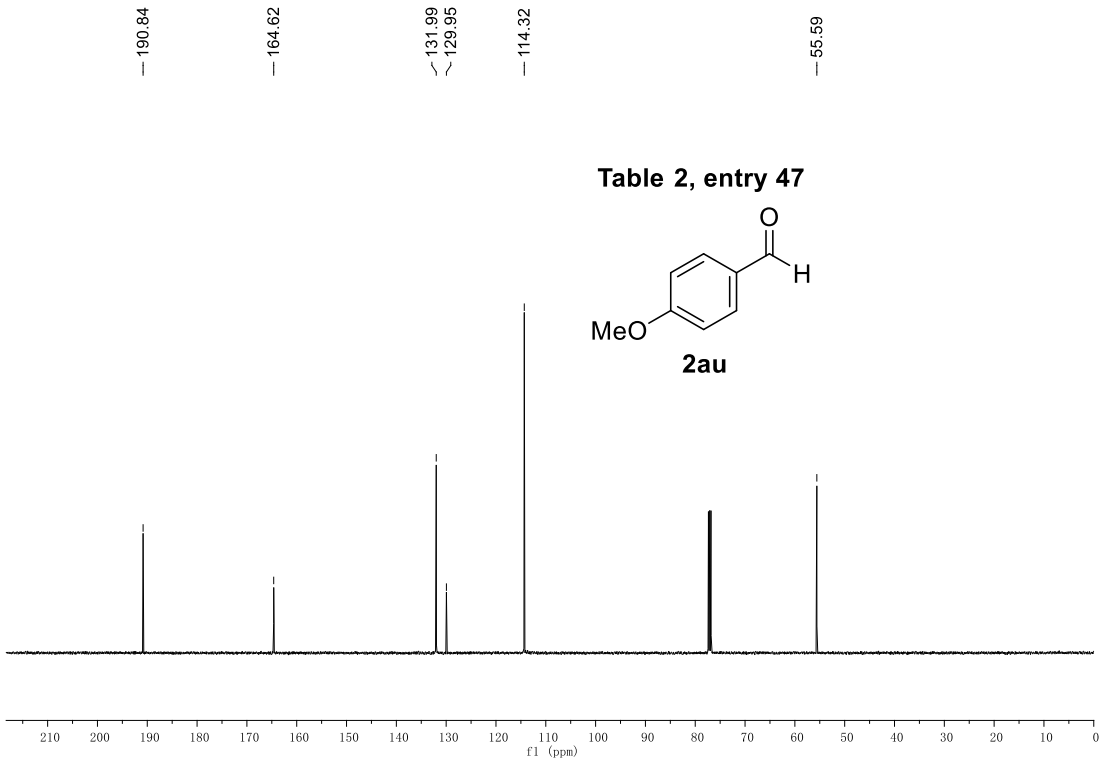

^{1}H NMR and ^{13}C NMR Spectrum of **2av**

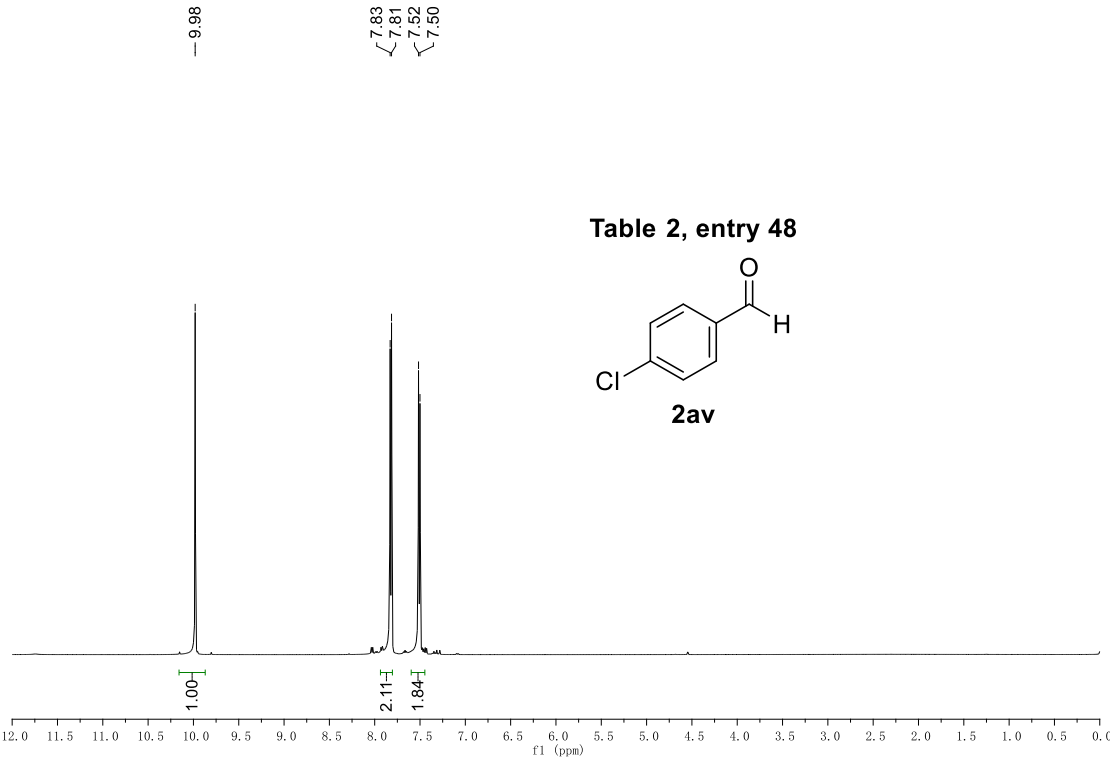

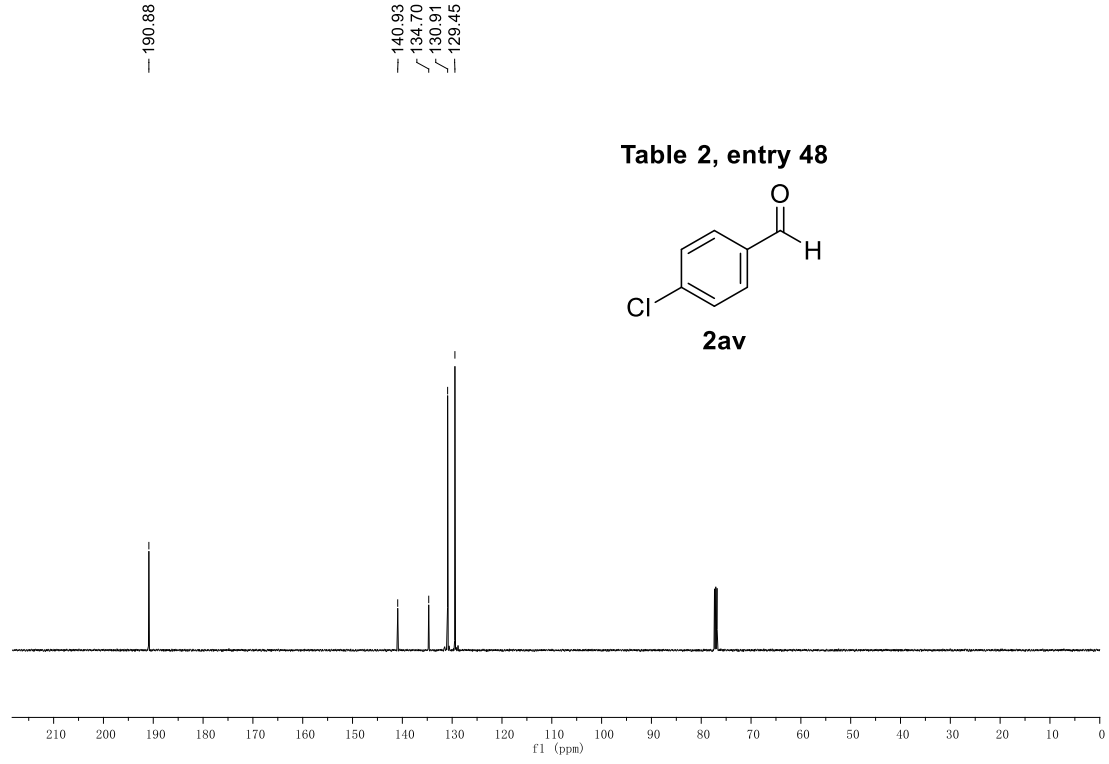

^{1}H NMR and ^{13}C NMR Spectrum of **2aw**

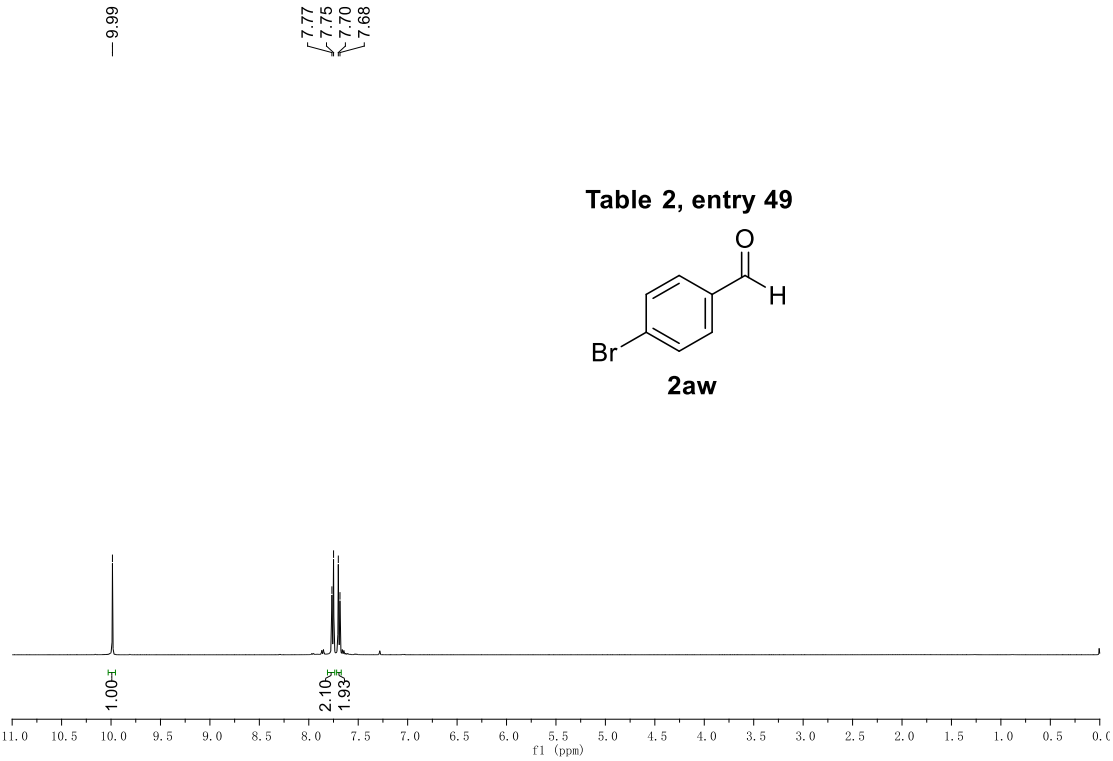

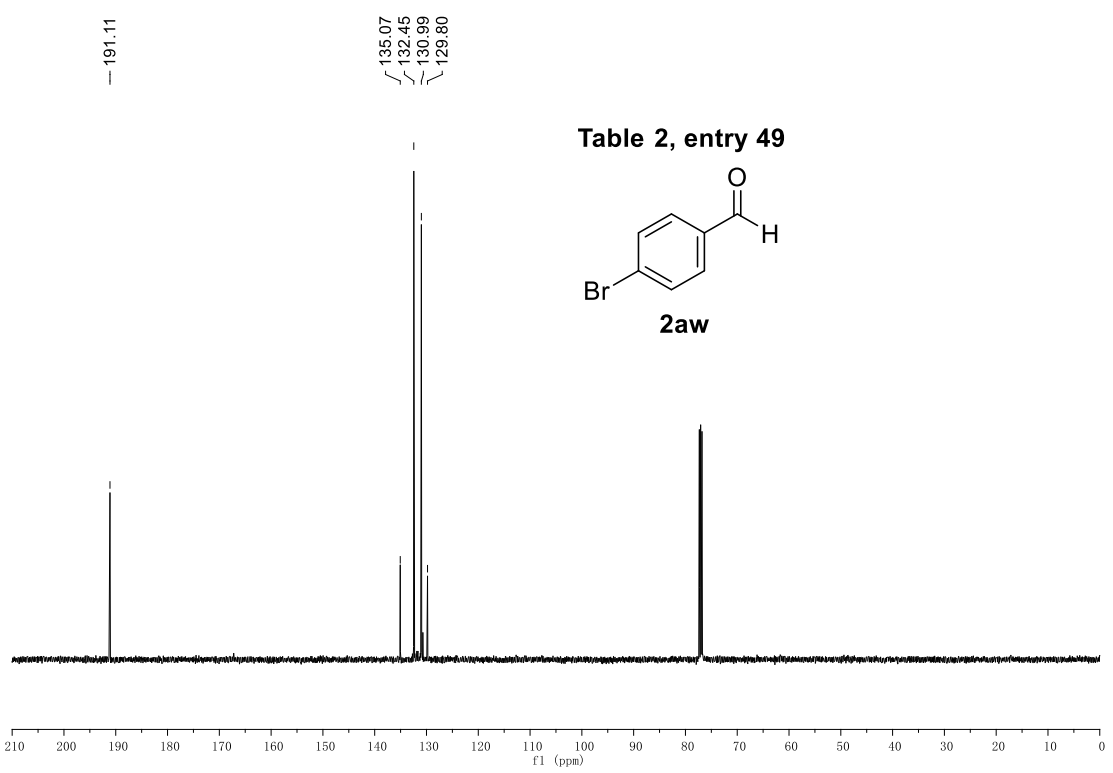

^{1}H NMR and ^{13}C NMR Spectrum of **2ax**

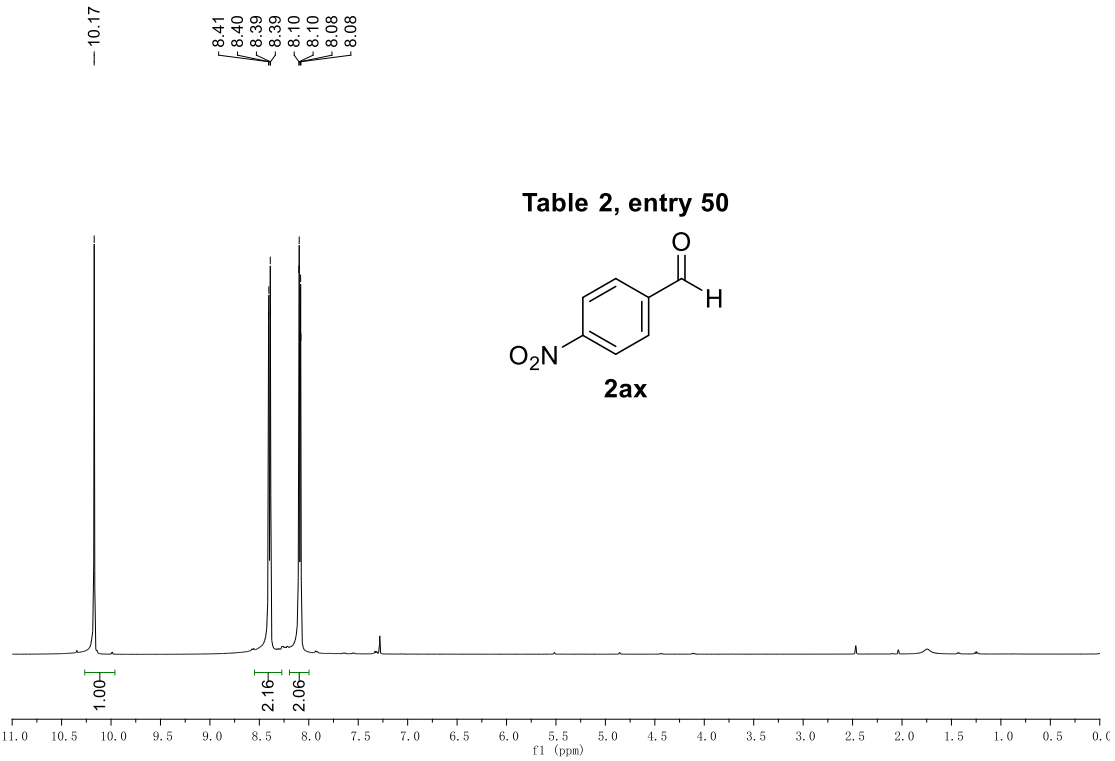

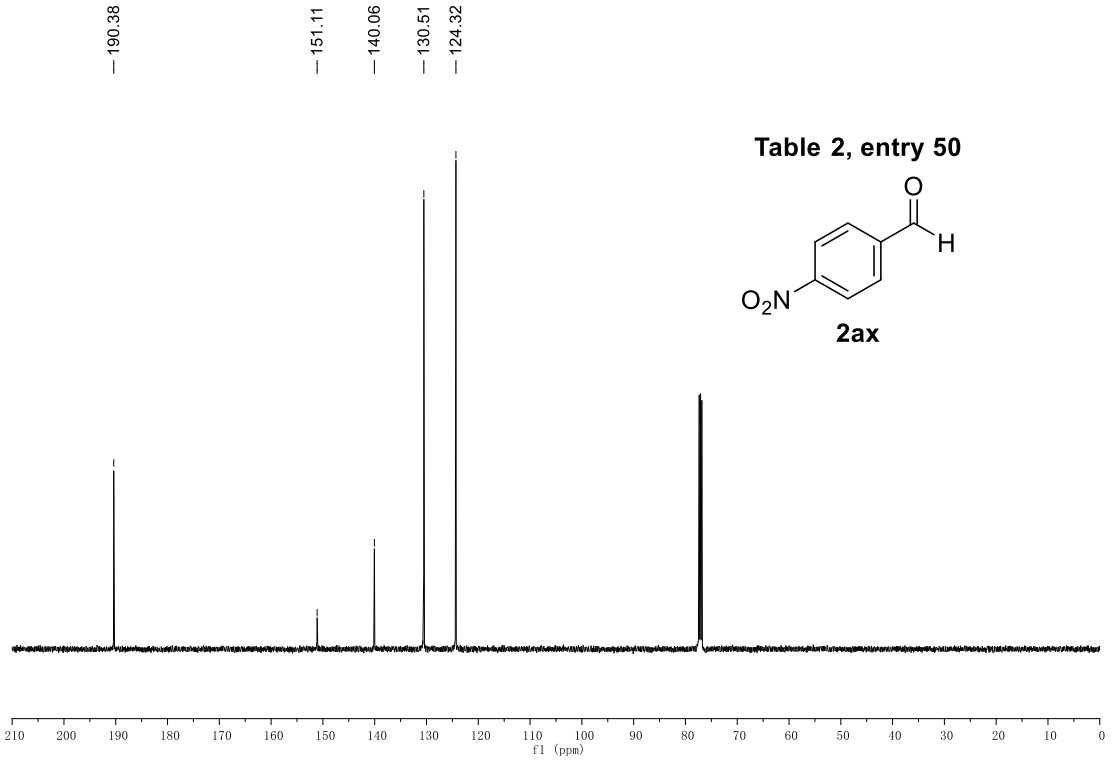

^{1}H NMR and ^{13}C NMR Spectrum of **2ay**

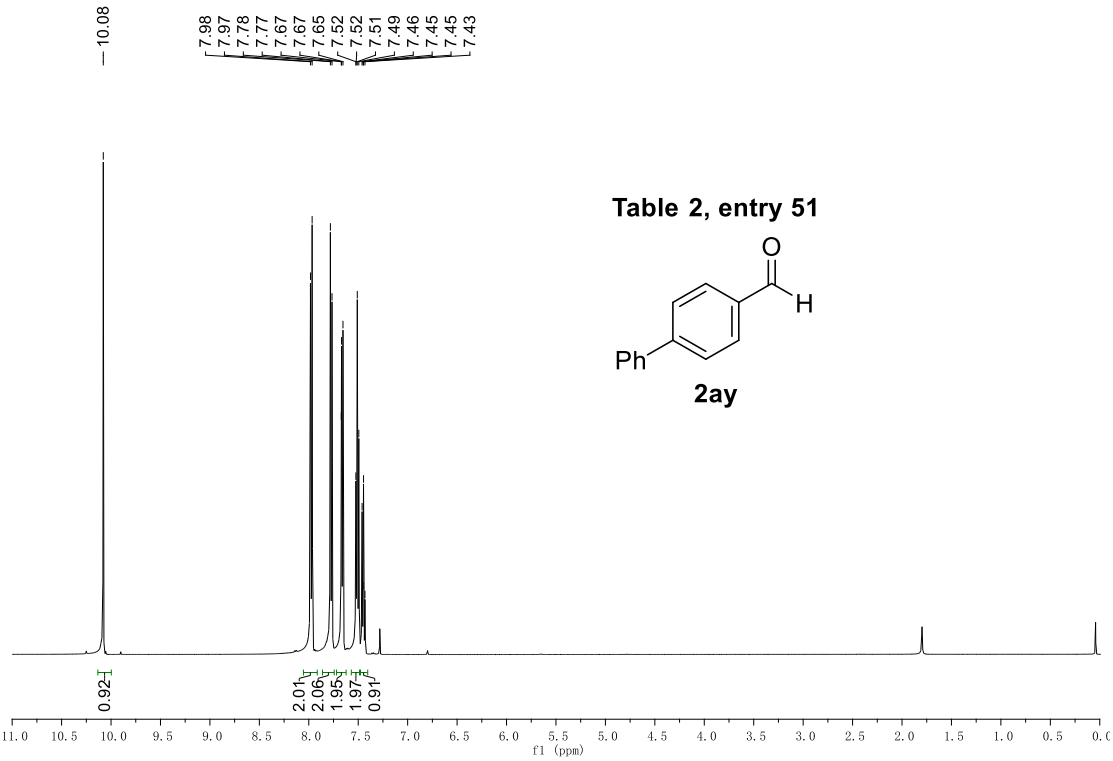

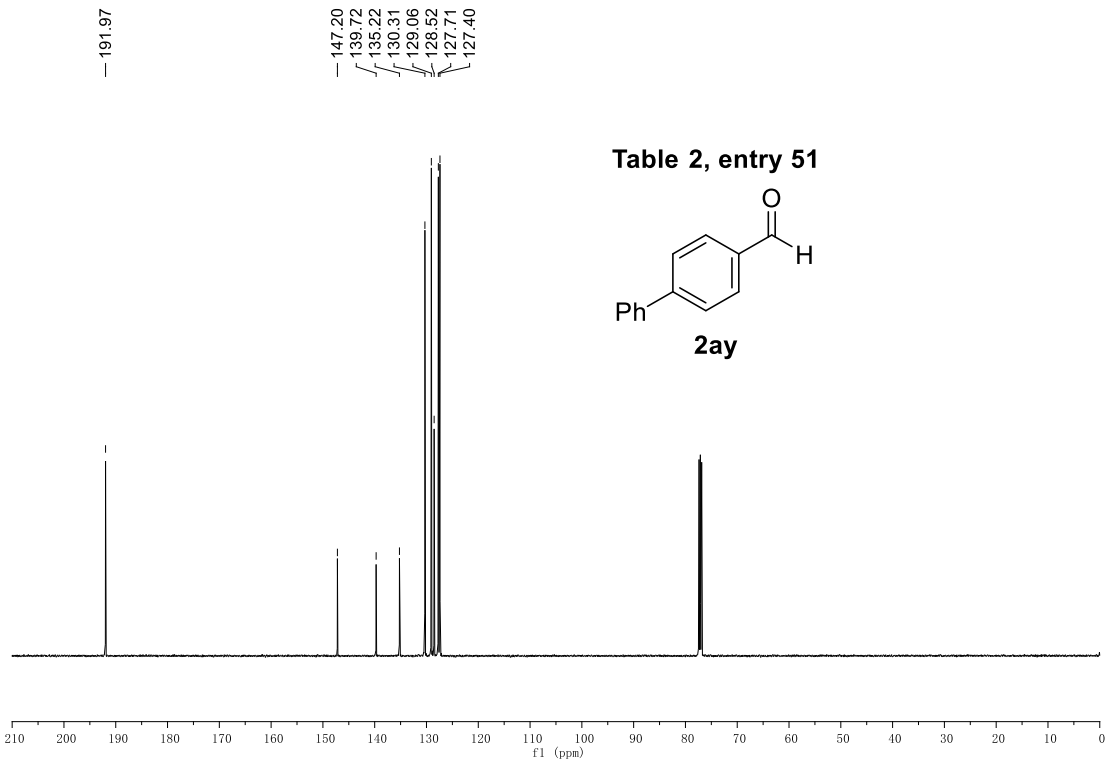

^{1}H NMR and ^{13}C NMR Spectrum of **2az**

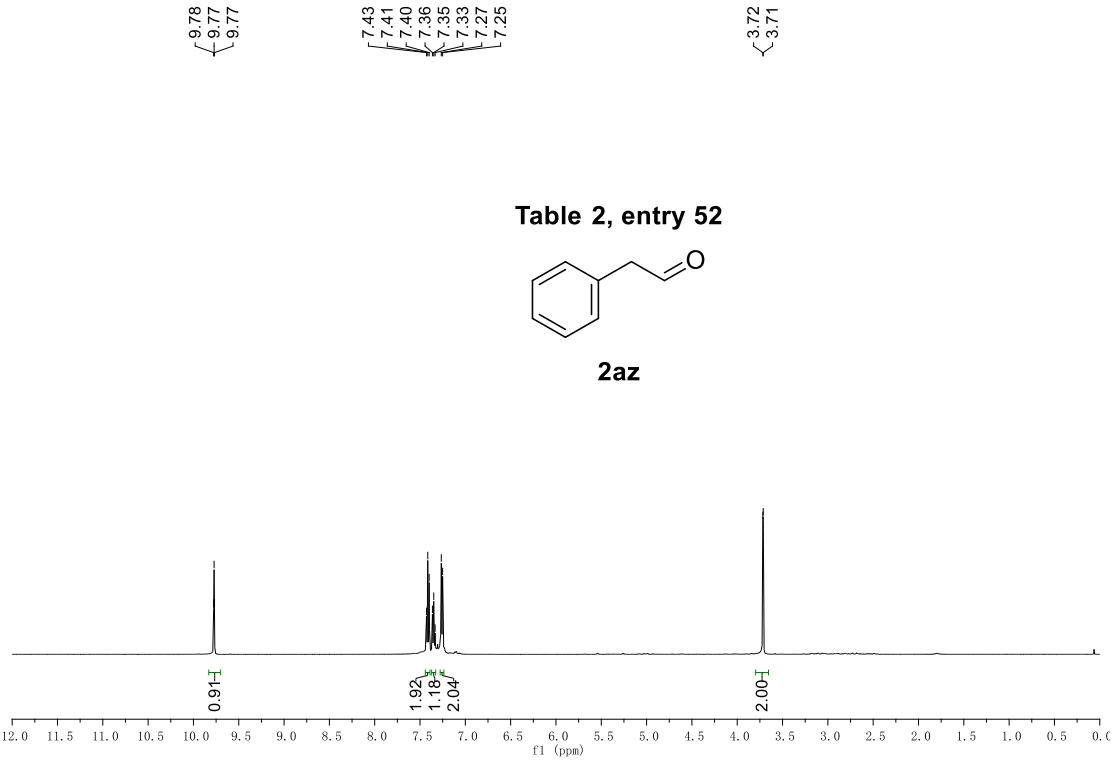

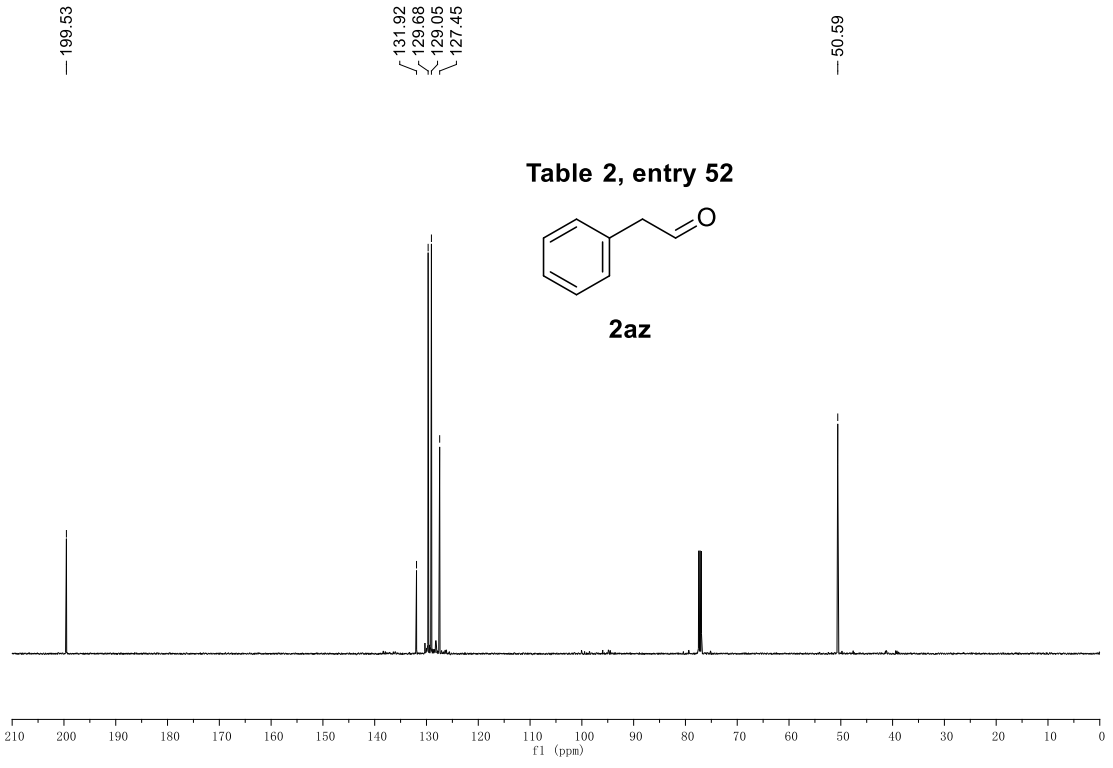

^{1}H NMR and ^{13}C NMR Spectrum of **2aaa**